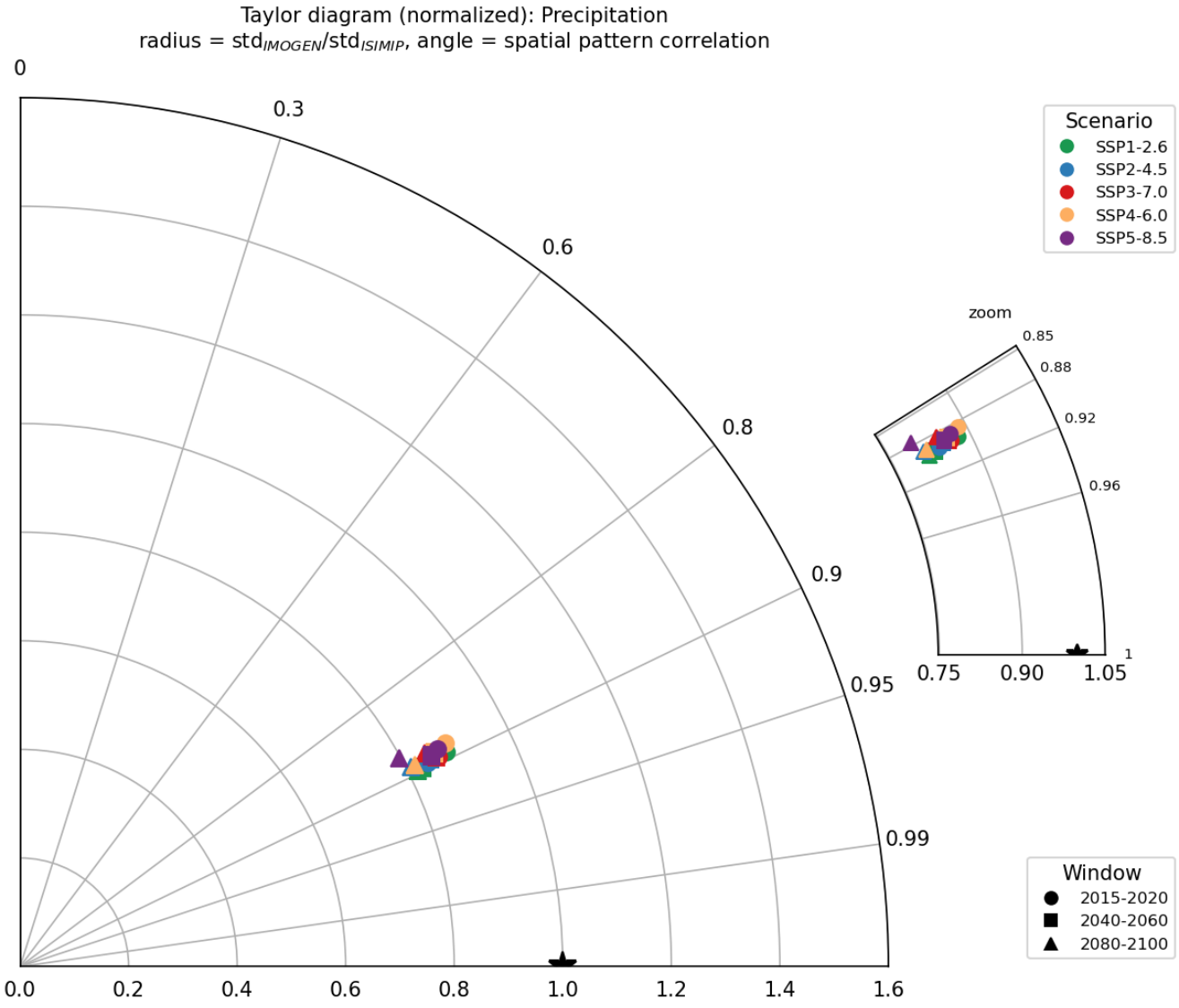
This Supplement provides the full per-scenario, per-window, and additional-variable statistics and figures that support the evaluation reported in the main text. Section S1 covers the climate-forcing evaluation (Sect. 3.3), Section S2 the atmospheric concentration evaluation (Sect. 3.2.2), Section S3 the ecosystem-state evaluation (Sect. 3.4), Section S4 the identical-emulator diagnostic (Sect. 4.4), Section S5 the detailed agricultural- and integrated-emission figures supporting Sects. 3.1 and 3.2.1, Section S6 the harmonised land-use forcing common to both configurations, Section S7 the per-scenario ecosystem-trajectory composites for the intermediate scenarios, Section S8 the raw-vs-smoothed integrated-emission time series, Section S9 the global-mean climate time-series, and Section S10 the absolute (offset-retaining) ecosystem-state difference maps.

S1 Climate-forcing evaluation

The IMOGEN-coupled climate is compared against the ISIMIP-3b MRI-ESM2-0 reference for all five SSP-RCP scenarios over three windows – 2015-2020 (scenario-overlap window; ISIMIP-3b scenario files begin in 2015), 2040-2060 (mid-century), and 2080-2100 (end of century) – and for six variables: near-surface air temperature (tas), precipitation (pr), surface downwelling shortwave radiation (rsds), daily minimum and maximum temperature (tasmin, tasmax), and the diurnal temperature range (dtr). The main text reports the headline variables (tas, pr, rsds) for the bracketing windows; the complete statistics for all five scenarios, three windows, and six variables are given in Table S1, and the supplementary Taylor diagrams and bias maps follow. Full-period (1900-2100) global-land-mean time-series of the three headline variables, over the whole simulation rather than in fixed windows, are provided in Section S9 (Figs S28-S30).

S1.1 Supplementary Taylor diagrams



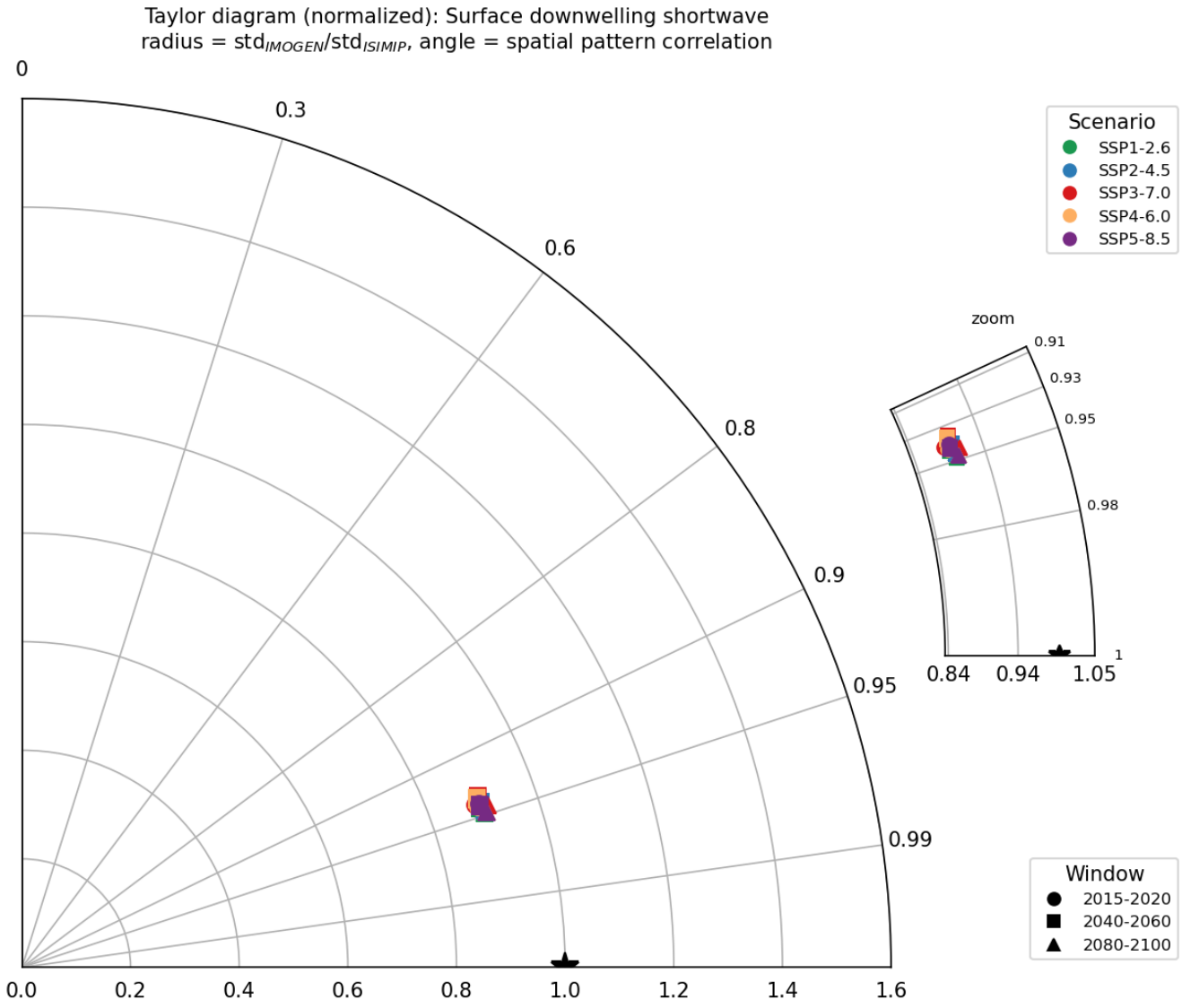
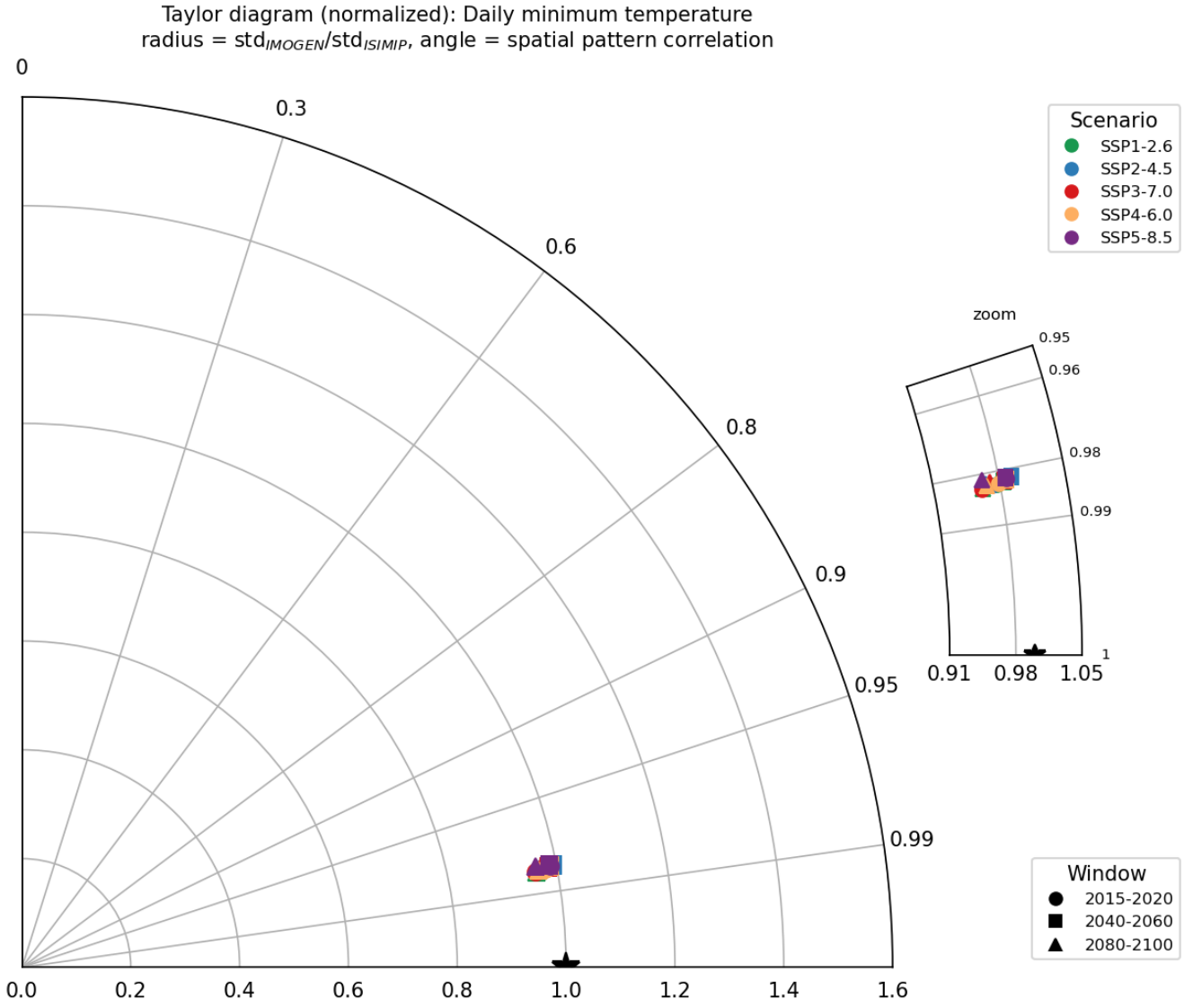
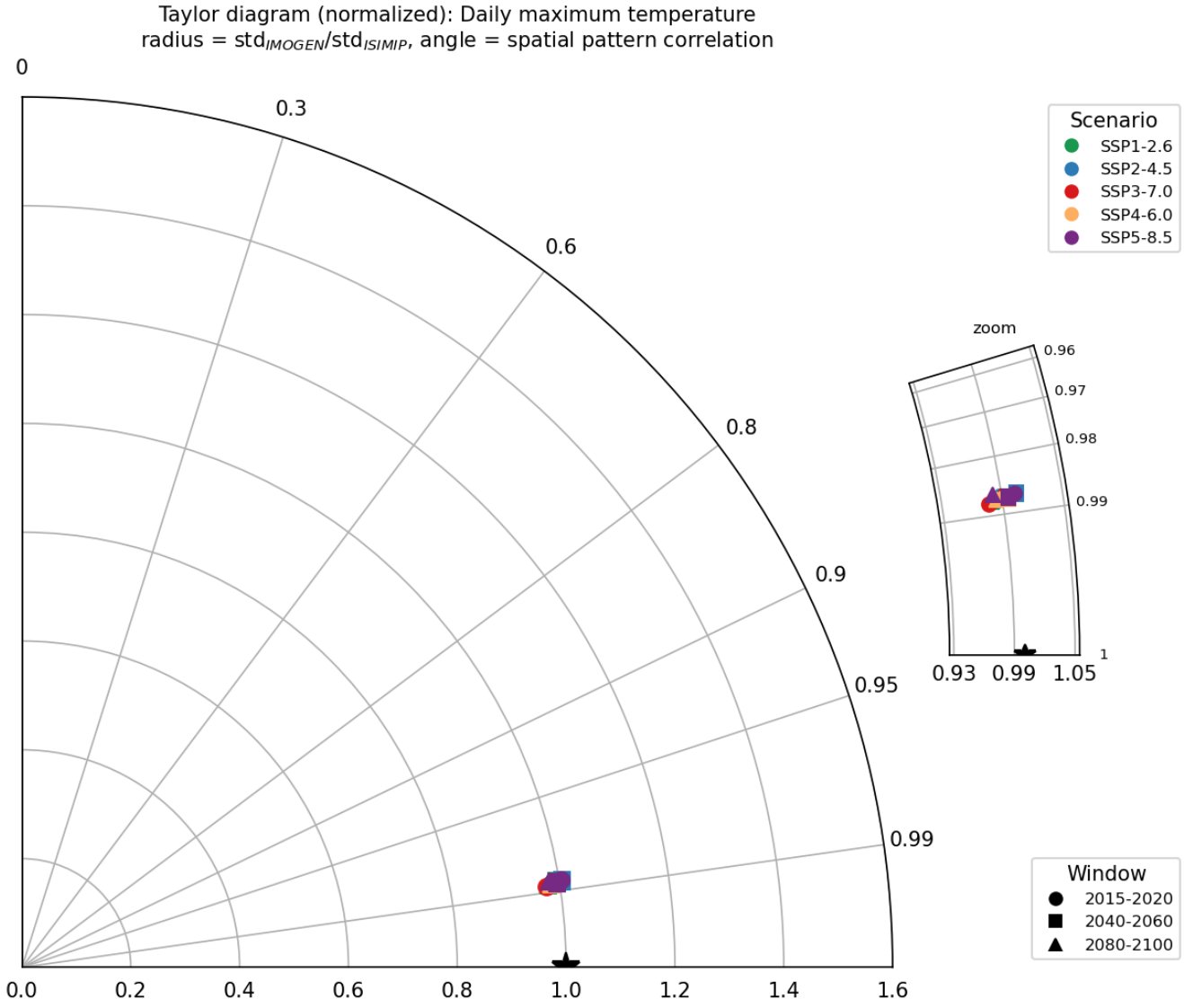


Figure S1. Taylor diagrams of the IMOGEN-coupled (top) precipitation and (bottom) surface downwelling shortwave radiation against the ISIMIP-3b MRI-ESM2-0 reference, for the five SSP-RCP scenarios and three analysis windows. These expand, per scenario and analysis window, the precipitation and shortwave panels of the four-variable summary Taylor diagram (Fig. 5) of the main text.


Taylor diagram (normalized): Daily minimum temperature
radius = std$_{IMOGEN}$/std$_{ISIMIP}$, angle = spatial pattern correlation
0
0.3
0.6
0.8
0.9
0.95
0.99
0.0
0.2
0.4
0.6
0.8
1.0
1.2
1.4
1.6
zoom
0.95
0.96
0.98
0.99
1
0.91
0.98
1.05
Scenario
SSP1-2.6
SSP2-4.5
SSP3-7.0
SSP4-6.0
SSP5-8.5
Window
2015-2020
2040-2060
2080-2100


Taylor diagram (normalized): Daily maximum temperature
radius = std$_{IMOGEN}$/std$_{ISIMIP}$, angle = spatial pattern correlation
0
0.3
0.6
0.8
0.9
0.95
0.99
0.0
0.2
0.4
0.6
0.8
1.0
1.2
1.4
1.6
Scenario
SSP1-2.6
SSP2-4.5
SSP3-7.0
SSP4-6.0
SSP5-8.5
zoom
0.96
0.97
0.98
0.99
1
0.93
0.99
1.05
Window
2015-2020
2040-2060
2080-2100

25

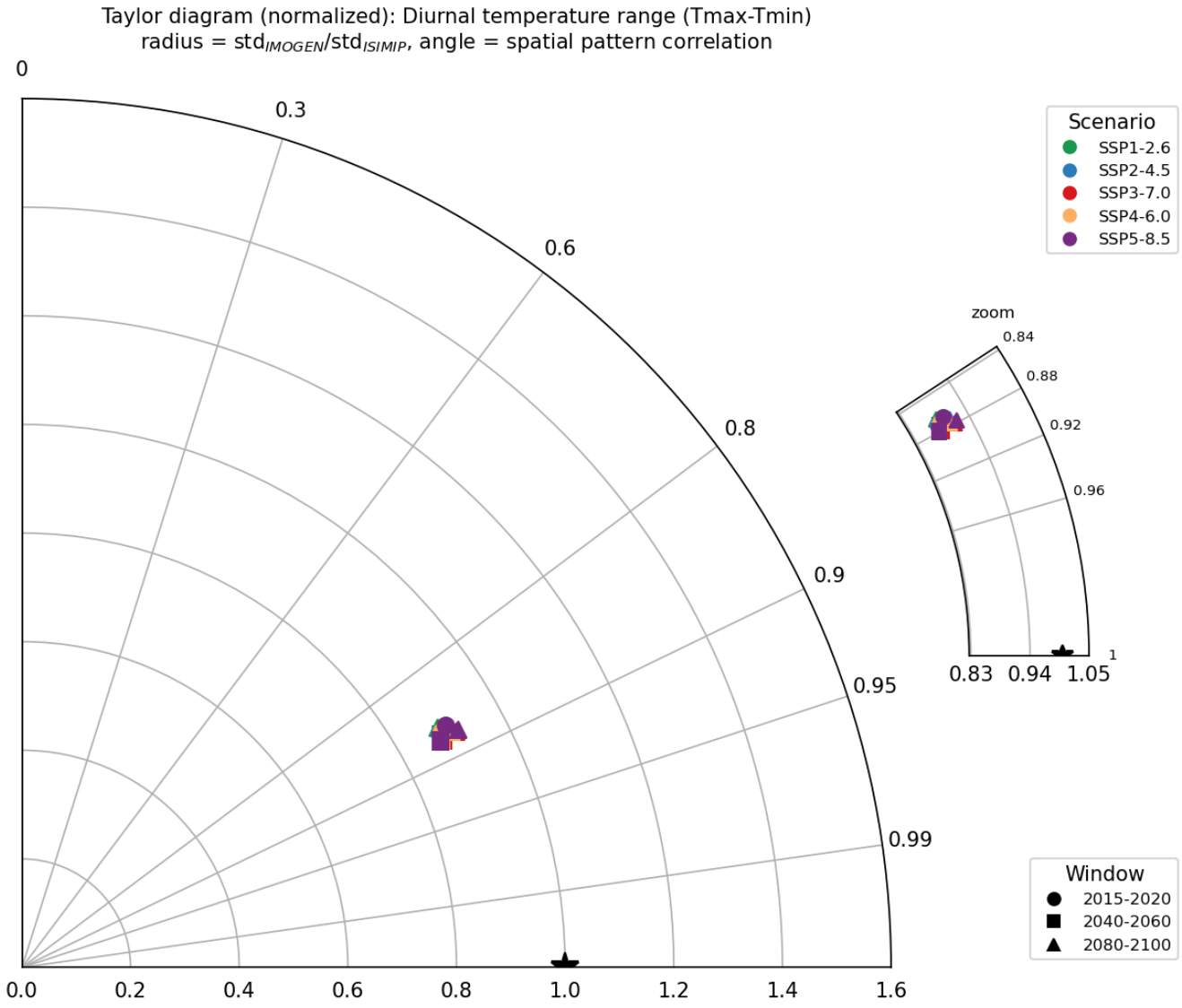
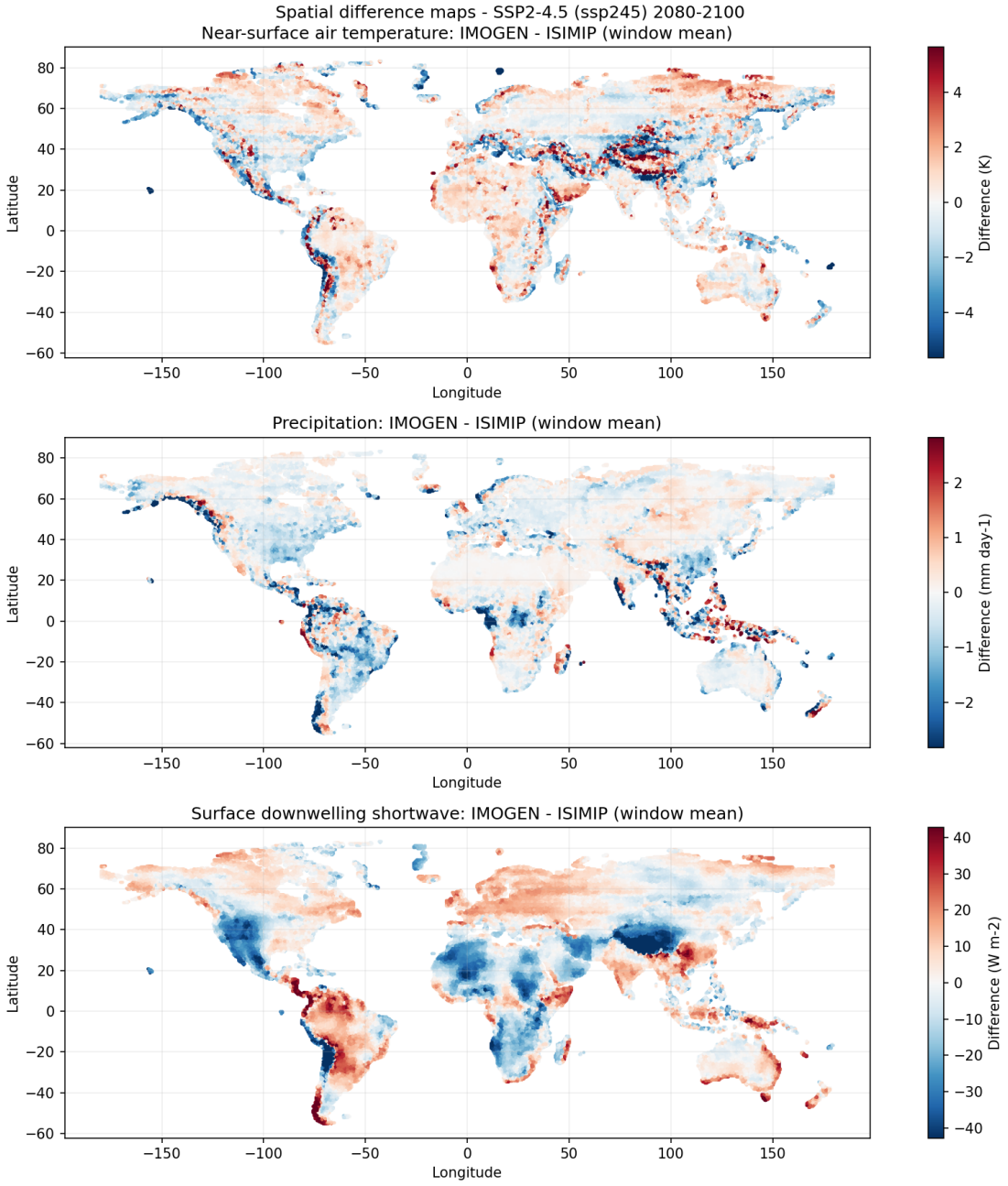
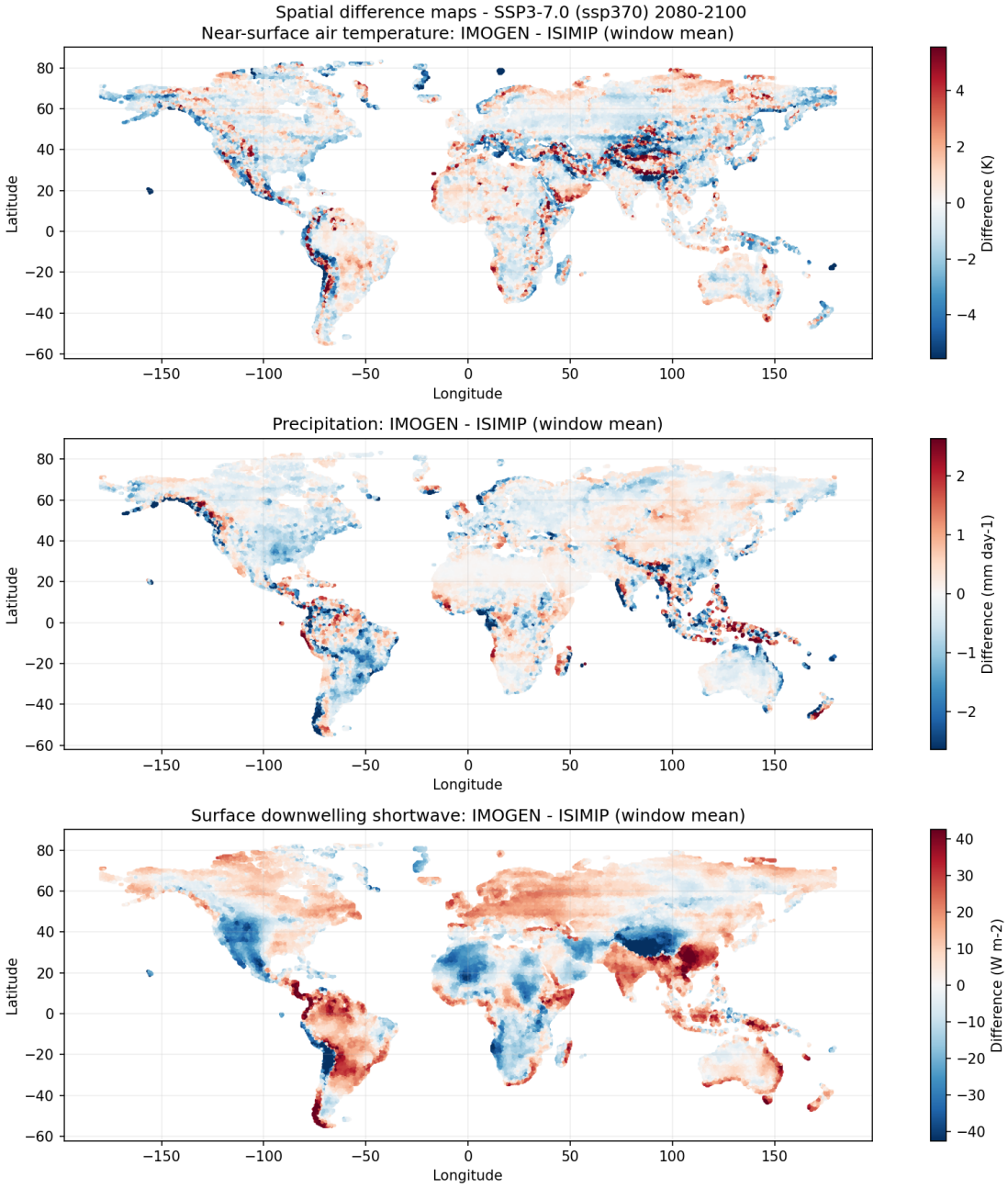


Figure S2. Taylor diagrams for the supplementary temperature variables: (top) daily minimum temperature, (middle) daily maximum temperature, and (bottom) diurnal temperature range, IMOGEN-coupled against the ISIMIP-3b MRI-ESM2-0 reference. The daily minimum and maximum temperatures track the near-surface mean temperature, with high spatial pattern agreement ($r \approx 0.98$); the diurnal temperature range is reproduced with a spatial pattern correlation of $r \approx 0.87$ (among the lowest of the climate variables, comparable to precipitation) and a sub-unity spatial-variability ratio (std ratio ≈ 0.89; Table S1).

S1.2 Supplementary bias maps




Spatial difference maps - SSP3-7.0 (ssp370) 2080-2100
Near-surface air temperature: IMOGEN - ISIMIP (window mean)
Latitude
Longitude
Difference (K)
Precipitation: IMOGEN - ISIMIP (window mean)
Latitude
Longitude
Difference (mm day-1)
Surface downwelling shortwave: IMOGEN - ISIMIP (window mean)
Latitude
Longitude
Difference (W m-2)

35

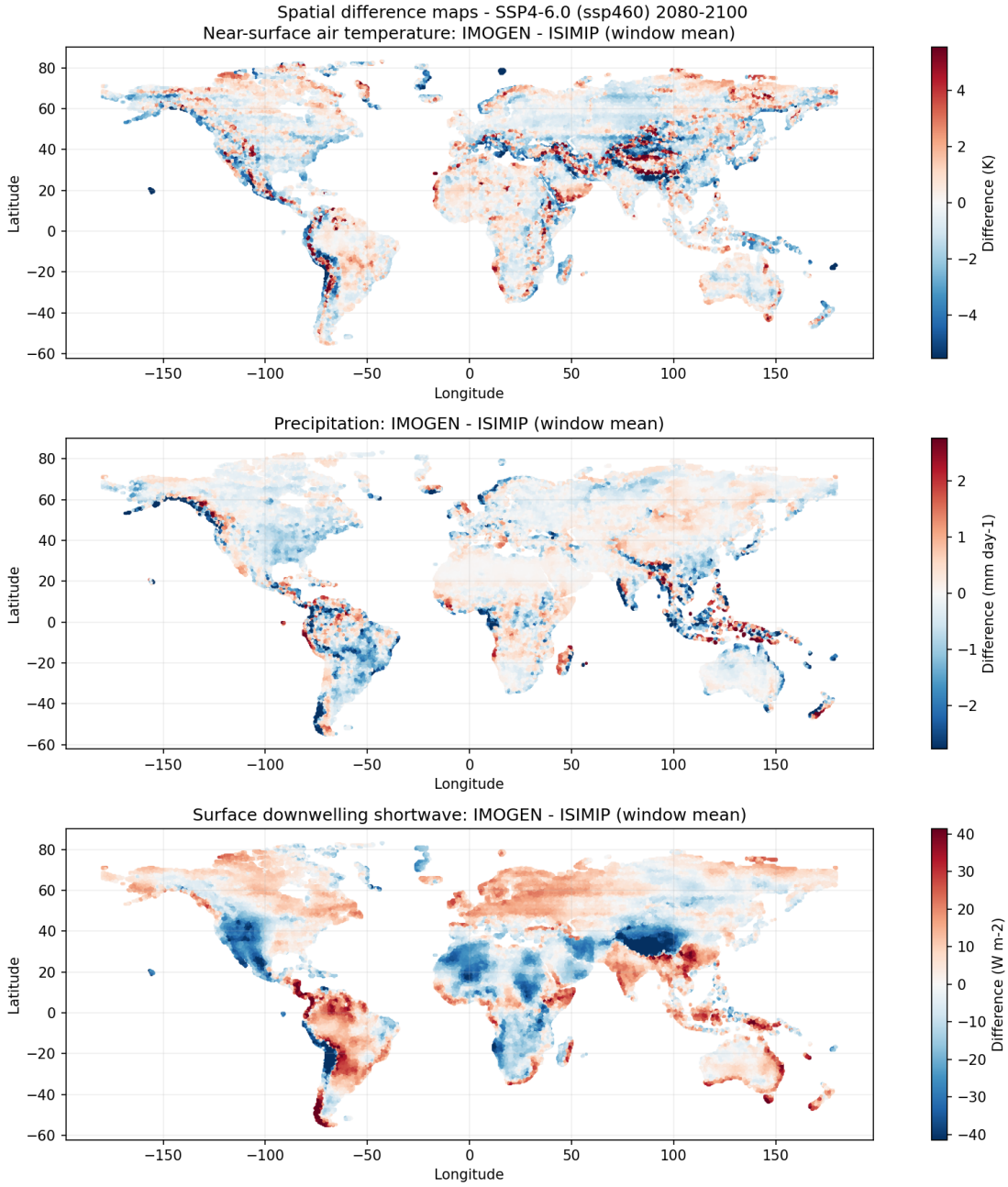


Figure S3. End-of-century (2080-2100) spatial difference (IMOGEN – ISIMIP-3b) in the headline climate variables (tas, pr, rsds) for the three intermediate scenarios not shown in the main text: (from top) SSP2-4.5, SSP3-7.0, and SSP4-6.0. The two bracketing scenarios (SSP1-2.6 and SSP5-8.5) end-of-century maps appear as Fig. 6 of the main text.

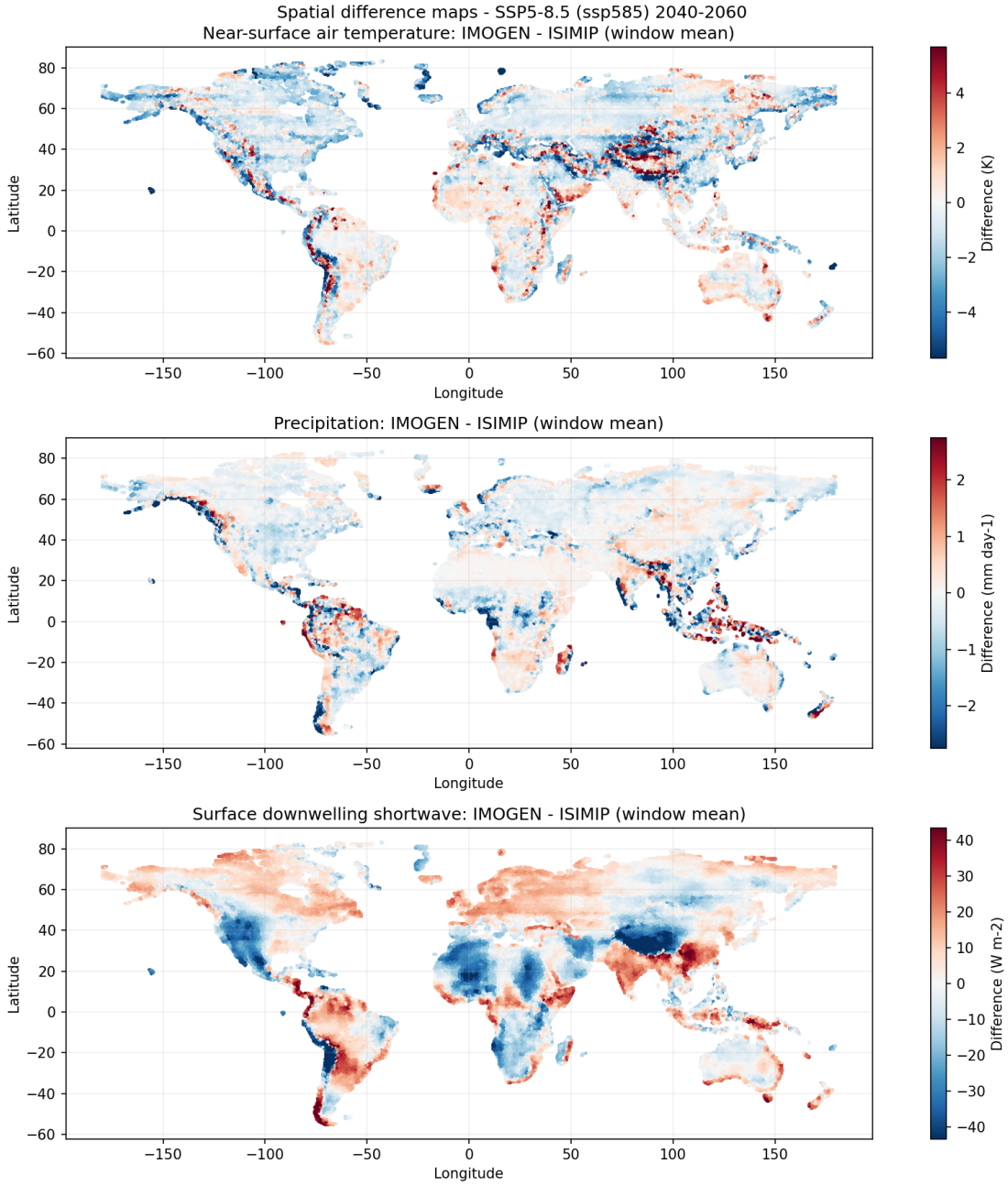


Figure S4. Mid-century (2040-2060) spatial difference (IMOGEN-coupled minus ISIMIP-3b) in the headline climate variables under SSP5-8.5, illustrating the small, regionally mixed difference at the intermediate window between the scenario-overlap and end-of-century periods.

Table S1: Full climate evaluation statistics

Table S1. Complete IMOGEN-coupled versus ISIMIP-3b MRI-ESM2-0 climate-evaluation statistics, for all five SSP-RCP scenarios, three analysis windows, and six variables. Mean bias is IMOGEN minus ISIMIP in native units; RMSD is the pooled root-mean-square difference; the spatial pattern correlation and the ratio of spatial standard deviations summarise the Taylor-diagram coordinates. All statistics are cosine-latitude (gridcell-area) weighted (Sect. 2.4.6).

Scenario	Window	Variable	Unit	Mean bias (IMOGEN – ISIMIP)	RMSD	Spatial pattern r	Std ratio
SSP1-2.6	2015-2020	tas	K	+0.04	3.03	0.987	1.002
SSP1-2.6	2015-2020	pr	mm day^{-1}	-0.19	2.44	0.893	0.878
SSP1-2.6	2015-2020	rsds	W m^{-2}	+2.72	26.29	0.941	0.891
SSP1-2.6	2015-2020	tasmin	K	-0.37	3.22	0.983	0.976
SSP1-2.6	2015-2020	tasmax	K	-0.12	3.23	0.988	0.992
SSP1-2.6	2015-2020	dtr	K	+0.25	2.02	0.869	0.897
SSP1-2.6	2040-2060	tas	K	-0.27	3.08	0.987	1.007
SSP1-2.6	2040-2060	pr	mm day^{-1}	-0.23	2.60	0.896	0.828
SSP1-2.6	2040-2060	rsds	W m^{-2}	-2.78	26.31	0.944	0.892
SSP1-2.6	2040-2060	tasmin	K	-0.61	3.28	0.982	0.984
SSP1-2.6	2040-2060	tasmax	K	-0.51	3.32	0.987	0.995
SSP1-2.6	2040-2060	dtr	K	+0.10	2.05	0.874	0.882
SSP1-2.6	2080-2100	tas	K	-0.07	3.03	0.987	0.988
SSP1-2.6	2080-2100	pr	mm day^{-1}	-0.23	2.52	0.897	0.817
SSP1-2.6	2080-2100	rsds	W m^{-2}	-2.22	25.06	0.948	0.898
SSP1-2.6	2080-2100	tasmin	K	-0.44	3.27	0.983	0.962
SSP1-2.6	2080-2100	tasmax	K	-0.26	3.28	0.988	0.979
SSP1-2.6	2080-2100	dtr	K	+0.18	2.08	0.866	0.884
SSP2-4.5	2015-2020	tas	K	+0.15	2.97	0.987	0.996
SSP2-4.5	2015-2020	pr	mm day^{-1}	-0.18	2.46	0.894	0.839
SSP2-4.5	2015-2020	rsds	W m^{-2}	+2.83	26.34	0.941	0.890
SSP2-4.5	2015-2020	tasmin	K	-0.26	3.15	0.983	0.971
SSP2-4.5	2015-2020	tasmax	K	-0.02	3.18	0.988	0.986
SSP2-4.5	2015-2020	dtr	K	+0.24	2.03	0.872	0.880
SSP2-4.5	2040-2060	tas	K	-0.30	3.04	0.986	1.017
SSP2-4.5	2040-2060	pr	mm day^{-1}	-0.17	2.48	0.892	0.849
SSP2-4.5	2040-2060	rsds	W m^{-2}	-0.62	26.33	0.941	0.897
SSP2-4.5	2040-2060	tasmin	K	-0.67	3.26	0.982	0.993
SSP2-4.5	2040-2060	tasmax	K	-0.50	3.27	0.987	1.005
SSP2-4.5	2040-2060	dtr	K	+0.17	2.05	0.875	0.883
SSP2-4.5	2080-2100	tas	K	+0.17	3.05	0.987	0.994
SSP2-4.5	2080-2100	pr	mm day^{-1}	-0.25	2.61	0.890	0.810
SSP2-4.5	2080-2100	rsds	W m^{-2}	-1.82	25.43	0.946	0.900
SSP2-4.5	2080-2100	tasmin	K	-0.23	3.24	0.982	0.966
SSP2-4.5	2080-2100	tasmax	K	-0.00	3.29	0.987	0.986
SSP2-4.5	2080-2100	dtr	K	+0.22	2.09	0.873	0.905
SSP3-7.0	2015-2020	tas	K	+0.10	2.95	0.987	0.985
SSP3-7.0	2015-2020	pr	mm day^{-1}	-0.16	2.39	0.894	0.863

Scenario	Window	Variable	Unit	Mean bias (IMOGEN – ISIMIP)	RMSD	Spatial pattern r	Std ratio
SSP3-7.0	2015-2020	rsds	W m^{-2}	+3.38	26.43	0.941	0.886
SSP3-7.0	2015-2020	tasmin	K	-0.31	3.17	0.983	0.960
SSP3-7.0	2015-2020	tasmax	K	-0.07	3.15	0.988	0.976
SSP3-7.0	2015-2020	dtr	K	+0.24	2.01	0.872	0.888
SSP3-7.0	2040-2060	tas	K	-0.22	3.02	0.987	1.008
SSP3-7.0	2040-2060	pr	mm day^{-1}	-0.15	2.50	0.893	0.859
SSP3-7.0	2040-2060	rsds	W m^{-2}	+1.66	26.94	0.936	0.896
SSP3-7.0	2040-2060	tasmin	K	-0.64	3.24	0.982	0.985
SSP3-7.0	2040-2060	tasmax	K	-0.39	3.26	0.988	0.995
SSP3-7.0	2040-2060	dtr	K	+0.25	2.05	0.880	0.883
SSP3-7.0	2080-2100	tas	K	-0.13	3.02	0.987	0.997
SSP3-7.0	2080-2100	pr	mm day^{-1}	-0.19	2.54	0.884	0.843
SSP3-7.0	2080-2100	rsds	W m^{-2}	+1.62	25.60	0.944	0.908
SSP3-7.0	2080-2100	tasmin	K	-0.60	3.23	0.982	0.970
SSP3-7.0	2080-2100	tasmax	K	-0.27	3.29	0.987	0.988
SSP3-7.0	2080-2100	dtr	K	+0.33	2.13	0.879	0.910
SSP4-6.0	2015-2020	tas	K	-0.03	3.01	0.987	1.002
SSP4-6.0	2015-2020	pr	mm day^{-1}	-0.14	2.38	0.885	0.885
SSP4-6.0	2015-2020	rsds	W m^{-2}	+3.07	26.21	0.943	0.890
SSP4-6.0	2015-2020	tasmin	K	-0.45	3.21	0.983	0.978
SSP4-6.0	2015-2020	tasmax	K	-0.19	3.21	0.988	0.991
SSP4-6.0	2015-2020	dtr	K	+0.26	2.04	0.871	0.887
SSP4-6.0	2040-2060	tas	K	-0.32	3.02	0.987	1.010
SSP4-6.0	2040-2060	pr	mm day^{-1}	-0.15	2.53	0.889	0.860
SSP4-6.0	2040-2060	rsds	W m^{-2}	+0.59	26.90	0.937	0.894
SSP4-6.0	2040-2060	tasmin	K	-0.71	3.24	0.982	0.988
SSP4-6.0	2040-2060	tasmax	K	-0.51	3.27	0.988	0.996
SSP4-6.0	2040-2060	dtr	K	+0.20	2.06	0.879	0.878
SSP4-6.0	2080-2100	tas	K	-0.12	3.01	0.987	0.993
SSP4-6.0	2080-2100	pr	mm day^{-1}	-0.21	2.55	0.890	0.816
SSP4-6.0	2080-2100	rsds	W m^{-2}	-0.59	25.29	0.948	0.903
SSP4-6.0	2080-2100	tasmin	K	-0.54	3.23	0.983	0.966
SSP4-6.0	2080-2100	tasmax	K	-0.29	3.26	0.988	0.984
SSP4-6.0	2080-2100	dtr	K	+0.26	2.09	0.876	0.902
SSP5-8.5	2015-2020	tas	K	+0.03	3.05	0.986	1.014
SSP5-8.5	2015-2020	pr	mm day^{-1}	-0.19	2.42	0.887	0.867
SSP5-8.5	2015-2020	rsds	W m^{-2}	+2.94	26.37	0.941	0.894
SSP5-8.5	2015-2020	tasmin	K	-0.41	3.25	0.982	0.988
SSP5-8.5	2015-2020	tasmax	K	-0.10	3.23	0.987	1.003
SSP5-8.5	2015-2020	dtr	K	+0.31	2.04	0.868	0.897
SSP5-8.5	2040-2060	tas	K	-0.31	3.05	0.986	1.010
SSP5-8.5	2040-2060	pr	mm day^{-1}	-0.18	2.54	0.890	0.851
SSP5-8.5	2040-2060	rsds	W m^{-2}	-1.24	26.31	0.943	0.893
SSP5-8.5	2040-2060	tasmin	K	-0.68	3.28	0.982	0.987
SSP5-8.5	2040-2060	tasmax	K	-0.52	3.30	0.988	0.996

Scenario	Window	Variable	Unit	Mean bias (IMOGEN – ISIMIP)	RMSD	Spatial pattern r	Std ratio
SSP5-8.5	2040-2060	dtr	K	+0.16	2.08	0.879	0.877
SSP5-8.5	2080-2100	tas	K	-0.03	3.05	0.986	0.990
SSP5-8.5	2080-2100	pr	mm day^{-1}	-0.24	2.69	0.876	0.798
SSP5-8.5	2080-2100	rsds	W m^{-2}	-2.33	25.49	0.948	0.902
SSP5-8.5	2080-2100	tasmin	K	-0.42	3.24	0.981	0.962
SSP5-8.5	2080-2100	tasmax	K	-0.25	3.35	0.987	0.982
SSP5-8.5	2080-2100	dtr	K	+0.17	2.16	0.878	0.915

S2 Atmospheric concentration evaluation

The prognostic atmospheric concentrations produced by the IMOGEN/FaIR module are evaluated against the observational records over the historical overlap (main-text Sect. 3.2.2). Figure S5 shows the concentration bias (IMOGEN/FaIR minus observed) for CO_2, CH_4, and N_2O by scenario, confirming that all three gases remain within their relaxed acceptance benchmarks over the historical period.

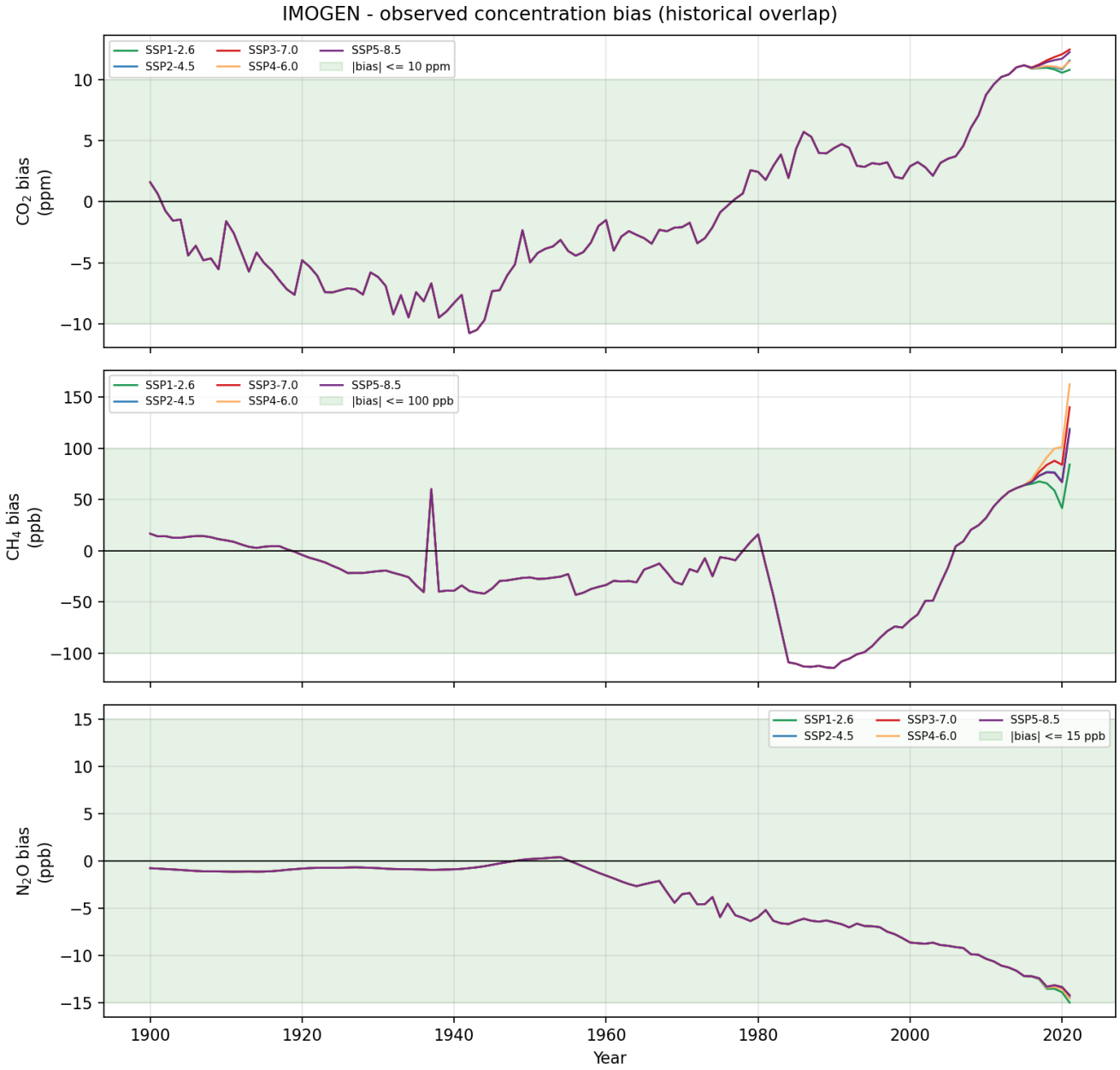


Figure S5. IMOGEN/FaIR minus observed atmospheric concentration bias over the historical overlap (~1900-2021) for CO_2, CH_4, and N_2O, by scenario. The shaded band marks the relaxed acceptance benchmark of Sect. 2.4.6 ($\pm$10 ppm for CO_2, $\pm$100 ppb for CH_4, $\pm$15 ppb for N_2O). The CO_2 bias crosses zero (low early, high late), and the CH_4 and N_2O biases are modest negative offsets that remain within their benchmarks (Sect. 3.2.2).

S3 Ecosystem-state evaluation

This section provides the full five-scenario ecosystem-state statistics that support the main-text comparison of the IMOGEN-coupled and ISIMIP-3b prescribed-climate configurations (Sect. 3.4). The two configurations share the same LPJ-GUESS version (v4.1, trunk revision r13078), gridlist (62,512 cells, the climate- and land-use-complete subset of the 62,892-cell HILDA+ remap of Sect. 2.3.3), land-use forcing, nitrogen deposition, population density, fire model, soil map, and bottom-up natural-emission inputs; the single differential is the climate forcing and its associated atmospheric CO_2 trajectory (Sect. 2.4). Table S2 reports the difference (Δ = IMOGEN-coupled – ISIMIP-3b) and the spatial pattern correlation (r, in parentheses) for every ecosystem-state variable over the end-of-century window (2080-2100), area-weighted over land, for all five SSP-RCP scenarios. The bracketing scenarios (SSP1-2.6, SSP5-8.5) are featured in the main text (Table 13; Figs. 7, 8). The present-day-to-end-of-century change-difference maps for carbon (Fig. S6) and crop yield (Fig. S7) are shown here for the three intermediate scenarios; the per-output global full-period (1901-2100) trajectories for all five scenarios are given in Figs. S8-S18; and the initial baseline offset and difference-in-change for all variables are tabulated in Table S3.

Table S2: Full ecosystem-state evaluation statistics

Table S2. Ecosystem-state differences (Δ = IMOGEN-coupled – ISIMIP-3b prescribed) over the end-of-century window (2080-2100), area-weighted over land (the crop yields production-weighted by harvested area), for all five SSP-RCP scenarios; the spatial pattern correlation between the two configurations is given in parentheses. Carbon-pool variables (VegC, LitterC, SoilC, Total) are time-mean stocks; the flux, productivity, yield, and hydrological variables are annual means. The Δ values are computed from unrounded fields and may differ from a subtraction of rounded quantities in the final digit.

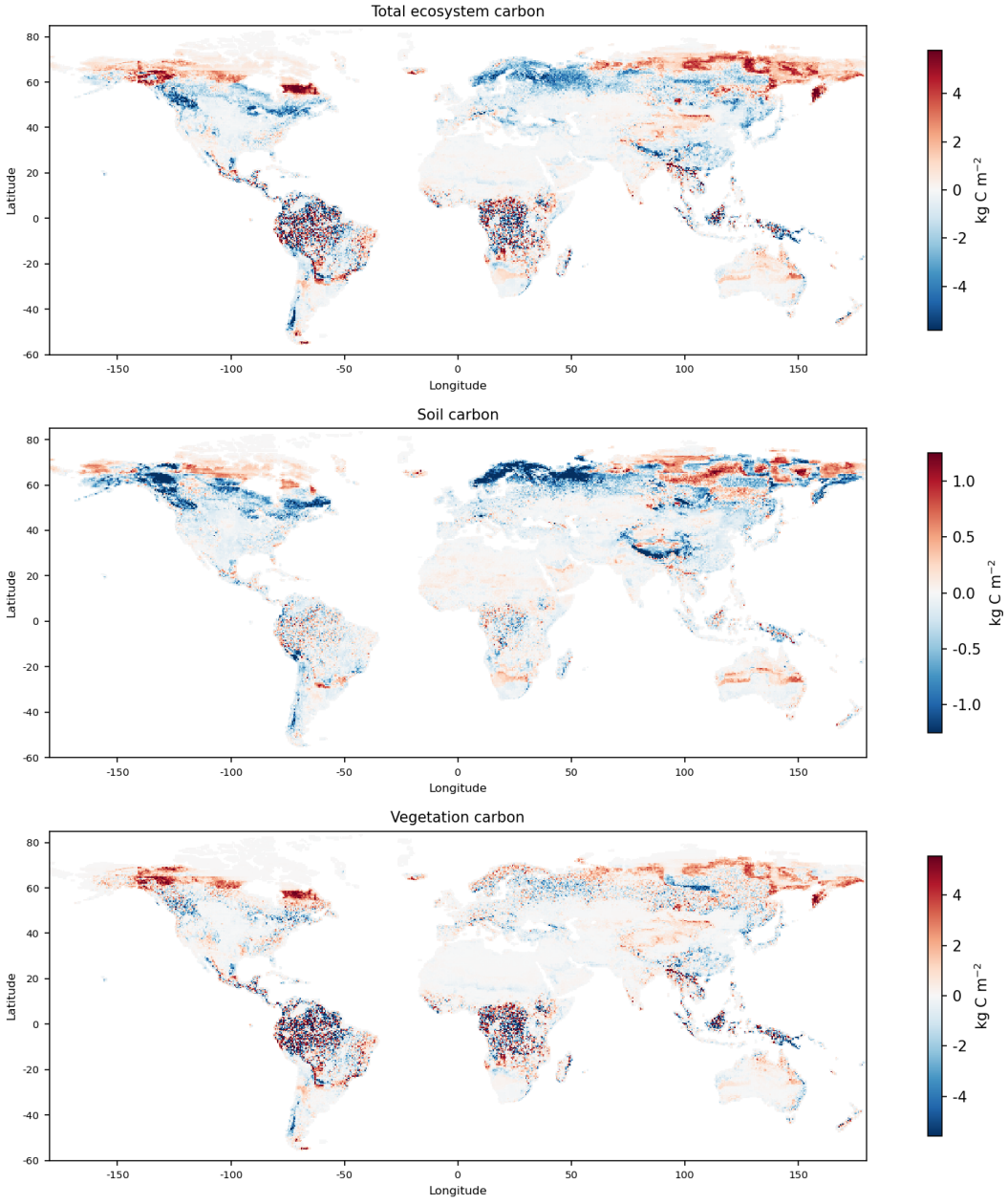
Variable	Unit	SSP1-2.6	SSP2-4.5	SSP3-7.0	SSP4-6.0	SSP5-8.5
Vegetation carbon	kg C m^{-2}	+0.71 (0.90)	+0.75 (0.90)	+0.80 (0.90)	+0.78 (0.90)	+0.77 (0.91)
Litter carbon	kg C m^{-2}	+0.83 (0.82)	+0.79 (0.83)	+0.81 (0.83)	+0.81 (0.82)	+0.76 (0.83)
Soil carbon	kg C m^{-2}	+2.81 (0.86)	+2.78 (0.86)	+2.78 (0.86)	+2.79 (0.86)	+2.75 (0.86)
Total ecosystem carbon	kg C m^{-2}	+4.35 (0.85)	+4.32 (0.85)	+4.39 (0.86)	+4.38 (0.86)	+4.28 (0.86)
Net primary production	kg C m^{-2} yr^{-1}	+0.060 (0.89)	+0.066 (0.88)	+0.072 (0.89)	+0.066 (0.89)	+0.065 (0.88)
Net land-atmosphere C flux (F_{net})	kg C m^{-2} yr^{-1}	+0.002 (0.07)	+0.005 (0.14)	+0.002 (0.23)	+0.004 (0.06)	+0.007 (0.21)
Vegetation C flux (uptake)	kg C m^{-2} yr^{-1}	-0.060 (0.89)	-0.066 (0.88)	-0.072 (0.89)	-0.066 (0.89)	-0.065 (0.88)
Soil C flux (respiration)	kg C m^{-2} yr^{-1}	+0.055 (0.92)	+0.060 (0.91)	+0.061 (0.91)	+0.059 (0.91)	+0.059 (0.91)
C3 cereal yield	kg C m^{-2} yr^{-1}	-0.007 (0.78)	-0.006 (0.76)	-0.009 (0.73)	-0.010 (0.76)	-0.005 (0.70)
C4 cereal yield	kg C m^{-2} yr^{-1}	+0.002 (0.94)	+0.017 (0.93)	+0.024 (0.92)	+0.017 (0.93)	+0.034 (0.91)
Rice yield	kg C m^{-2} yr^{-1}	+0.022 (0.84)	+0.043 (0.87)	+0.063 (0.86)	+0.045 (0.86)	+0.106 (0.85)
N-fixing oil-crop yield	kg C m^{-2} yr^{-1}	+0.075 (0.83)	+0.094 (0.82)	+0.116 (0.80)	+0.093 (0.81)	+0.128 (0.77)
Other oil-crop yield	kg C m^{-2} yr^{-1}	-0.008 (0.75)	-0.009 (0.73)	-0.025 (0.71)	-0.017 (0.73)	-0.018 (0.66)

Variable	Unit	SSP1-2.6	SSP2-4.5	SSP3-7.0	SSP4-6.0	SSP5-8.5
Pulse yield	kg C m^{-2} yr^{-1}	+0.045 (0.83)	+0.087 (0.82)	+0.115 (0.80)	+0.099 (0.81)	+0.135 (0.77)
Total nitrogen pool	kg N m^{-2}	+0.284 (0.85)	+0.282 (0.85)	+0.282 (0.85)	+0.283 (0.85)	+0.280 (0.85)
Soil N_2O flux	kg N ha^{-1} yr^{-1}	+0.071 (0.57)	+0.057 (0.50)	-0.029 (0.40)	+0.024 (0.52)	+0.046 (0.42)
Total soil N-gas flux (N_2+N_2O+NO+NH_3)	kg N ha^{-1} yr^{-1}	+0.154 (0.53)	+0.058 (0.48)	-0.335 (0.40)	-0.080 (0.48)	-0.087 (0.44)
Nitrogen leaching	kg N ha^{-1} yr^{-1}	-0.838 (0.65)	-1.124 (0.53)	-1.058 (0.47)	-1.090 (0.52)	-0.846 (0.49)
Wetland CH_4	g CH_4 m^{-2} yr^{-1}	+0.155 (0.96)	+0.167 (0.95)	+0.173 (0.95)	+0.160 (0.95)	+0.178 (0.95)
Leaf area index	m^2 m^{-2}	+0.339 (0.91)	+0.384 (0.90)	+0.405 (0.90)	+0.387 (0.90)	+0.391 (0.90)
Total runoff	mm yr^{-1}	-144.7 (0.74)	-149.8 (0.72)	-134.3 (0.73)	-140.6 (0.73)	-138.4 (0.72)

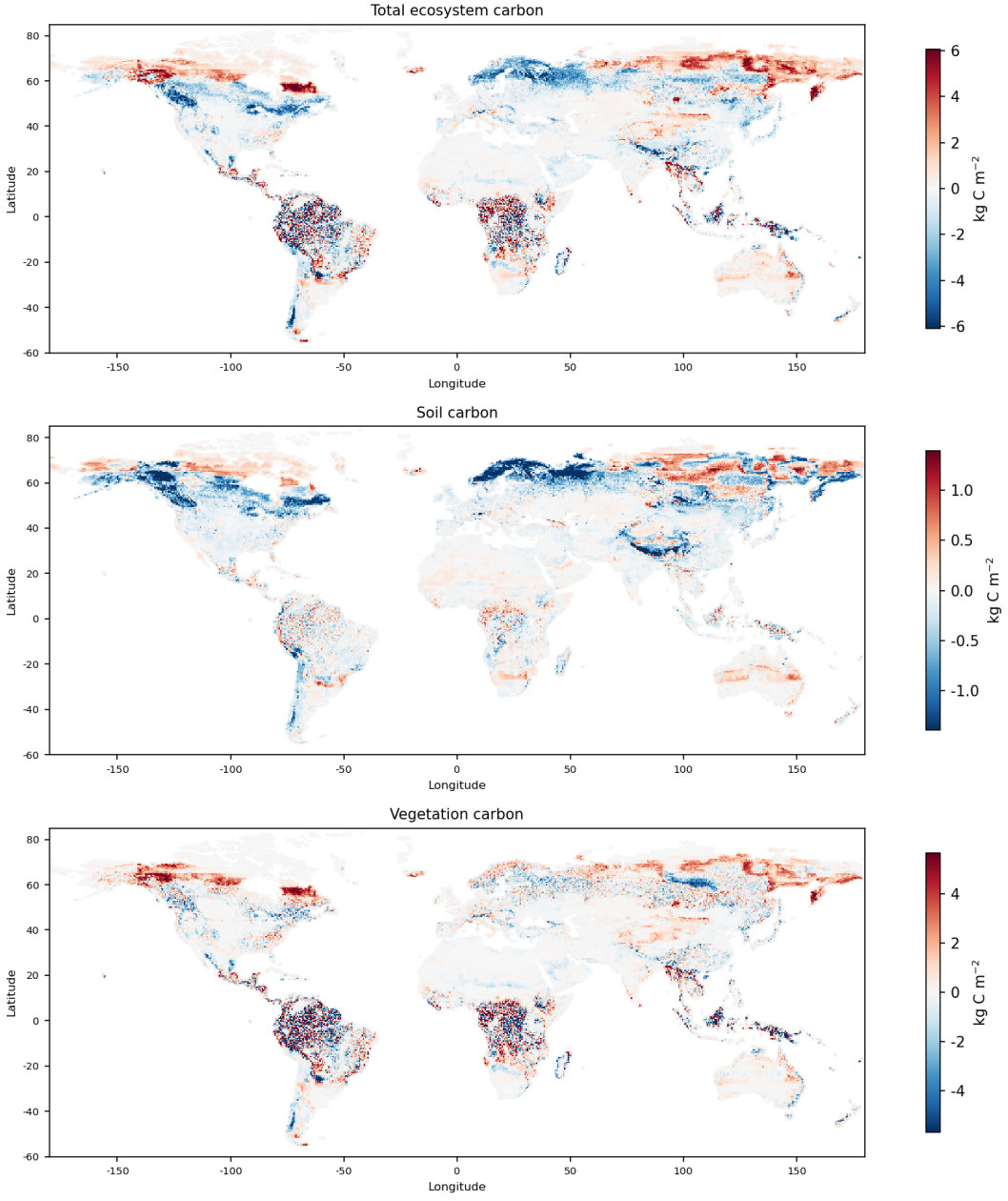
The difference statistics are consistent across the five scenarios in sign and spatial structure: the total-carbon surplus is roughly constant across the forcing range (about +4.3 kg C m^{-2}), and the crop-yield, nitrogen-gas-flux, and wetland-CH_4 differences are small and vary only weakly with forcing, consistent with a persistent mean-state offset rather than a forcing-
80 dependent feedback (Sect. 3.4.1). The net land-atmosphere carbon flux (F_{net}) has a small difference and a low spatial pattern correlation ($r \leq 0.23$), because the larger vegetation-uptake and soil-respiration fluxes of the coupled configuration nearly cancel (Sect. 3.4.1).

S3.1 Supplementary ecosystem difference maps

Difference in the present-day-to-end-of-century carbon change (IMOGEN-coupled - ISIMIP-3b), SSP2-4.5 (2005-2025 to 2080-2100)



Difference in the present-day-to-end-of-century carbon change (IMOGEN-coupled - ISIMIP-3b), SSP3-7.0 (2005-2025 to 2080-2100)



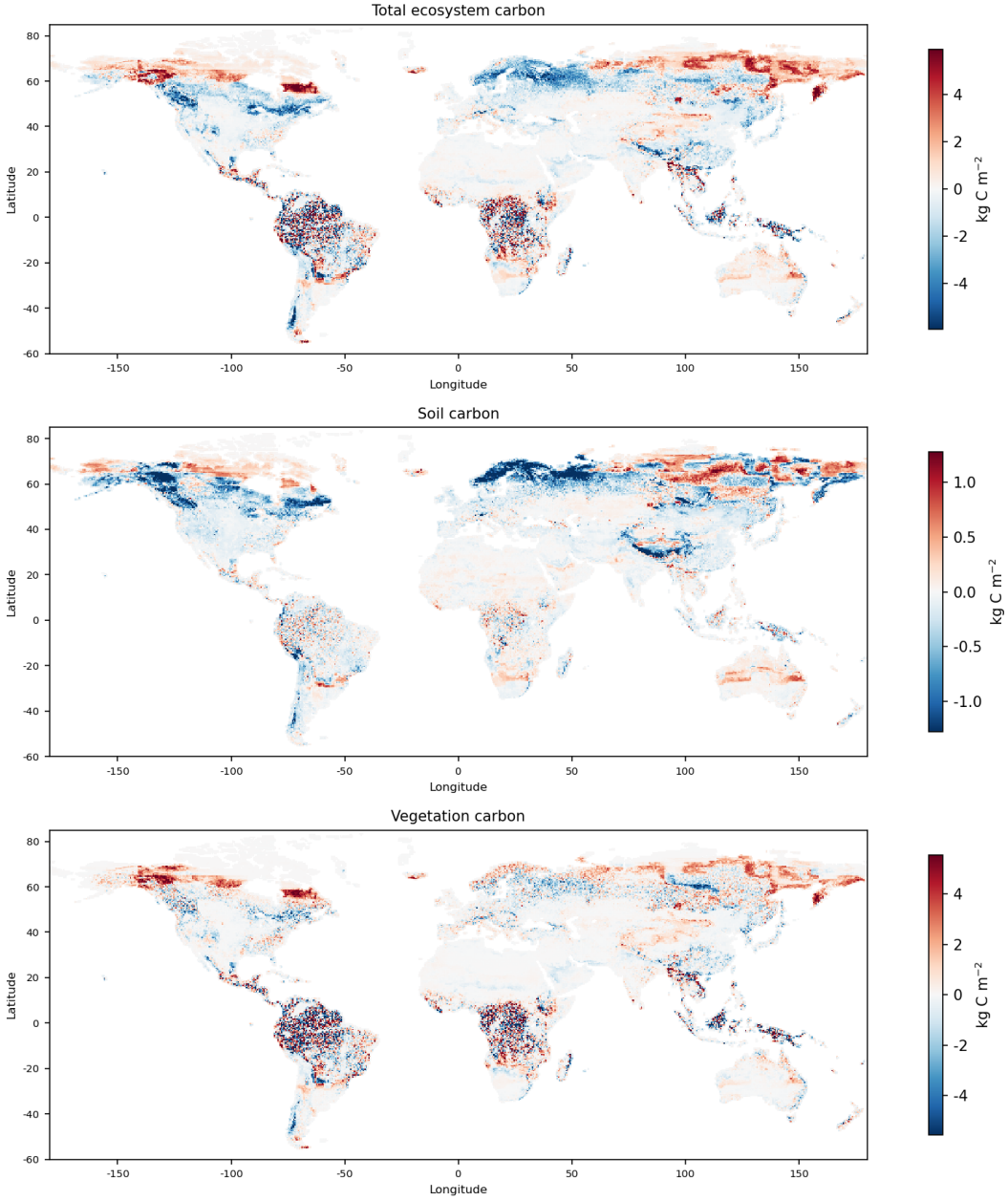
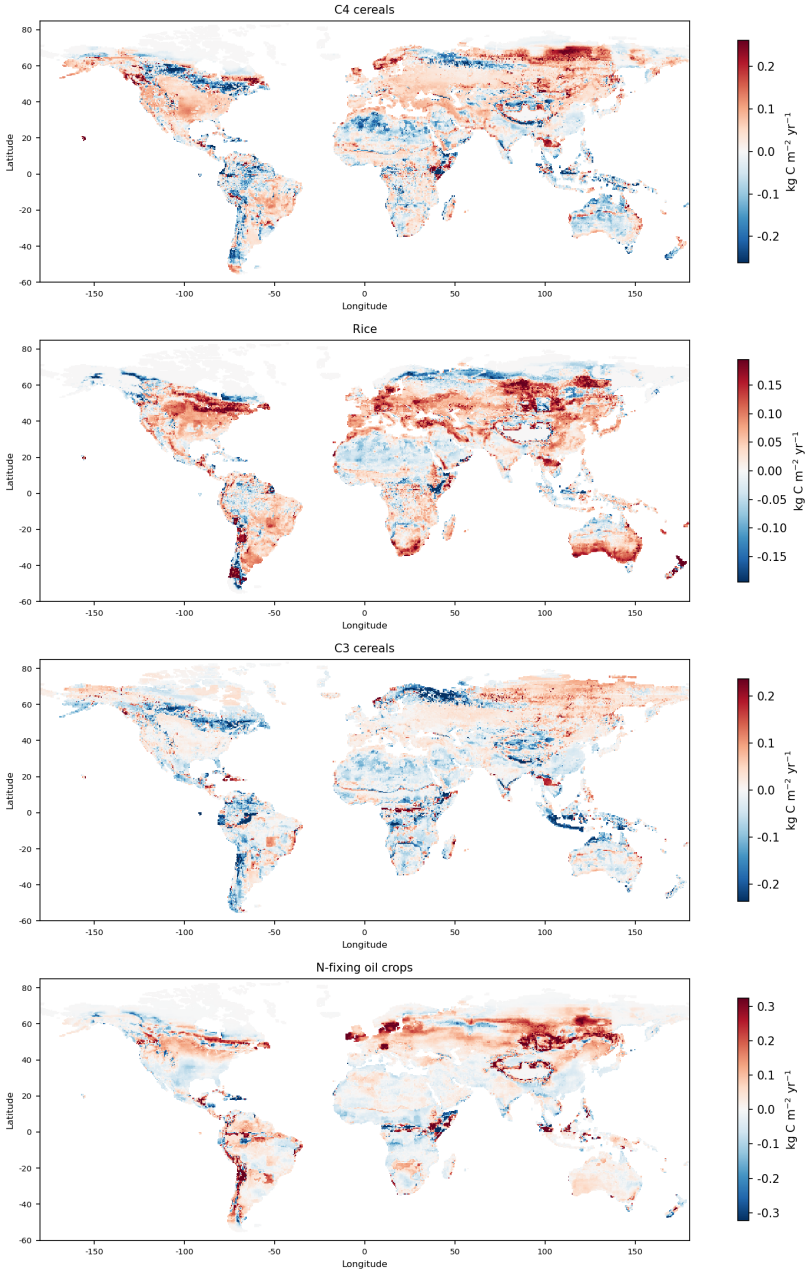
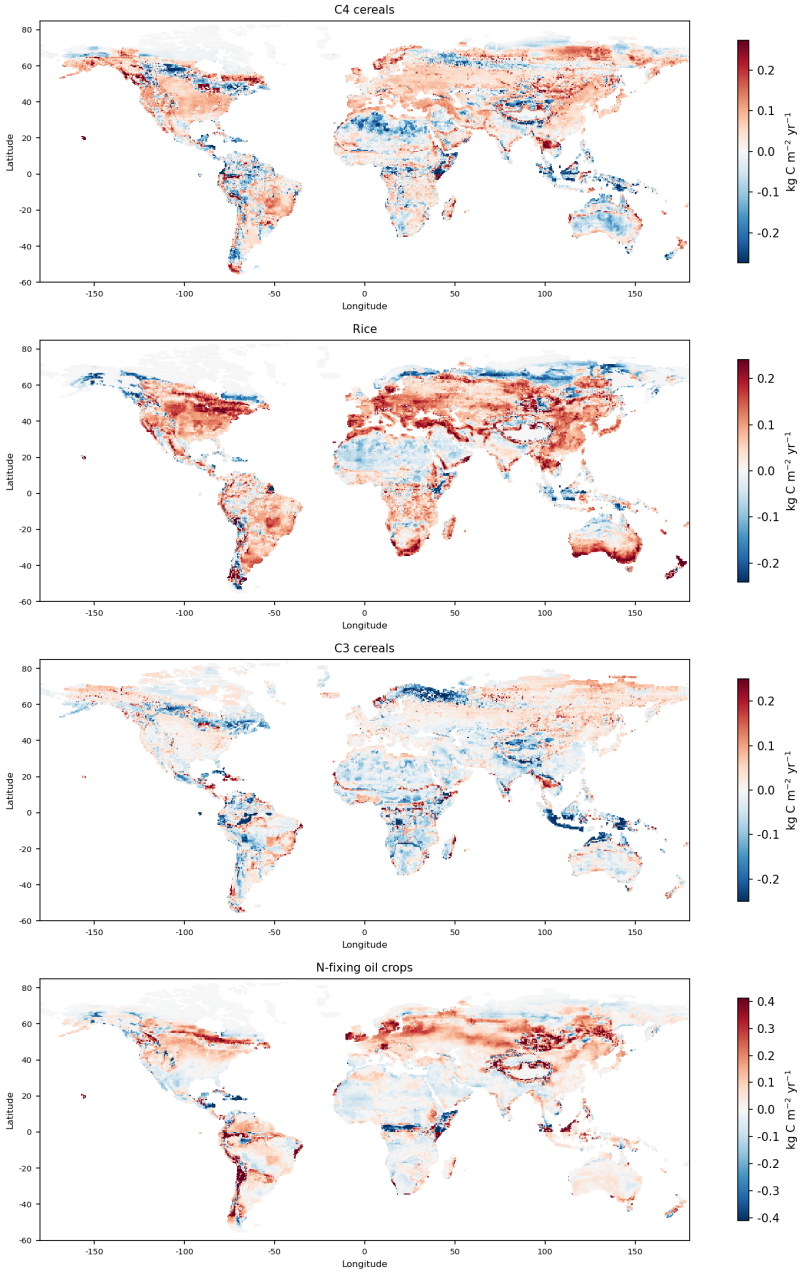


Figure S6. Difference in the present-day-to-end-of-century change (2005-2025 to 2080-2100) in ecosystem carbon (total ecosystem carbon, soil carbon, vegetation carbon), IMOGEN-coupled minus ISIMIP-3b prescribed, for the three intermediate scenarios not shown in the main text: (from top) SSP2-4.5, SSP3-7.0, and SSP4-6.0. As in Fig. 7, differencing the change removes the time-invariant baseline-climatology offset, so the maps show where the two configurations' carbon responses differ; the differences are small and regionally mixed in sign. The bracketing-scenario maps (SSP1-2.6, SSP5-8.5) appear as Fig. 7 of the main text.

Difference in the present-day-to-end-of-century crop-yield change (IMOGEN-coupled - ISIMIP-3b), SSP2-4.5 (2005-2025 to 2080-2100)



Difference in the present-day-to-end-of-century crop-yield change (IMOGEN-coupled - ISIMIP-3b), SSP3-7.0 (2005-2025 to 2080-2100)



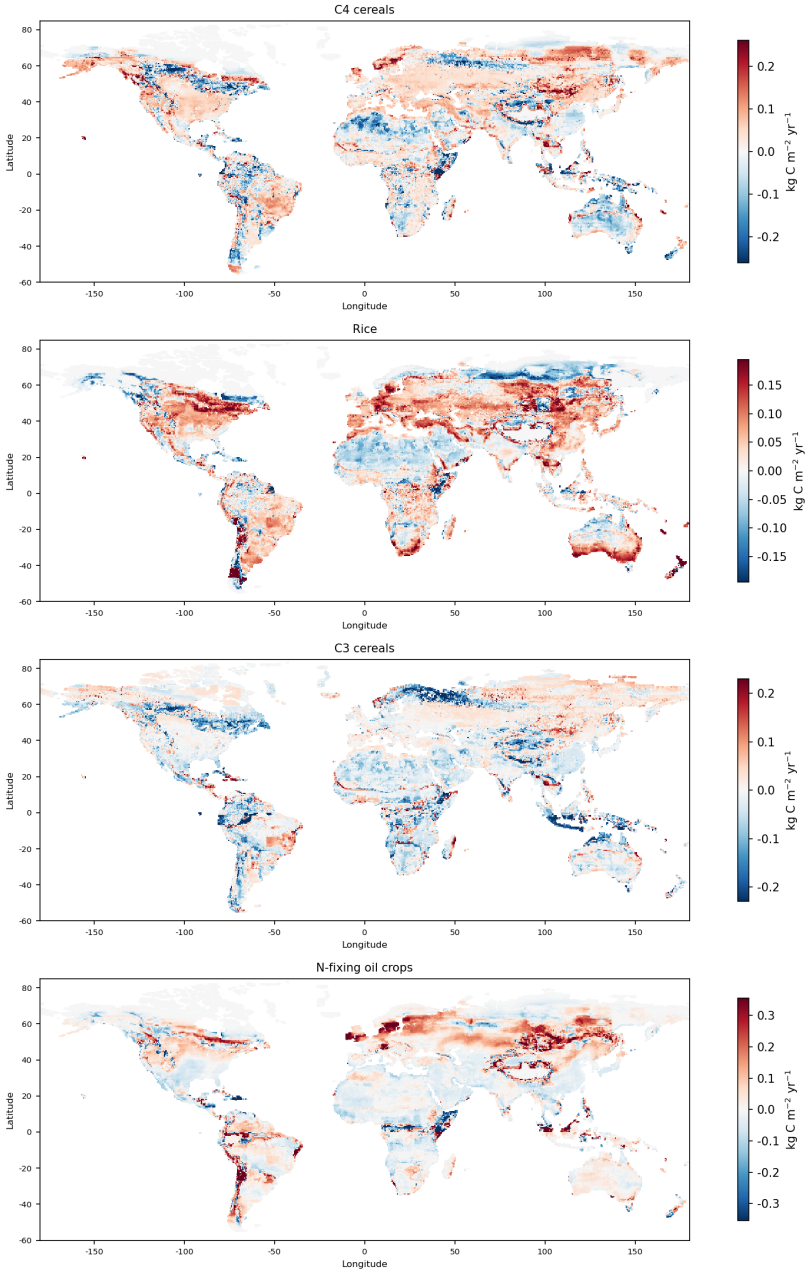


Figure S7. Difference in the present-day-to-end-of-century change (2005-2025 to 2080-2100) in crop yield (C4 cereals, rice, C3 cereals, N-fixing oil crops), IMOGEN-coupled minus ISIMIP-3b prescribed, for the three intermediate scenarios: (from top) SSP2-4.5, SSP3-7.0, and SSP4-6.0. As in Fig. 8, differencing the change removes the time-invariant baseline-climatology offset; the differences are small and regionally mixed in sign. The bracketing-scenario maps appear as Fig. 8 of the main text.

S3.2 Baseline offset and change decomposition

The full-period trajectories (Figs. S8-S18) show that the IMOGEN-coupled and ISIMIP-3b prescribed configurations differ throughout the simulation rather than agreeing in the historical period and diverging thereafter, because the coupled configuration is driven by the IMOGEN-emulated climate over the full 1901-2100 period (Sect. 2.4). For the global total ecosystem carbon a persistent baseline offset of +624 Pg C is present already in 1901 – reflecting the regional mean-state difference between the observation-based baseline climatology and the reference (Sect. 3.3) rather than a scenario feedback – and it is essentially unchanged over the historical period (+626 Pg C by 2020). The scenario-period change is small and weakly negative (an order of magnitude smaller than the persistent offset; quantified for all variables in Table S3). The end-of-century difference reported in the main text (Table 13; Sect. 3.4) is therefore dominated by the persistent mean-state offset, with only a small scenario-period change; the bottom-up-emission-pathway component of that change is isolated at the climate level by the identical-emulator diagnostic (Sect. 4.4, 4.5).

This decomposition generalises to all ecosystem-state variables in Table S3: the initial baseline offset is present at the present-day reference and is essentially scenario-independent, whereas the difference in the present-day-to-end-of-century change between the two configurations (Δ_{chg} = coupled change – prescribed change) is, for every variable, small relative to that offset and to each configuration's own change (Table 13). The projected changes therefore track closely between the two climate baselines, so the large absolute offset is a spin-up artefact of the baseline-climatology choice rather than a coupling signal.

Table S3. Change-based decomposition for all ecosystem-state variables, present-day reference (2005-2025) to end of century (2080-2100), consistent with the main-text Table 13. For each variable: the initial baseline offset (IMOGEN-coupled minus ISIMIP-3b at the present-day reference, scenario-mean) and the difference in the change between the two configurations (Δ_{chg}) for each SSP-RCP scenario. Carbon and nitrogen pools and fluxes are global totals (Pg C, Pg N, Pg C yr^{-1}); the per-area intensities are in their native units, as in Table S2. The initial offset is quoted at the present-day reference (2005-2025); for total ecosystem carbon it is +627 Pg C here and +624 Pg C at 1901, i.e. essentially time-invariant. The Δ_{chg} values use the same 2005-2025 to 2080-2100 window as the main-text Table 13.

Variable	Unit	Initial offset	Δ_{chg} SSP1-2.6	SSP2-4.5	SSP3-7.0	SSP4-6.0	SSP5-8.5
Total ecosystem C	Pg C	+627	-16.6	-21.1	-11.5	-13.3	-26.3
Soil C	Pg C	+402	-8.4	-12.2	-12.6	-11.1	-16.1
Litter C	Pg C	+122	-4.9	-10.9	-8.7	-8.7	-15.8
Vegetation C	Pg C	+103	-2.7	+2.4	+10.1	+7.0	+6.0
Net primary production	Pg C yr^{-1}	+10.6	-2.0	-1.2	-0.7	-1.6	-1.4
Net land-atmosphere C flux (F_{net})	Pg C yr^{-1}	-0.1	+0.2	+0.7	+0.5	+0.7	+0.9
Total nitrogen pool	Pg N	+40.3	-0.5	-0.8	-0.9	-0.7	-1.0
Soil N_2O	kg N ha^{-1} yr^{-1}	+0.013	+0.054	+0.047	-0.039	+0.013	+0.033
Nitrogen leaching	kg N ha^{-1} yr^{-1}	-1.326	+0.473	+0.211	+0.272	+0.236	+0.483

Variable	Unit	Initial offset	Δ_{chg} SSP1-2.6	SSP2-4.5	SSP3-7.0	SSP4-6.0	SSP5-8.5
Wetland CH_4	g CH_4 m^{-2} yr^{-1}	+0.173	-0.018	-0.006	+0.001	-0.015	+0.007
Leaf area index	m^2 m^{-2}	+0.420	-0.077	-0.034	-0.017	-0.038	-0.027
Total runoff	mm yr^{-1}	-135	-6.7	-13.7	-1.5	-6.3	-4.0
C4 cereal yield	kg C m^{-2} yr^{-1}	-0.006	+0.010	+0.021	+0.029	+0.022	+0.042
Rice yield	kg C m^{-2} yr^{-1}	+0.021	+0.003	+0.021	+0.043	+0.018	+0.086
C3 cereal yield	kg C m^{-2} yr^{-1}	-0.013	+0.004	+0.008	+0.005	+0.004	+0.009
N-fixing oil-crop yield	kg C m^{-2} yr^{-1}	+0.084	-0.002	+0.012	+0.032	+0.002	+0.043

S3.3 Global full-period trajectories by output

Figures S8-S18 show, for each ecosystem-state output, the global trajectories (1901-2100) of every reported column for all five SSP-RCP scenarios, as the area-weighted mean (native units) and the global total (Pg C, Pg N, Tg N yr^{-1}, Tg CH_4 yr^{-1}, or km^3 yr^{-1}). For the per-land-cover carbon (Fig. S9) and net-primary-production (Fig. S10) components, the global total is the within-land-cover density weighted by the land-cover area fraction taken from the harmonised land-use forcing (Sect. S6), so the four land-cover totals sum to the gridcell total; the per-crop yields are shown as the production-weighted mean (weighted by harvested area = crop-fraction x cropland x cell area). In all panels the solid line is the ISIMIP-3b prescribed configuration and the dashed line the IMOGEN-coupled configuration; the dotted vertical line marks the 2020 historical-scenario land-use transition. The net primary production (Fig. S10) and crop-yield (Fig. S12) figures are shown over the internally consistent scenario period (2022-2100). Per-scenario four-panel composites (carbon pools, carbon fluxes, nitrogen pools, nitrogen fluxes) equivalent to the bracketing-scenario main-text Figs 9 and 10 are provided for the three intermediate scenarios in Section S7 (Figs S24-S26).

Table S4. Scenario-period (2022-2100) time-mean crop-yield difference (IMOGEN-coupled – ISIMIP-3b prescribed; kg C m^{-2} yr^{-1}, production-weighted by harvested area: crop-fraction x cropland x cell area) for all five SSP-RCP scenarios. These summarise the yield trajectories of Fig. S12 over the internally consistent scenario period, complementing the end-of-century statistics of Tables 13 and S2.

Crop	SSP1-2.6	SSP2-4.5	SSP3-7.0	SSP4-6.0	SSP5-8.5
C3 cereals	-0.007	-0.009	-0.011	-0.010	-0.009
C4 cereals	-0.002	+0.005	+0.008	+0.006	+0.011
Rice	+0.024	+0.032	+0.039	+0.039	+0.059
N-fixing oil crops	+0.076	+0.088	+0.099	+0.091	+0.103
Other oil crops	-0.007	-0.007	-0.015	-0.009	-0.009
Pulses	+0.050	+0.070	+0.082	+0.078	+0.090

Table S5. Scenario-period (2022-2100) time-mean net-primary-production difference (IMOGEN-coupled – ISIMIP-3b prescribed; kg C m^{-2} yr^{-1}) by land cover, for all five SSP-RCP scenarios. Each per-land-cover value is the mean within-stand NPP density (per unit area of that land cover), area-weighted across gridcells by that land cover's extent; the gridcell Total is the area-weighted mean of the whole-gridcell density. Because the per-land-cover entries and the Total use different area normalisations, the four land-cover values are not expected to sum to the Total.

NPP component	SSP1-2.6	SSP2-4.5	SSP3-7.0	SSP4-6.0	SSP5-8.5
Total (gridcell)	+0.067	+0.072	+0.076	+0.075	+0.073
Natural	+0.081	+0.088	+0.095	+0.092	+0.090
Cropland	+0.012	+0.014	+0.015	+0.017	+0.015
Pasture	+0.095	+0.102	+0.106	+0.105	+0.105
Wetland	+0.086	+0.085	+0.084	+0.084	+0.079

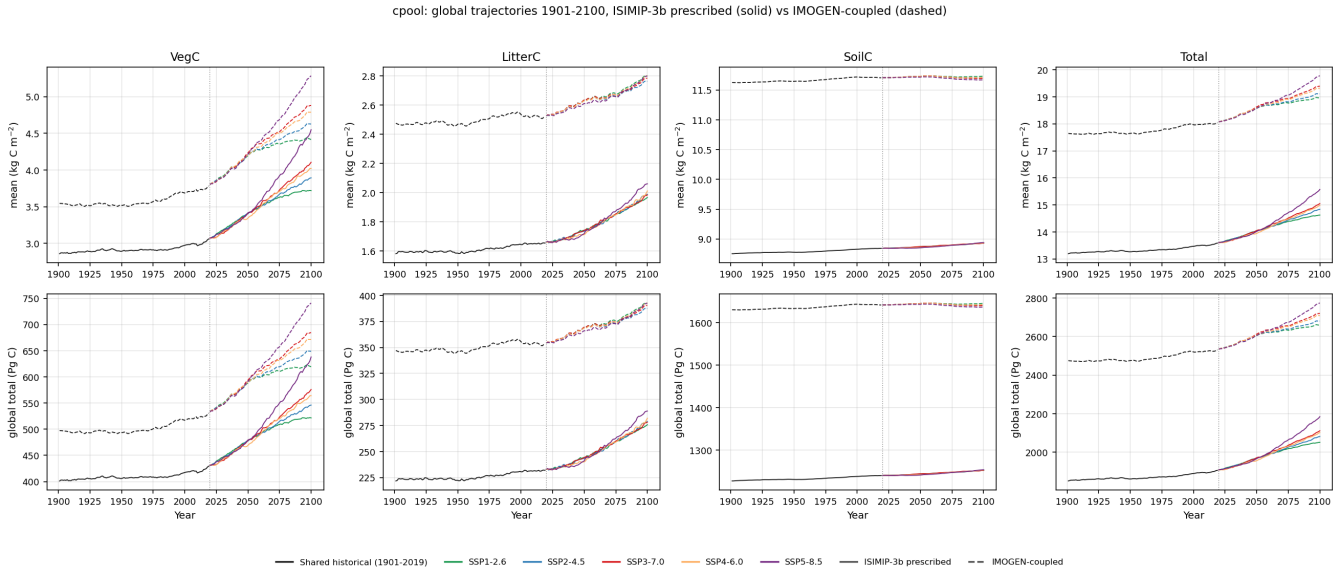


Figure S8. Carbon pools (cpool): VegC, LitterC, SoilC, and total.

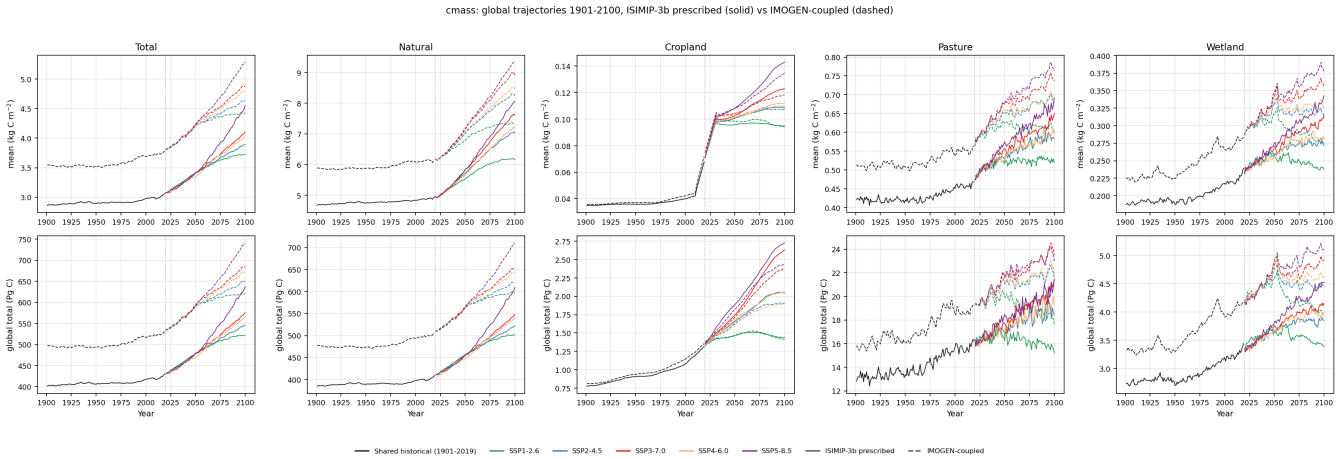


Figure S9. Vegetation carbon by land cover (cmass): the gridcell total and the natural, cropland, pasture, and wetland components, shown as the within-land-cover area-weighted mean density (top row) and the global total (bottom row). The per-land-cover global totals are obtained by weighting each density by its land-cover area fraction from the harmonised land-use forcing (Sect. S6), so the four land-cover totals sum to the gridcell total. The cropland component is drawn with a 21-year running mean for legibility. The modest residual step around 2020 in the cropland component reflects the historical-to-scenario crop-management forcing handover (the static crop-type mix and fertiliser switching to the time-varying PLUM values in

2021); it is present near-identically in both configurations, and is therefore a land-management-forcing feature rather than a coupling or climate signal.

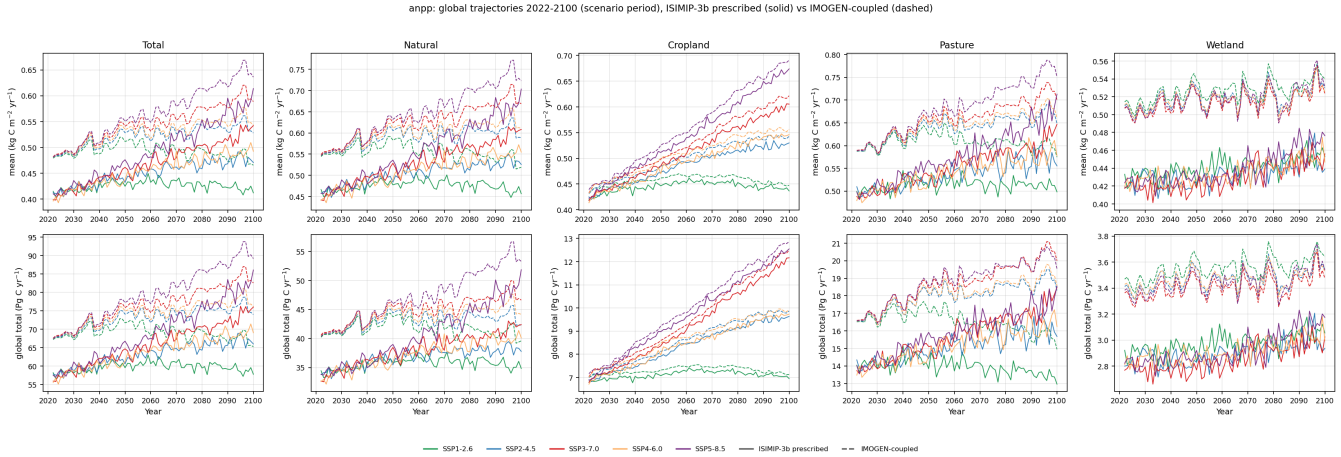


Figure S10. Net primary production (anpp): the gridcell total and the natural, cropland, pasture, and wetland components, shown (top row) as the gridcell area-weighted mean for the total and, for each land cover, the land-cover-area-weighted mean of the within-stand density (per unit area of that land cover, and therefore not additive to the gridcell total), and (bottom row) the global total (per-land-cover totals weighted by land-cover area fraction as in Fig. S9). Shown over the scenario period (2022-2100).

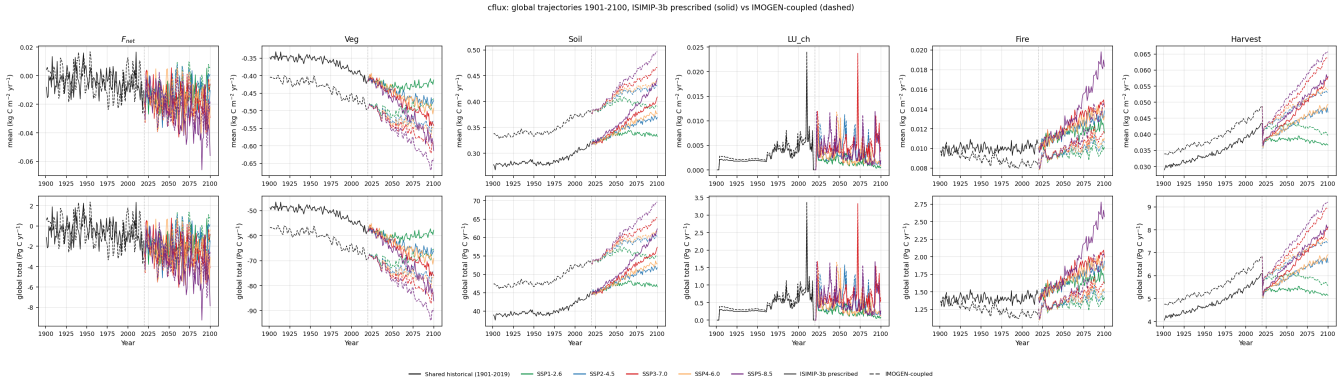


Figure S11. Carbon fluxes (cflux): F_{net} (net land-atmosphere C flux), vegetation uptake, soil respiration, land-use change, fire, and harvest.

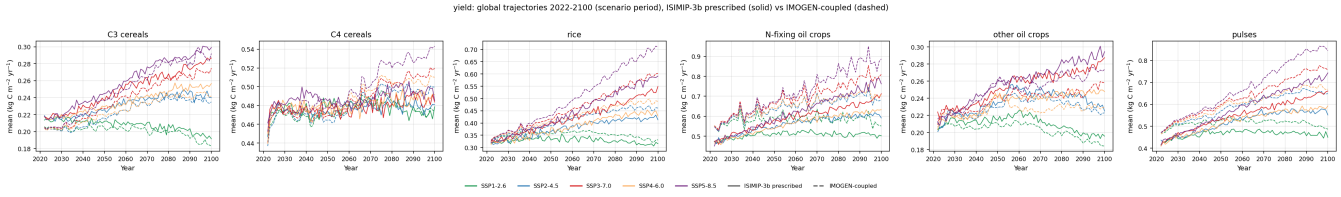


Figure S12. Crop yields (yield): C3 cereals, C4 cereals, rice, N-fixing oil crops, other oil crops, and pulses, shown as the production-weighted mean (weighted by harvested area = crop-fraction x cropland x cell area). Shown over the scenario period (2022-2100).



Figure S13. Nitrogen pools (npool): VegN, LitterN, SoilN, and total.

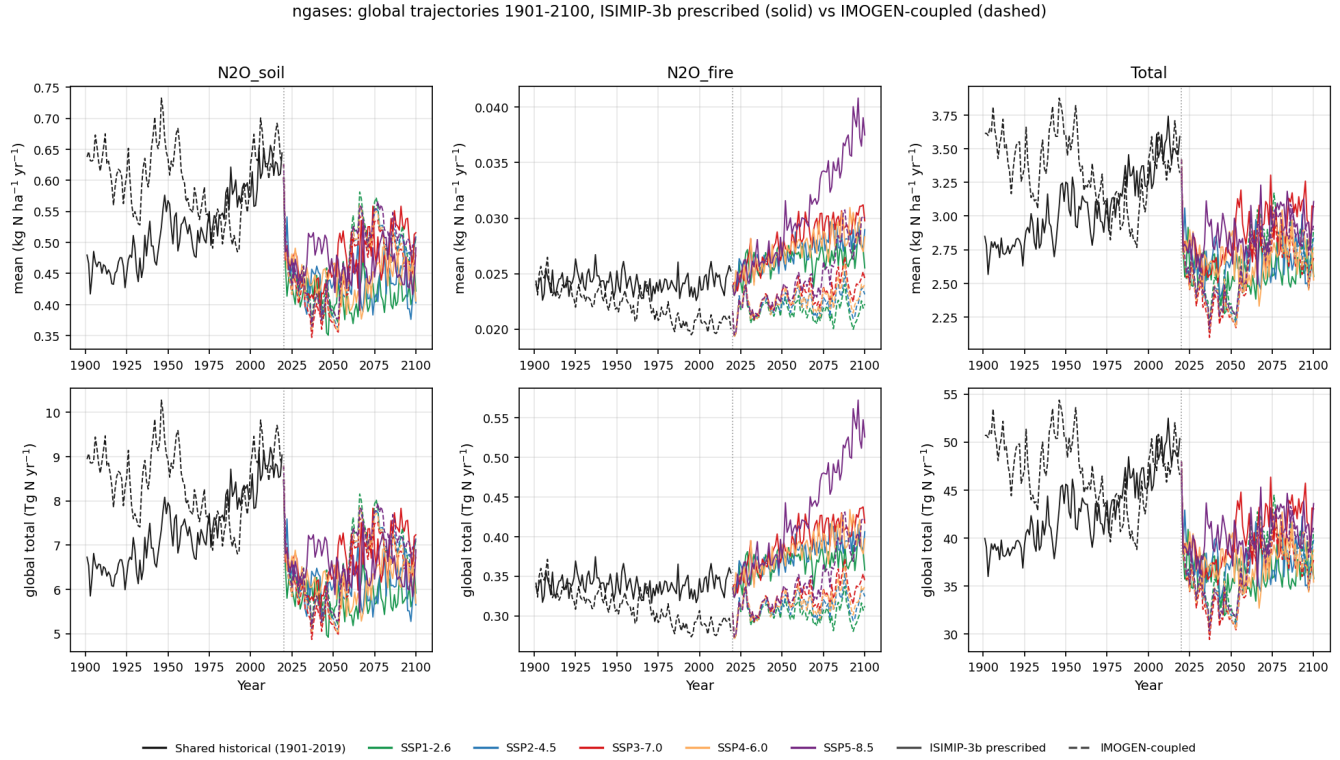


Figure S14. Nitrogen gases (ngases): soil N_2O, fire N_2O, and the total soil gaseous-nitrogen loss (the "Total" panel is N_2+N_2O+NO+NH_3, not total N_2O).

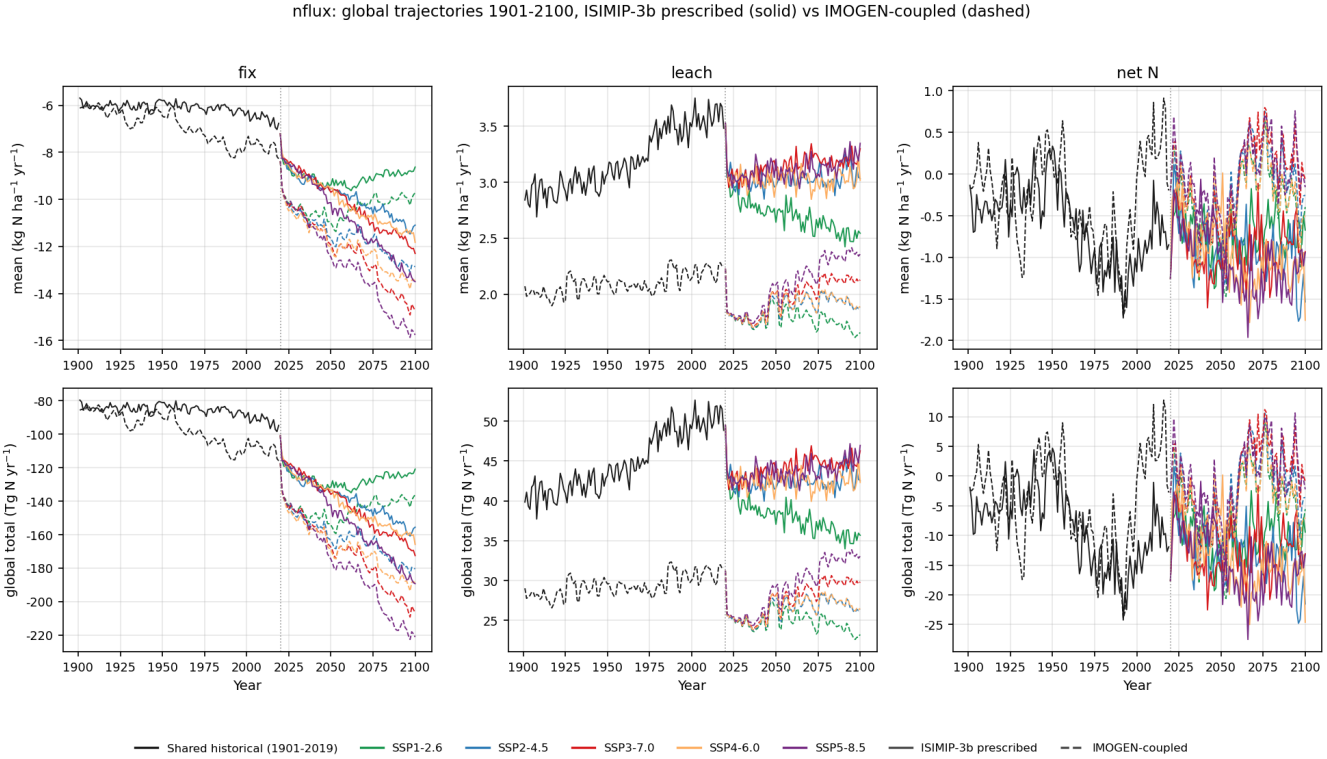


Figure S15. Nitrogen fluxes (nflux): fixation, leaching, and net exchange (net N).

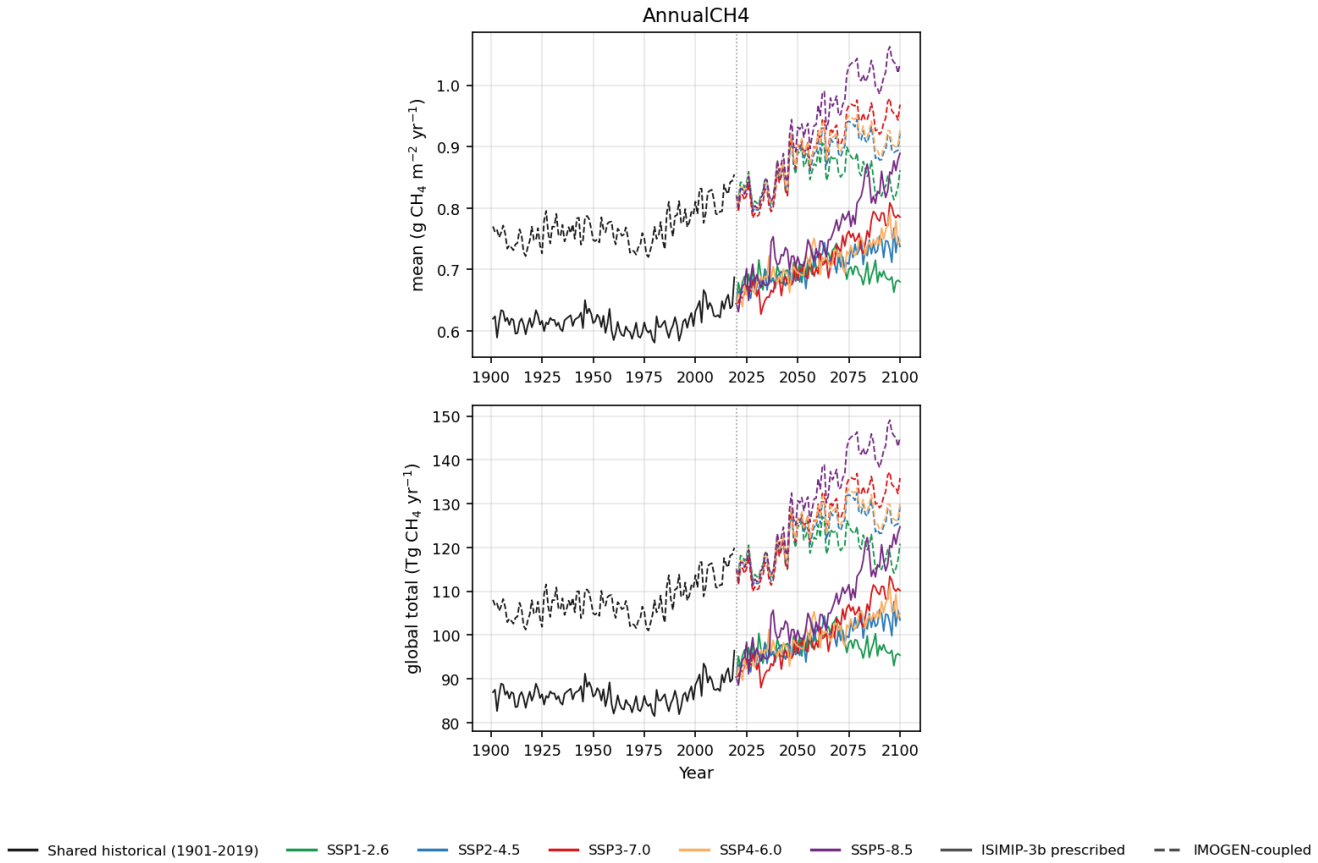


Figure S16. Wetland methane (mch4): annual CH_4 flux, computed by the LPJ-GUESS wetland (LPJ-WHyMe/Spahni) scheme over the time-invariant GLWD3 wetland mask (Sect. 2.2.7). The static-area treatment is a conservative, transparent choice (wetland-area dynamics are an open problem across Earth system models); combined with the prescribed inland-freshwater and reservoir terms, the resulting integrated CH_4 reconciles with the Global Methane Budget to within a few per cent and reproduces the observed concentration (Table 10; Fig. 4b), so the constant area does not inflate the total natural source.

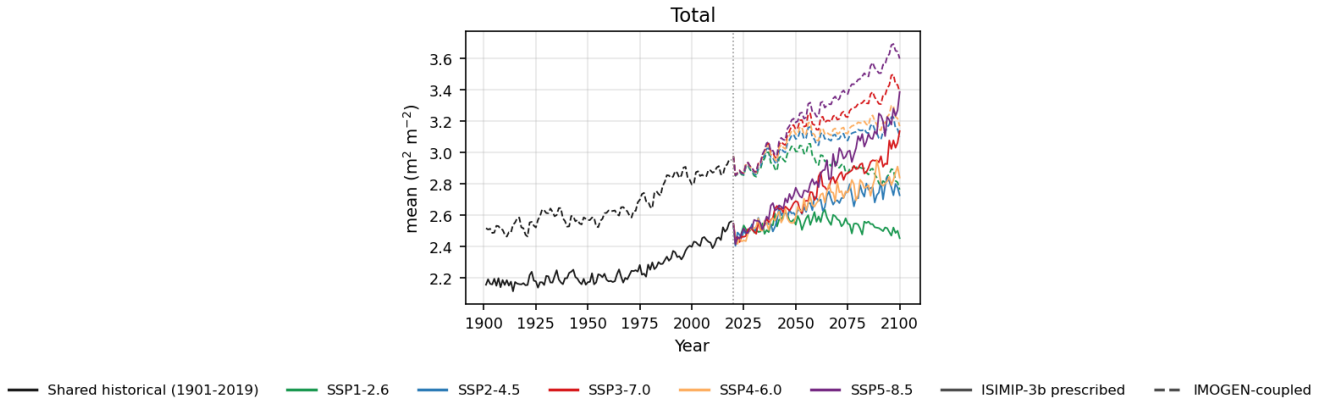


Figure S17. Leaf area index (lai): total (area-weighted mean only).

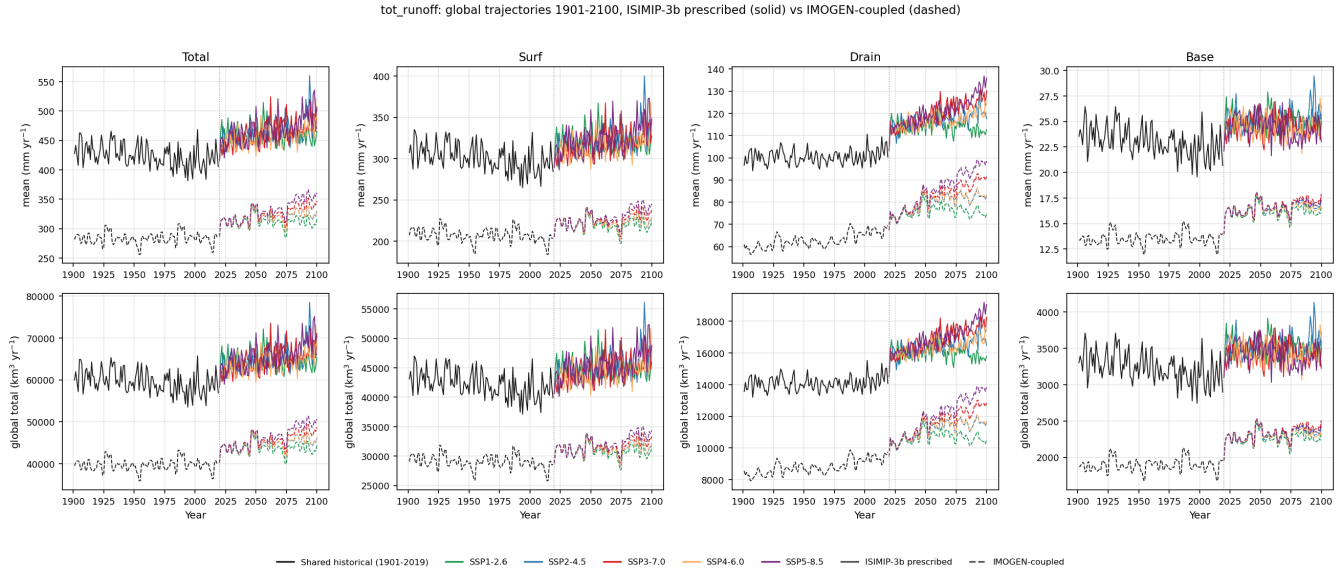


Figure S18. Total runoff (tot_runoff): total, surface, drainage, and baseflow.

S4 Identical-emulator diagnostic: emission-pathway feedback on temperature

The identical-emulator diagnostic (Sect. 4.4) isolates the emission-pathway feedback on the emulated climate by running the IMOGEN engine twice for each bracketing scenario: once forced by the framework's integrated emissions (the coupled configuration) and once by the unmodified RCMIP+FaIR emissions (the control), with all other inputs and the pattern and energy-balance calibration held fixed. Because both arms pass through the identical emulator, the emulator's mean-state and transient-response terms cancel in the difference, leaving the emission-pathway signal. The feedback is reported as the area-weighted (cosine-latitude) global-land-mean of the annual-mean field over the three analysis windows.

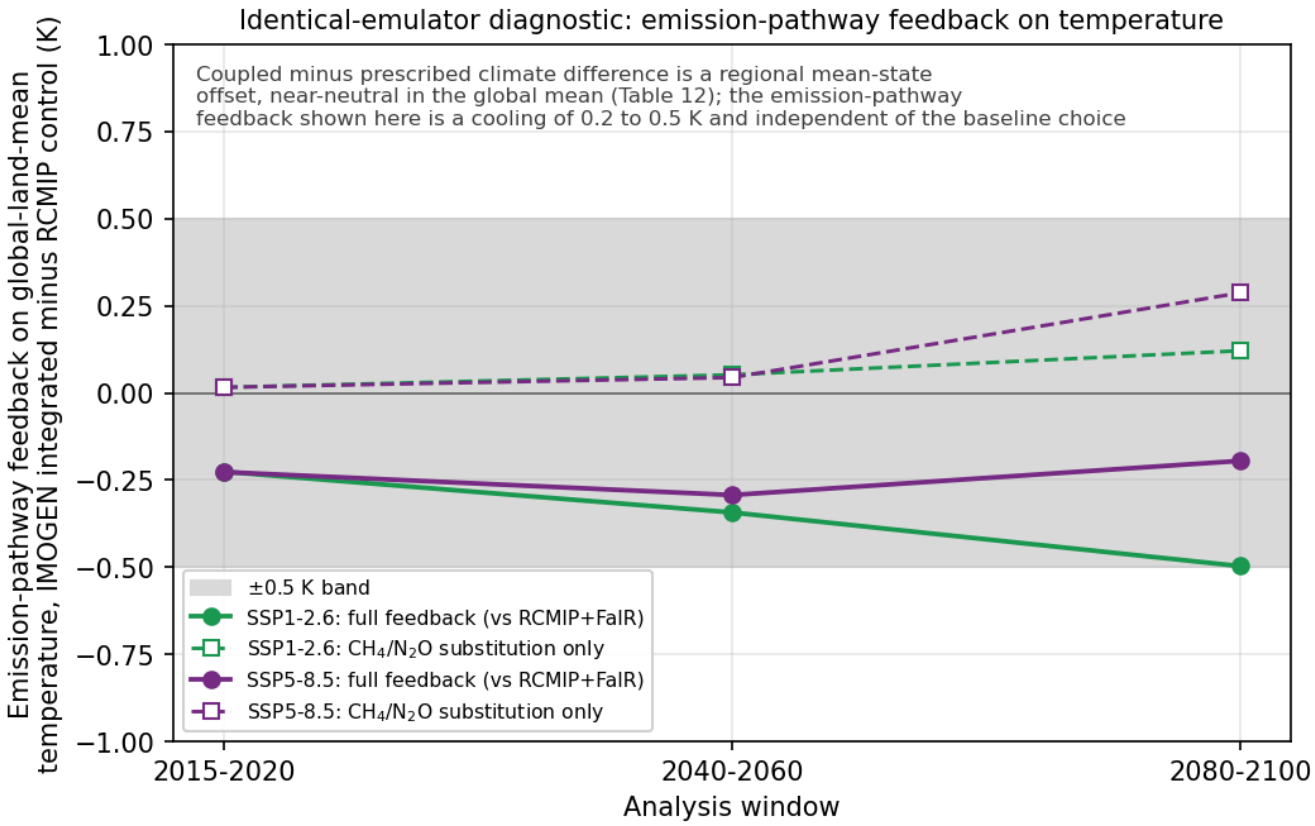


Figure S19. Emission-pathway feedback on global-land-mean near-surface temperature (IMOGEN forced by the integrated emissions minus IMOGEN forced by the unmodified RCMIP+FaIR emissions), for the two bracketing scenarios over the three analysis windows. The full feedback (solid; against the RCMIP+FaIR reference of Sect. 3.2.1) is a cooling of 0.2 to 0.5 K; the variant isolating only the CH_4/N_2O Tier-1 substitution (dashed) is a warming (≤ 0.3 K), more than offset by the CO_2 land-sink cooling in the full feedback. The full-feedback cooling is somewhat larger under SSP1-2.6 (about -0.5 K by end of century) than under SSP5-8.5 (about -0.2 K), consistent with the diminishing marginal radiative effect of the land-sink CO_2 difference as the background CO_2 concentration rises. The residual coupled-versus-prescribed climate difference is a regional mean-state difference from the observation-based baseline choice (Sect. 3.3), near-neutral in the global mean, rather than an emission-pathway feedback.

Table S6. Identical-emulator diagnostic: emission-pathway feedback on global-land-mean near-surface temperature (K), by scenario and window. The full feedback is IMOGEN(integrated) – IMOGEN(RCMIP+FaIR reference); the substitution-only column is IMOGEN(integrated) – IMOGEN(RCMIP anthropogenic + LPJ-GUESS natural), which differs from the full feedback only in the CH_4/N_2O Tier-1 substitution. Negative values denote a cooler integrated-emission climate.

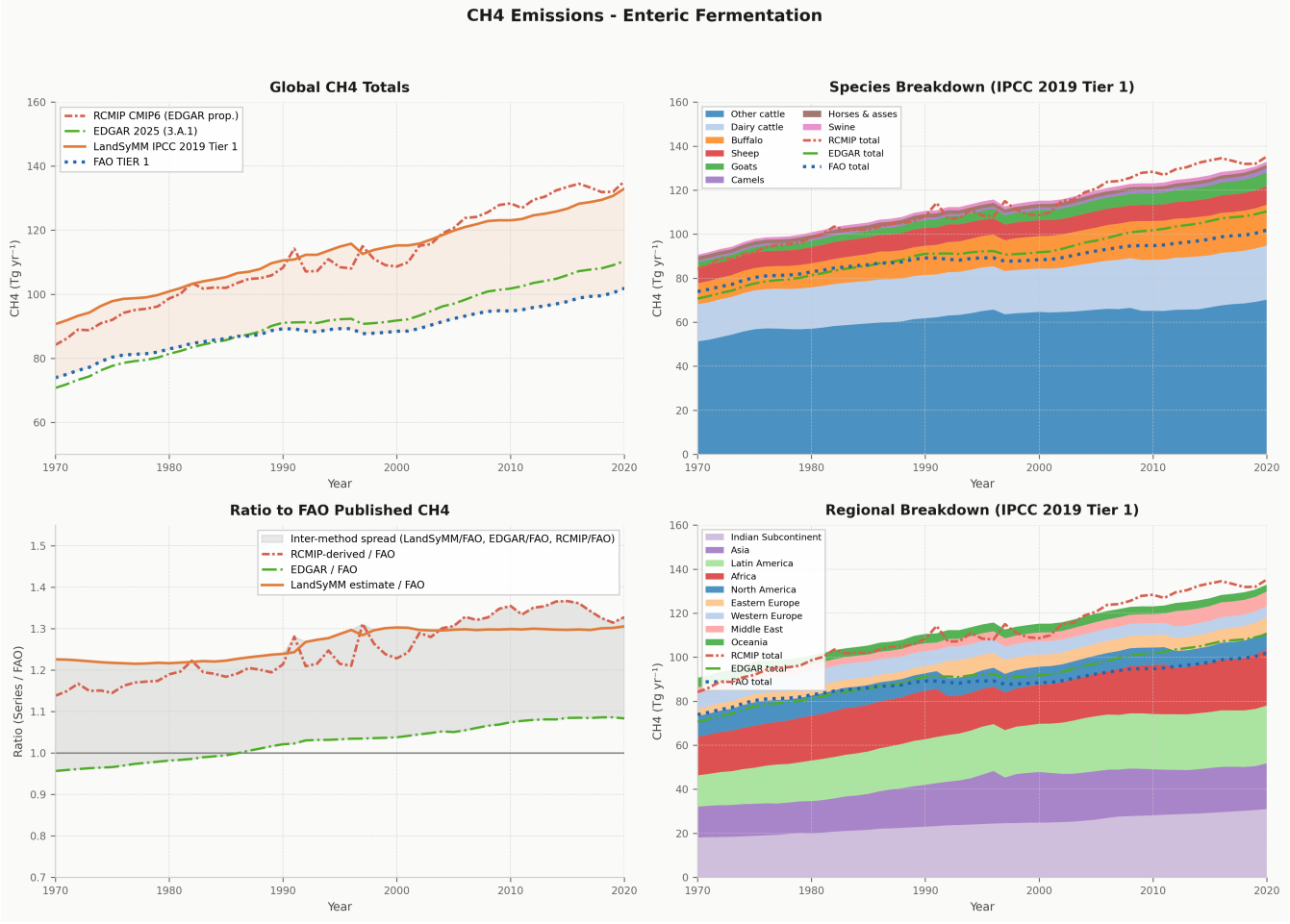
Scenario	Window	Full feedback (K)	Substitution-only (K)
SSP1-2.6	2015-2020	-0.23	+0.02
SSP1-2.6	2040-2060	-0.34	+0.05
SSP1-2.6	2080-2100	-0.50	+0.12
SSP5-8.5	2015-2020	-0.23	+0.02
SSP5-8.5	2040-2060	-0.29	+0.04
SSP5-8.5	2080-2100	-0.20	+0.29

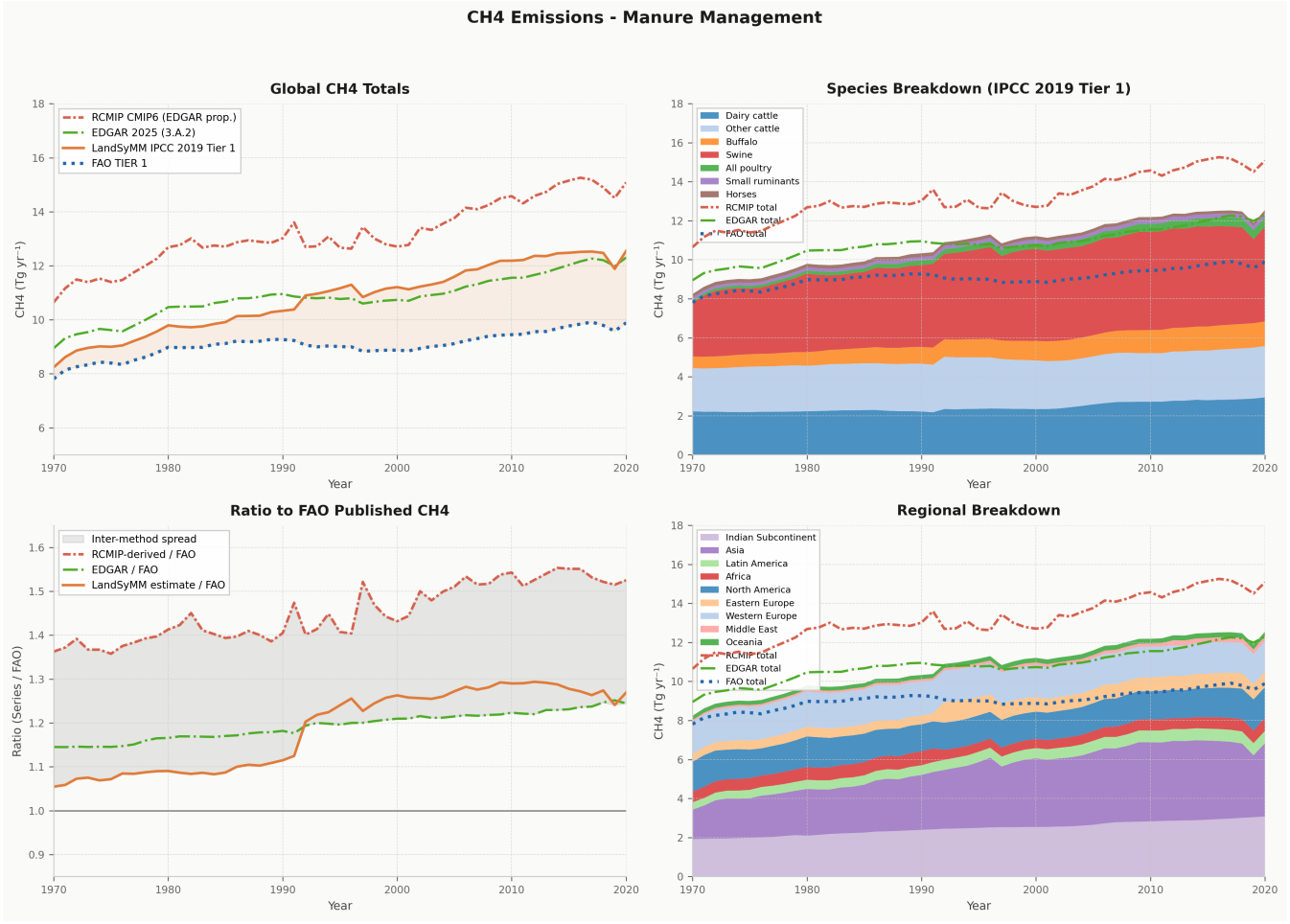
Precipitation feedback is negligible (≤ 0.01 mm day^{-1}); the shortwave-radiation feedback is +0.3 to +0.7 W m^{-2} (full feedback).

S5 Supplementary agricultural- and integrated-emission figures

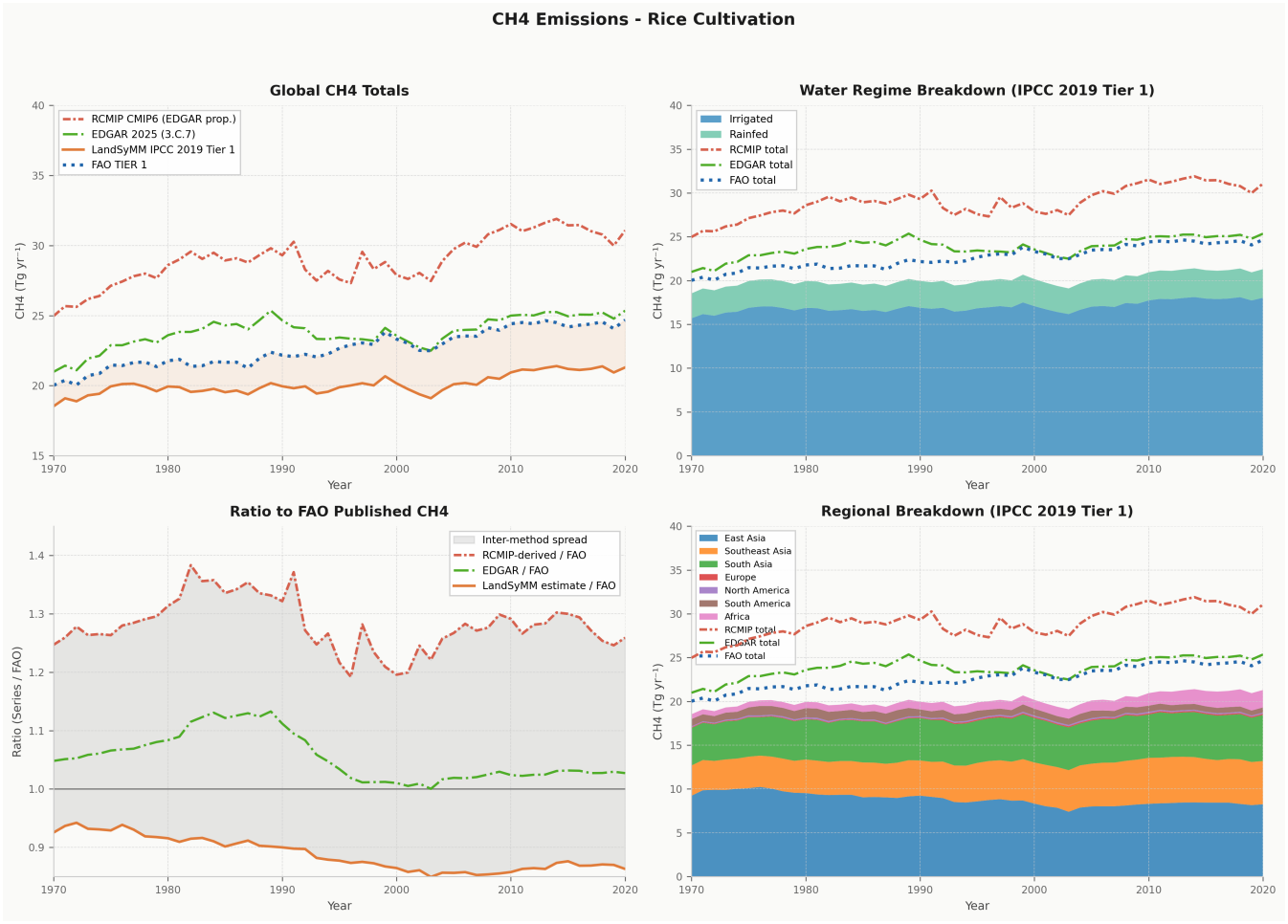
This section provides the detailed source-category breakdowns underlying the historical agricultural-emission evaluation (main Sect. 3.1, Fig. 2, Table 9) and the scenario-baseline reference (Fig. S21) that supplements the observation-anchored integrated-emission trajectories of main Sect. 3.2.1 (Fig. 3).

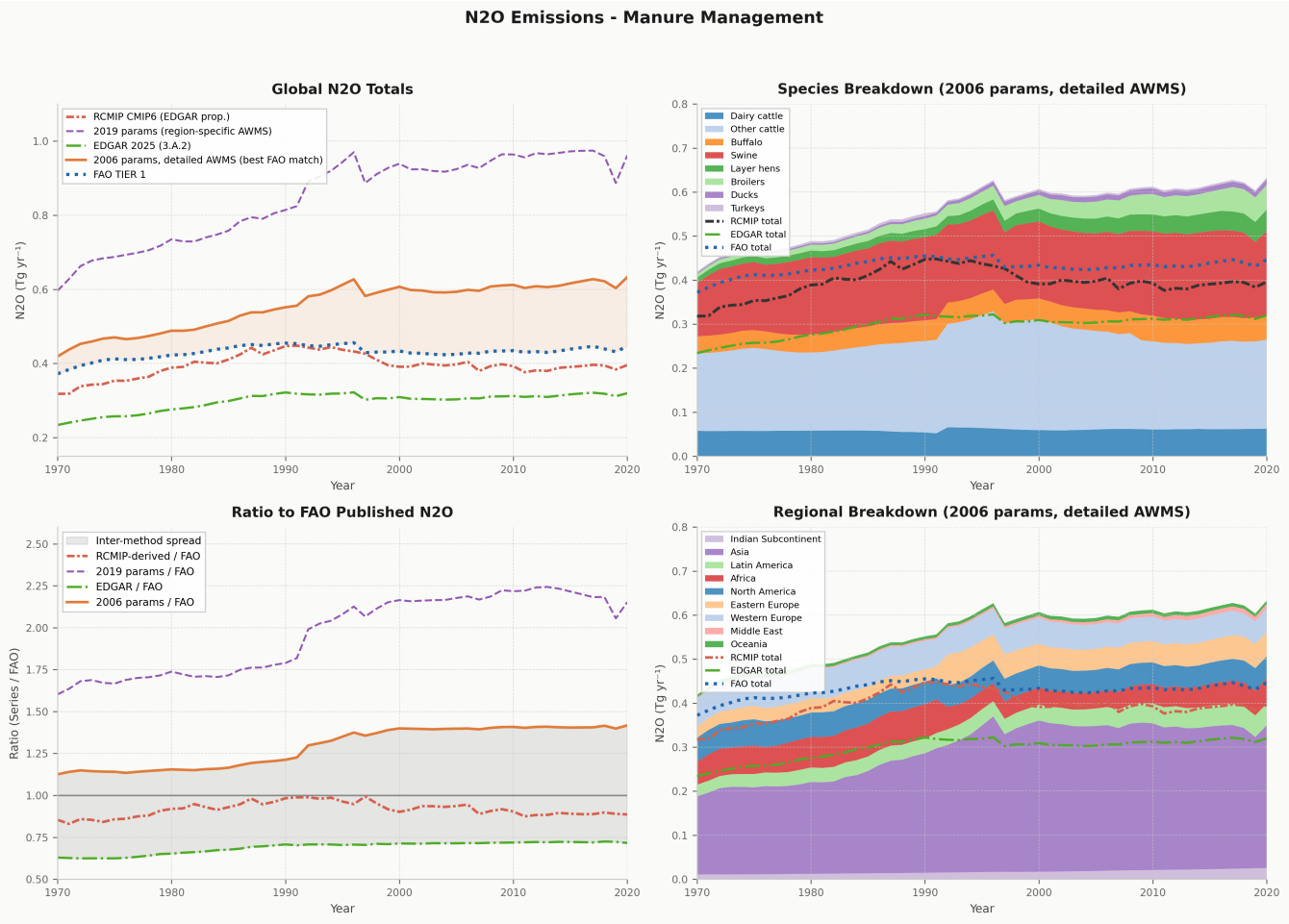
S5.1 Per-category agricultural-emission breakdowns

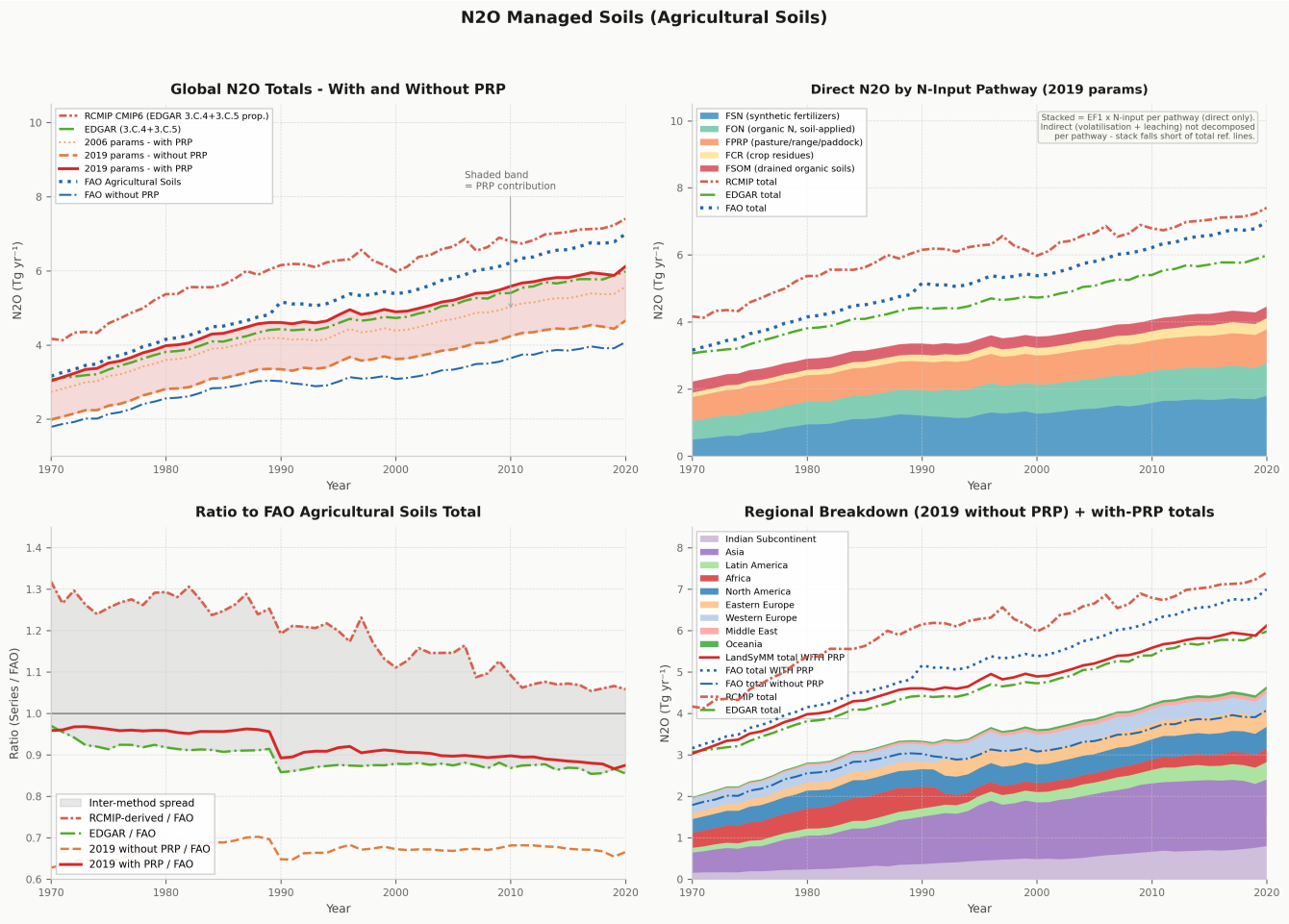



CH4 Emissions - Manure Management
Global CH4 Totals
RCMIP CMIP6 (EDGAR prop.)
EDGAR 2025 (3.A.2)
LandSyMM IPCC 2019 Tier 1
FAO TIER 1
CH4 (Tg yr⁻¹)
Year
Species Breakdown (IPCC 2019 Tier 1)
Dairy cattle
Other cattle
Buffalo
Swine
All poultry
Small ruminants
Horses
RCMIP total
EDGAR total
FAO total
CH4 (Tg yr⁻¹)
Year
Ratio to FAO Published CH4
Inter-method spread
RCMIP-derived / FAO
EDGAR / FAO
LandSyMM estimate / FAO
Ratio (Series / FAO)
Year
Regional Breakdown
Indian Subcontinent
Asia
Latin America
Africa
North America
Eastern Europe
Western Europe
Middle East
Oceania
RCMIP total
EDGAR total
FAO total
CH4 (Tg yr⁻¹)
Year

215


CH4 Emissions - Rice Cultivation
Global CH4 Totals
RCMIP CMIP6 (EDGAR prop.)
EDGAR 2025 (3.C.7)
LandSyMM IPCC 2019 Tier 1
FAO TIER 1
CH4 (Tg yr⁻¹)
Year
Water Regime Breakdown (IPCC 2019 Tier 1)
Irrigated
Rainfed
RCMIP total
EDGAR total
FAO total
CH4 (Tg yr⁻¹)
Year
Ratio to FAO Published CH4
Inter-method spread
RCMIP-derived / FAO
EDGAR / FAO
LandSyMM estimate / FAO
Ratio (Series / FAO)
Year
Regional Breakdown (IPCC 2019 Tier 1)
East Asia
Southeast Asia
South Asia
Europe
North America
South America
Africa
RCMIP total
EDGAR total
FAO total
CH4 (Tg yr⁻¹)
Year


N2O Emissions - Manure Management
Global N2O Totals
RCMIP CMIP6 (EDGAR prop.)
2019 params (region-specific AWMS)
EDGAR 2025 (3.A.2)
2006 params, detailed AWMS (best FAO match)
FAO TIER 1
N2O (Tg yr⁻¹)
Year
Species Breakdown (2006 params, detailed AWMS)
Dairy cattle
Other cattle
Buffalo
Swine
Layer hens
Broilers
Ducks
Turkeys
RCMIP total
EDGAR total
FAO total
N2O (Tg yr⁻¹)
Year
Ratio to FAO Published N2O
Inter-method spread
RCMIP-derived / FAO
2019 params / FAO
EDGAR / FAO
2006 params / FAO
Ratio (Series / FAO)
Year
Regional Breakdown (2006 params, detailed AWMS)
Indian Subcontinent
Asia
Latin America
Africa
North America
Eastern Europe
Western Europe
Middle East
Oceania
RCMIP total
EDGAR total
FAO total
N2O (Tg yr⁻¹)
Year


N2O Managed Soils (Agricultural Soils)
Global N2O Totals - With and Without PRP
RCMIP CMIP6 (EDGAR 3.C.4+3.C.5 prop.)
EDGAR (3.C.4+3.C.5)
2006 params - with PRP
2019 params - without PRP
2019 params - with PRP
FAO Agricultural Soils
FAO without PRP
Shaded band
= PRP contribution
N2O (Tg yr⁻¹)
Year
Direct N2O by N-Input Pathway (2019 params)
FSN (synthetic fertilizers)
FON (organic N, soil-applied)
FPRP (pasture/range/paddock)
FCR (crop residues)
FSOM (drained organic soils)
RCMIP total
EDGAR total
FAO total
Stacked = EF1 x N-input per pathway (direct only).
Indirect (volatilisation + leaching) not decomposed
per pathway - stack falls short of total ref. lines.
Ratio to FAO Agricultural Soils Total
Ratio (Series / FAO)
Inter-method spread
RCMIP-derived / FAO
EDGAR / FAO
2019 without PRP / FAO
2019 with PRP / FAO
Regional Breakdown (2019 without PRP) + with-PRP totals
Indian Subcontinent
Asia
Latin America
Africa
North America
Eastern Europe
Western Europe
Middle East
Oceania
LandSyMM total WITH PRP
FAO total WITH PRP
FAO total without PRP
RCMIP total
EDGAR total

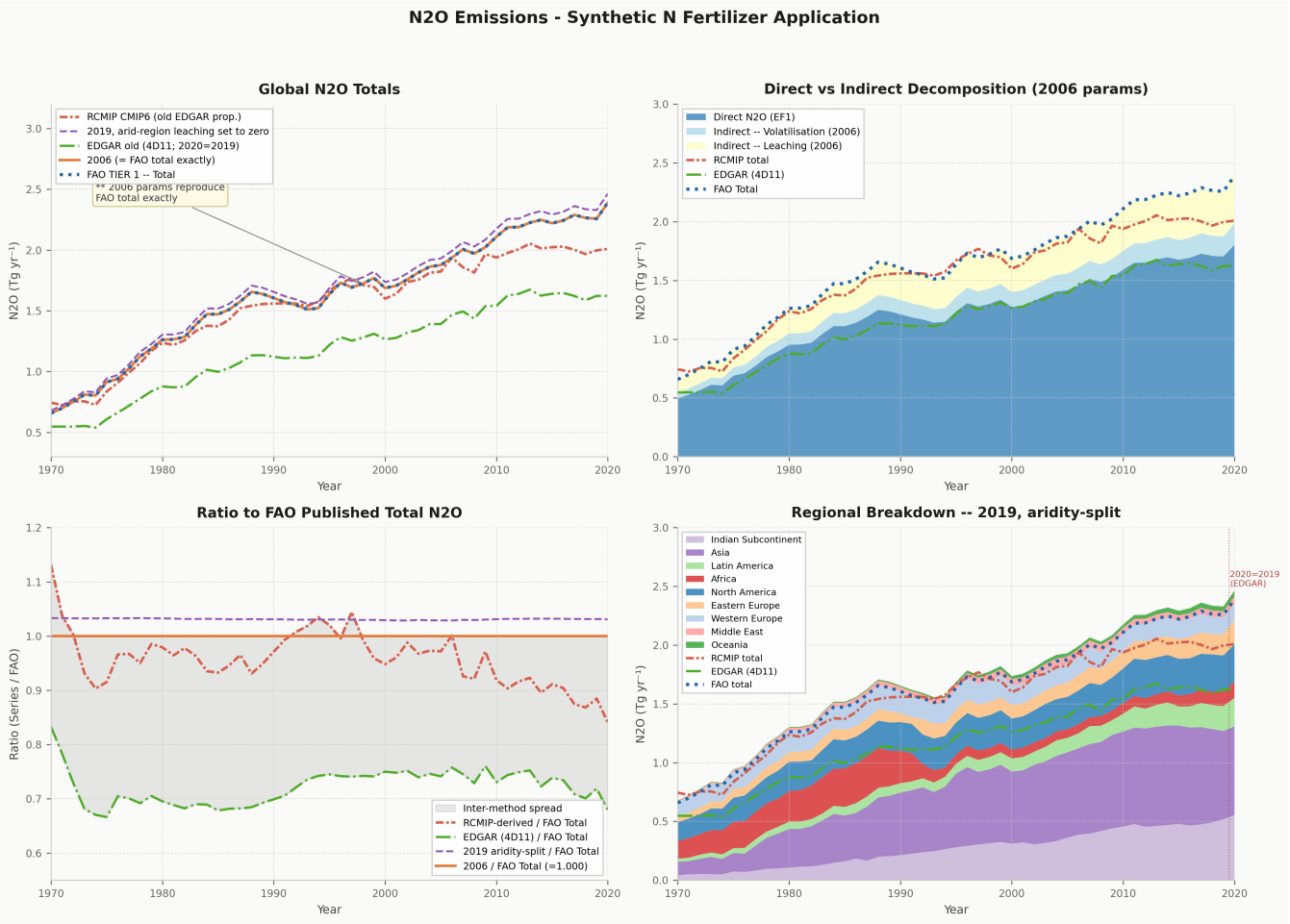


Figure S20. Detailed historical evaluation (1970-2020) of the bottom-up Tier-1 agricultural-emission modules, by source category: (a) enteric-fermentation CH_4, (b) manure-management CH_4, (c) rice-cultivation CH_4, (d) manure-management N_2O, (e) managed-soils N_2O, and (f) the synthetic-fertiliser N_2O sub-component of managed soils. Each panel comprises four sub-plots: the global total (LandSyMM IPCC Tier-1, FAOSTAT, EDGAR 2025, and the RCMIP-derived series; this is the panel reproduced in main Fig. 2); the species or N-input-pathway decomposition of the LandSyMM estimate; the ratio of each series to the FAOSTAT total with the inter-method spread shaded; and the regional decomposition. Manure-management N_2O (d) and managed-soils N_2O (e) show both the 2006 IPCC Guidelines and 2019 Refinement bases; managed soils (e) resolves the five IPCC direct-N_2O input pathways (synthetic fertiliser, organic N, pasture/range/paddock, crop residues, and drained organic soils), of which panel (f) isolates the synthetic-fertiliser (FSN) pathway – the single largest direct managed-soil N_2O source and a primary mitigation lever. Aggregate PBIAS and 2020 totals are reported in main Table 9.

S5.2 Scenario-baseline reference and source decomposition

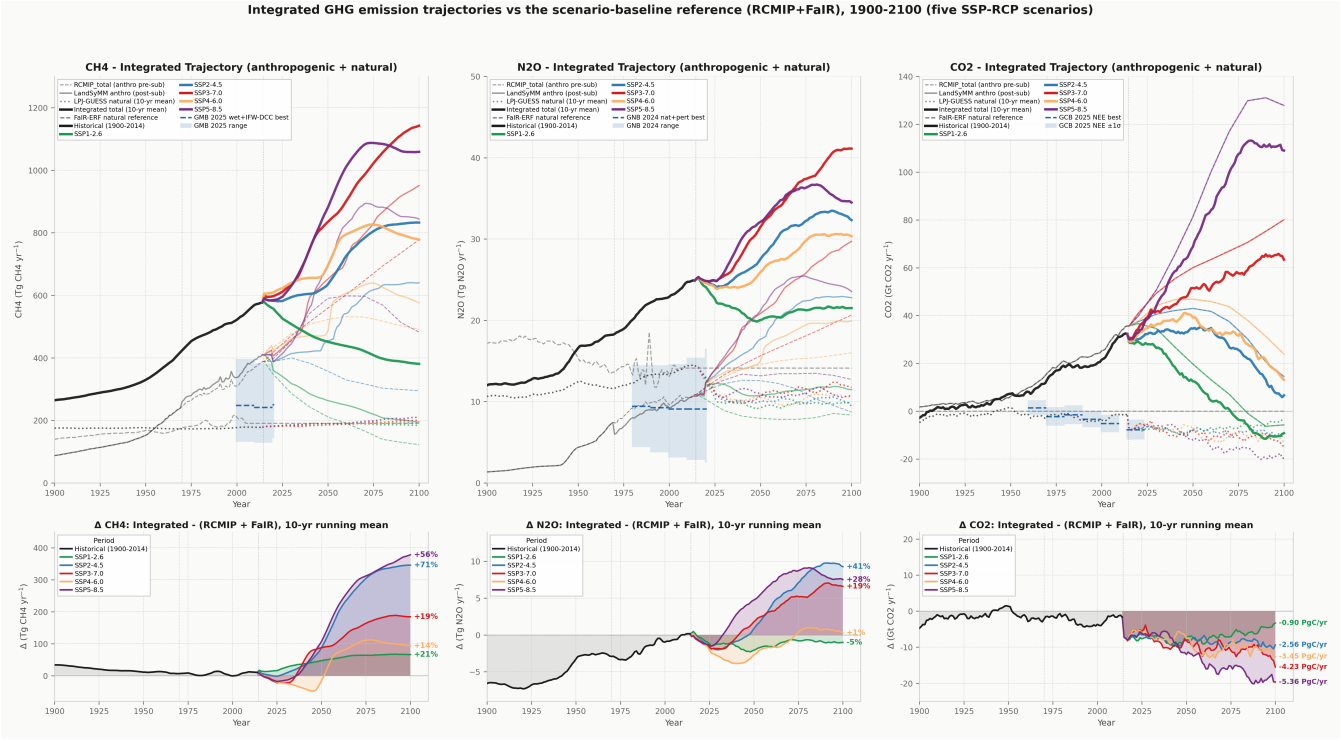


Figure S21. Integrated GHG emission trajectories (anthropogenic + natural), 1900-2100, for the five SSP-RCP scenarios, shown against the scenario-baseline reference (Option A of Sect. 2.3.4; the RCMIP+FaIR trajectory applied throughout, retained as a supplementary diagnostic to the observation-anchored reference of main Fig. 3). Top row: per-gas integrated trajectories with the anthropogenic and natural components decomposed (RCMIP anthropogenic total before substitution, LPJ-GUESS natural flux, the integrated total, and the FaIR effective-radiative-forcing natural baseline), with the observationally constrained global budgets (Global Methane, Nitrous Oxide and Carbon Budgets) overlaid over their observational periods. Bottom row: the difference (integrated minus the RCMIP+FaIR scenario-baseline reference, 10-year running mean) by scenario, with 2100 values annotated. For CH_4 and N_2O the scenario-period divergence is the same as for the observation-anchored reference (main Fig. 3), since the two references coincide outside the 1980-2020 anchored window; for CO_2 they differ, because the observation-anchored reference applies a land-sink (SLAND) correction (Sect. 2.3.4), so against this scenario-baseline reference the integrated CO_2 source is lower by 0.9-5.4 Pg C yr^{-1} (3.3-19.7 Gt CO_2 yr^{-1}) across scenarios. In the CO_2 panels the Global Carbon Budget reference is shown under its native label "NEE," corresponding here to the net land-atmosphere carbon flux (F_{net}, Sect. 2.2.6). The overlaid budget series are labelled by vintage and variant: for CH_4, the Global Methane Budget best estimate (wetland plus inland-freshwater, double-counting-corrected, Saunois et al., 2025) shown with its reported uncertainty range; for N_2O, the Global Nitrous Oxide Budget 2024 net-plus-perturbation best estimate and range (Tian et al., 2024); and for CO_2, the Global Carbon Budget net-ecosystem-exchange best estimate and $\pm 1\sigma$ range (Friedlingstein et al., 2025).

S6 Land-use forcing

The land-use forcing common to both configurations is the harmonised HILDA+ (historical) and PLUM (scenario) land-cover product (Sect. 2.3.3), supplying the per-gridcell, per-year fractions of natural vegetation, cropland, pasture and wetland that

partition each grid cell among the simulated stands. These same fractions are used to convert the within-land-cover carbon and net-primary-production densities to the global totals shown in Figs. S9 and S10.

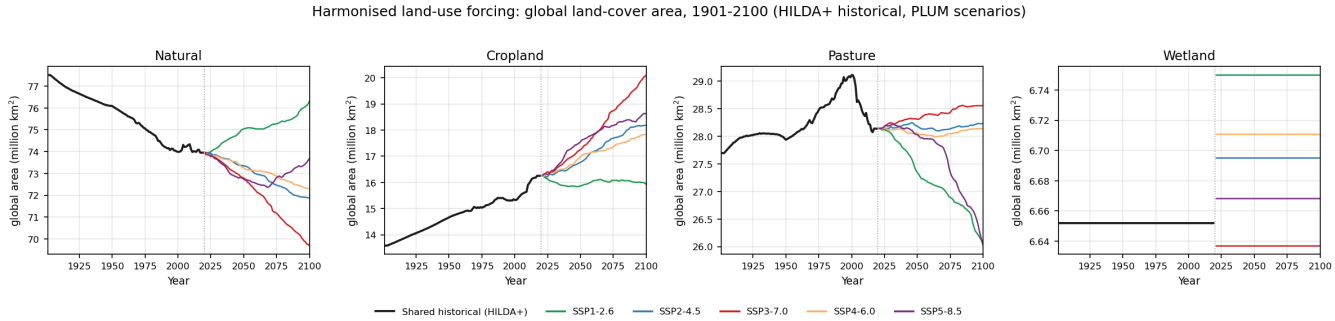


Figure S22. Global land-cover area, 1901-2100, for natural vegetation, cropland, pasture and wetland, from the harmonised land-use forcing (HILDA+ historical, shared across scenarios in black to 2019; PLUM scenarios coloured from 2020). Areas are the cosine-latitude gridcell-area sums of the land-cover fractions. Cropland expands and natural vegetation contracts under all scenarios, most strongly under SSP3-7.0; pasture peaks around 2000 and then diverges by scenario; the wetland area is time-invariant within each scenario by construction, and the small cross-scenario differences arise because the carved wetland fraction depends on the scenario-specific minimum natural fraction (Eq. 27, Sect. 2.3.3).

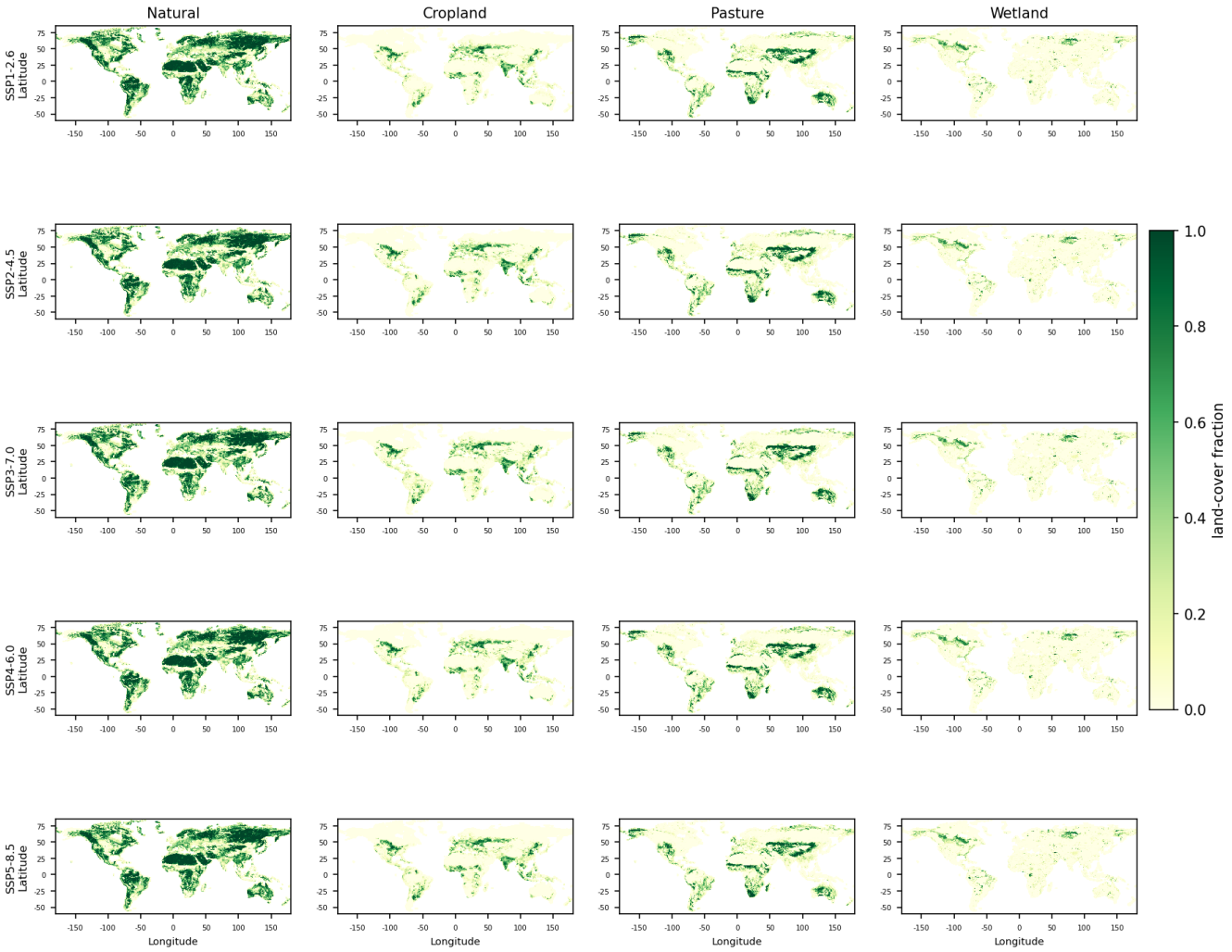


Figure S23. End-of-century (2080-2100) mean land-cover fraction for natural vegetation, cropland, pasture and wetland under all five SSP-RCP scenarios (rows), from the harmonised land-use forcing. The fractions sum to unity with the (small) barren fraction in each cell and define the stand areas used throughout the coupled simulations.

S7 Per-scenario ecosystem-trajectory composites (intermediate scenarios)

These figures provide, for the three intermediate scenarios, the per-scenario four-panel composite of carbon pools (cpool), carbon fluxes (cflux), nitrogen pools (npool), and nitrogen fluxes (nflux) – the same view as main-text Fig. 9 (SSP1-2.6) and Fig. 10 (SSP5-8.5). In each panel the solid line is the ISIMIP-3b prescribed configuration and the dashed line the IMOGEN-

coupled configuration; lines are coloured by output component, and the dotted vertical line marks the 2020 historical-scenario
270 transition.

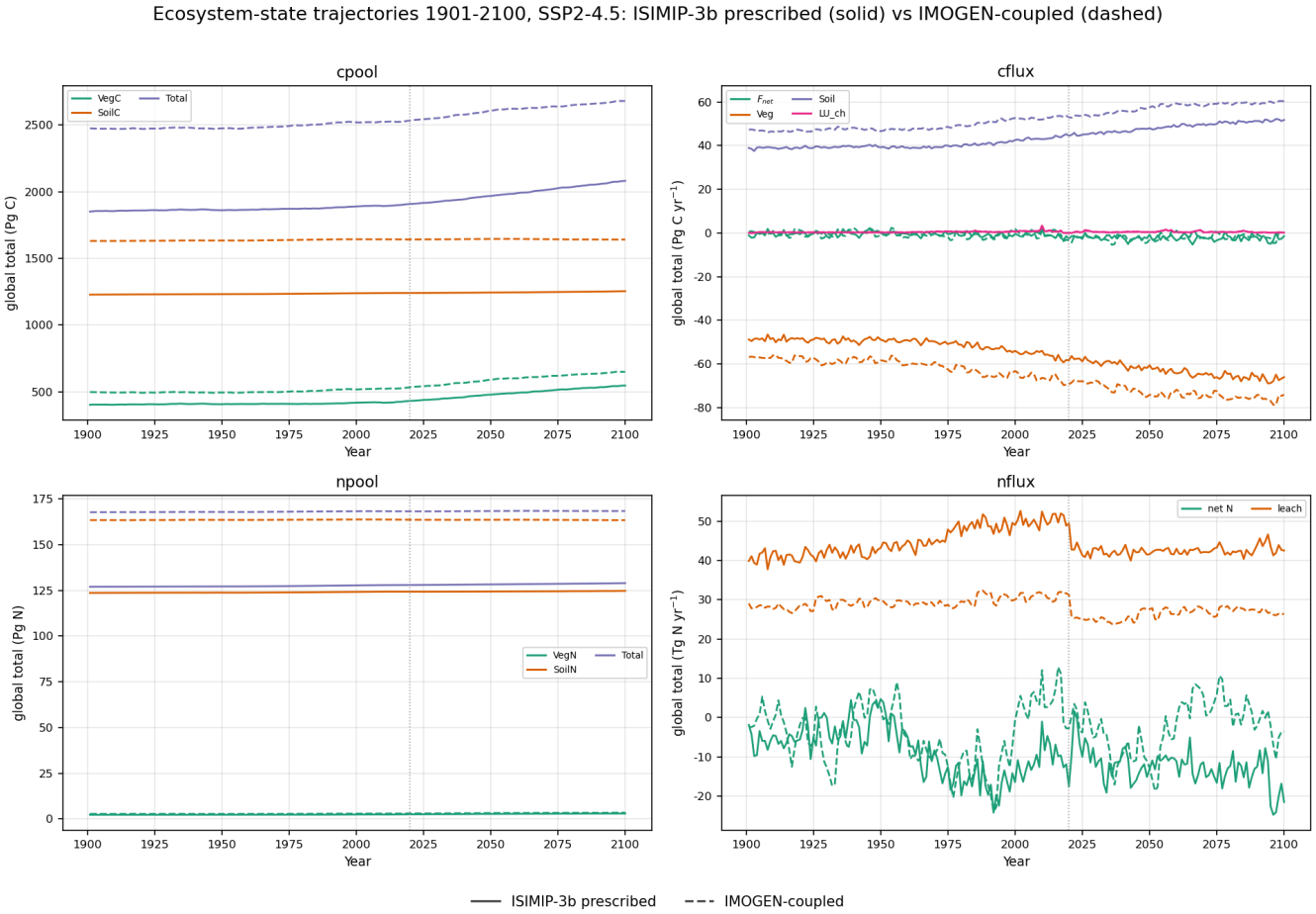


Figure S24. Per-scenario ecosystem-state trajectories (1901-2100), SSP2-4.5.

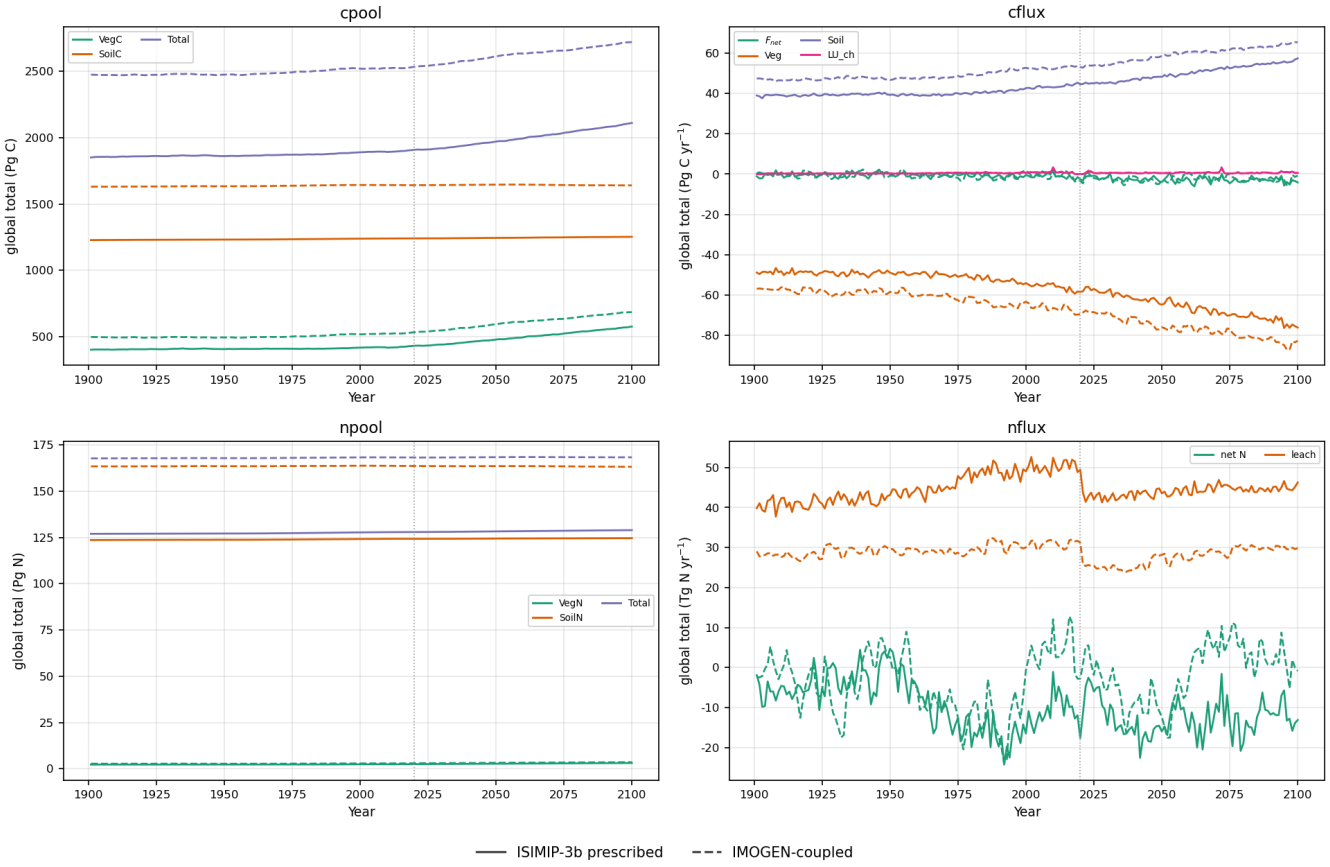


Figure S25. Per-scenario ecosystem-state trajectories (1901-2100), SSP3-7.0.

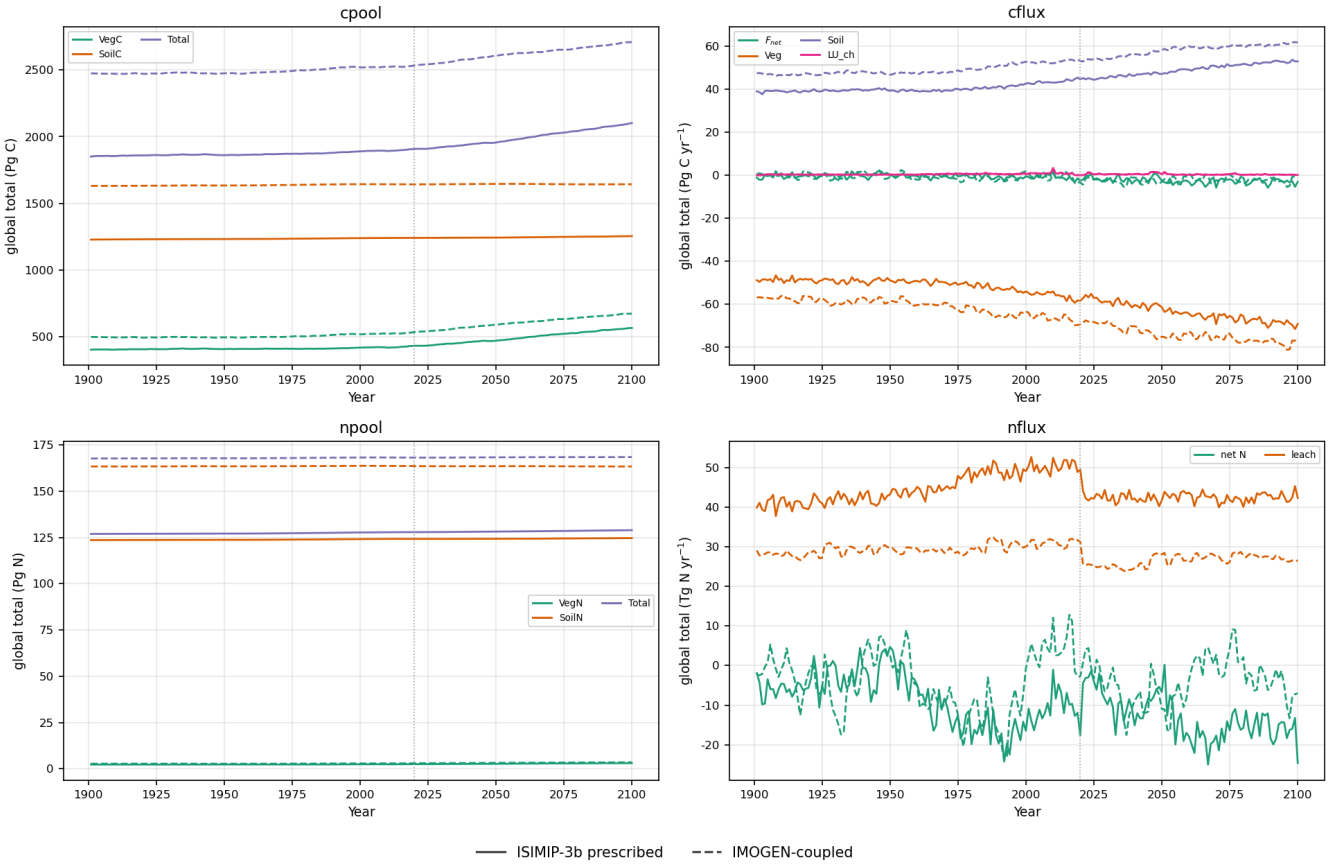


Figure S26. Per-scenario ecosystem-state trajectories (1901-2100), SSP4-6.0.

S8 Integrated-emission time series: raw and smoothed

This figure shows the integrated GHG emissions handed to IMOGEN both as the raw annual series and as the 10-year centred running mean (Sect. 2.3.2, 2.3.4). It makes explicit (i) the genuine methodological step discontinuities that are retained in the forcing at the 1970 (Tier-1 inventory start) and 2020 (FAO-to-PLUM activity-data hand-off) transitions, and (ii) that the running mean is applied only for the figures and the reference series of Fig. 3, never to the driving emissions.

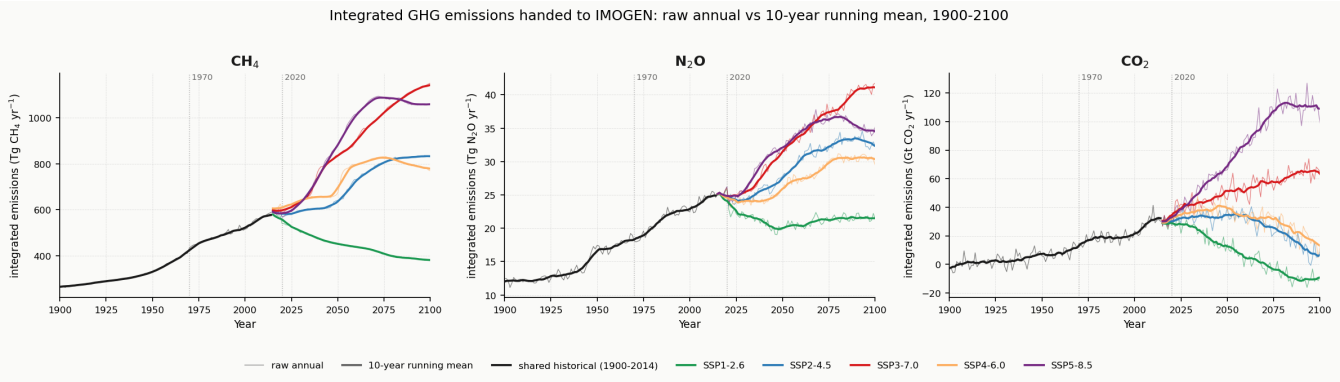


Figure S27. Integrated GHG emissions (anthropogenic + natural) handed to IMOGEN, 1900-2100, by gas (CH_4, N_2O, CO_2), for the five SSP-RCP scenarios: raw annual series (thin) and the 10-year centred running mean (thick), with the shared historical period (1900-2014) in black. Vertical dotted lines mark the 1970 Tier-1 inventory start and the 2020 FAO-to-PLUM activity-data transition; the step at 2020 (and the interannual variability, most visible in the CO_2 net source) is retained in the forcing and only smoothed for display. The 10-year running mean is computed separately on the historical and scenario segments so the 2015 scenario divergence is not smoothed across. The raw and smoothed CH_4 series appear nearly coincident because the integrated CH_4 emissions have low interannual variability (the raw-minus-smoothed scatter is about 2% of the total, against about 13% for CO_2, whose net land-atmosphere flux dominates the year-to-year variability).

S9 Global-mean climate time-series

Complementing the windowed spatial statistics of Section S1, Figures S28-S30 show the full-period (1900-2100) cosine-latitude area-weighted global-land annual mean of the three headline climate variables – near-surface air temperature, precipitation, and surface downwelling shortwave radiation – for the IMOGEN-coupled climate and the ISIMIP-3b MRI-ESM2-0 reference, for all five SSP-RCP scenarios. The ISIMIP-3b reference is extended before 2015 with the MRI-ESM2-0 historical simulation; all means are taken over the IMOGEN land grid. These trajectories show, over the full period rather than in fixed windows, the close correspondence of the emulated global-land-mean temperature with the reference throughout (within about 0.3 K, without systematic forcing dependence; Sect. 3.3.1), and of precipitation and shortwave radiation between the two configurations.

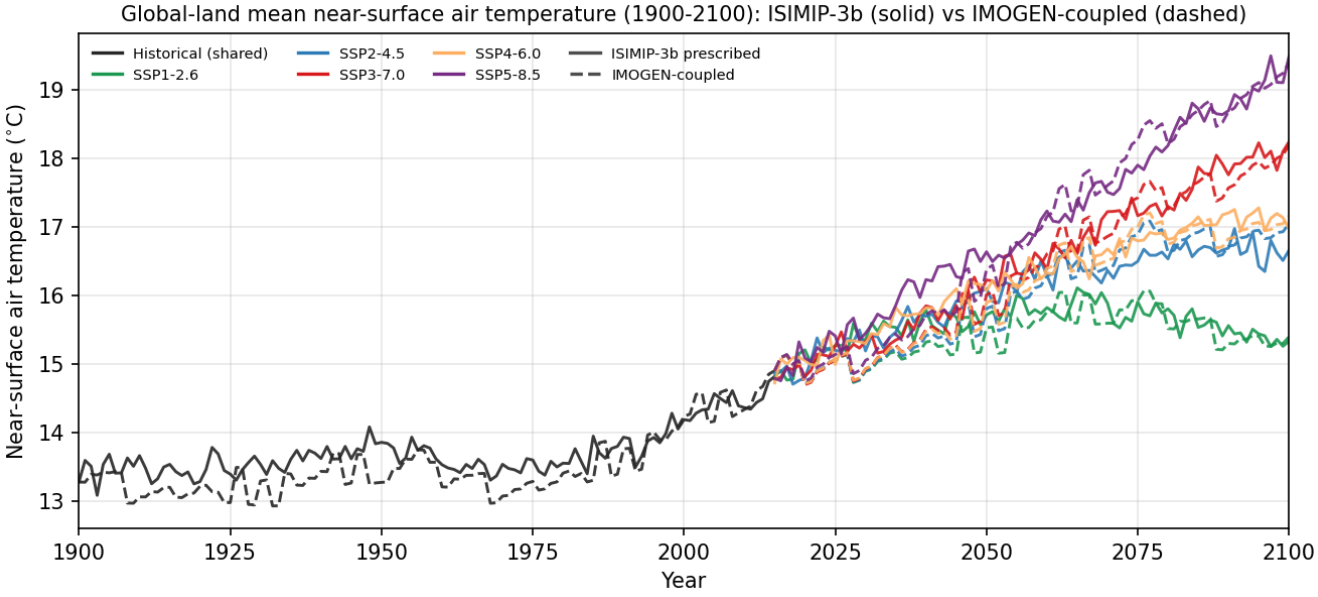


Figure S28. Global-land mean near-surface air temperature (1900-2100), ISIMIP-3b MRI-ESM2-0 (solid) versus IMOGEN-coupled (dashed); the projection period is coloured by scenario and the shared historical period (to 2015) is shown in black. The emulated temperature closely tracks the reference global-land mean, to within about 0.3 K over the analysis windows, with no systematic forcing dependence (consistent with the windowed statistics of Table S1 and Sect. 3.3.1).

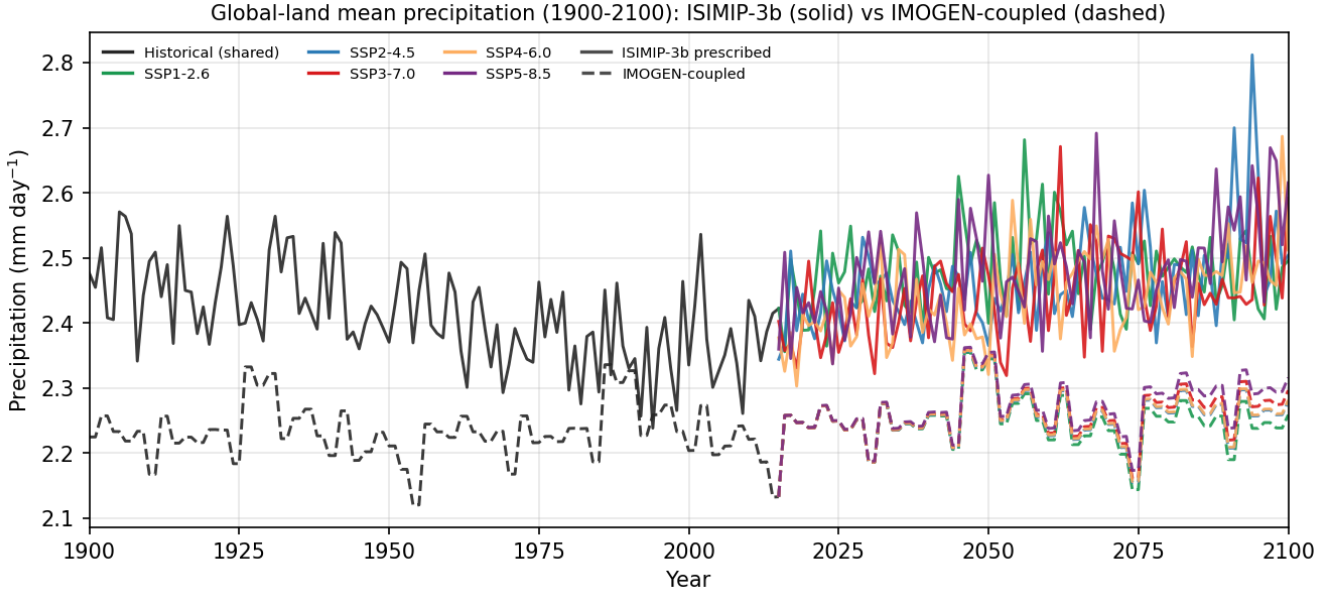


Figure S29. Global-land mean precipitation (1900-2100), ISIMIP-3b MRI-ESM2-0 (solid) versus IMOGEN-coupled (dashed); the projection period is coloured by scenario and the shared historical period (to 2015) is shown in black.

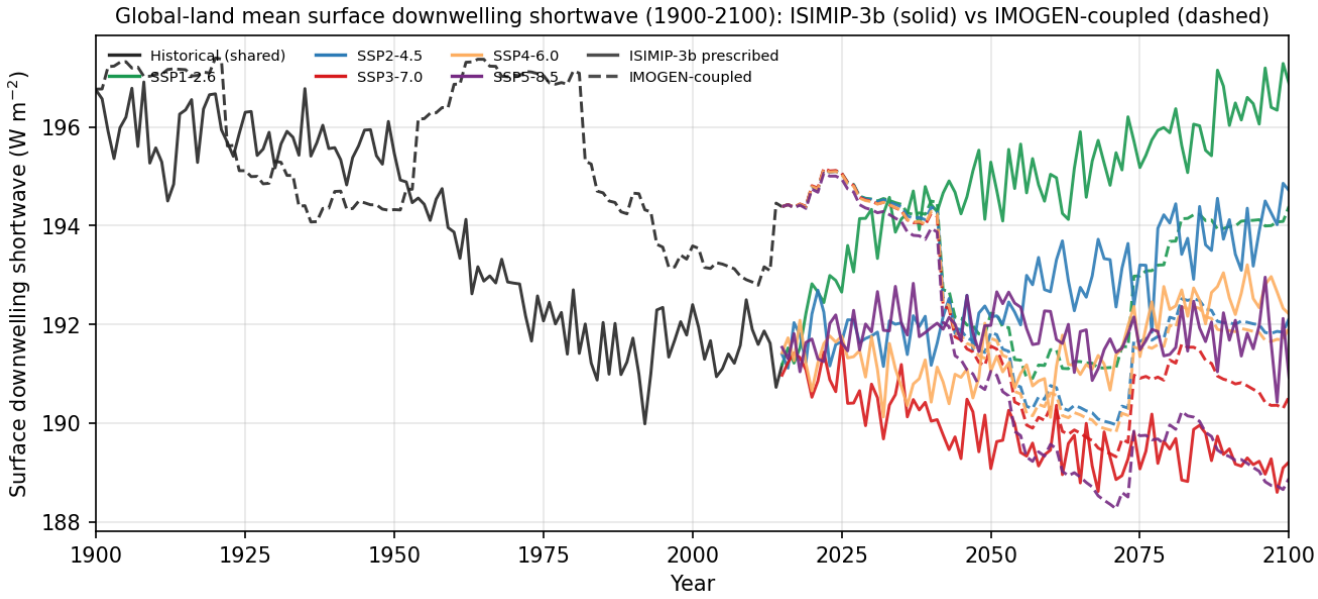
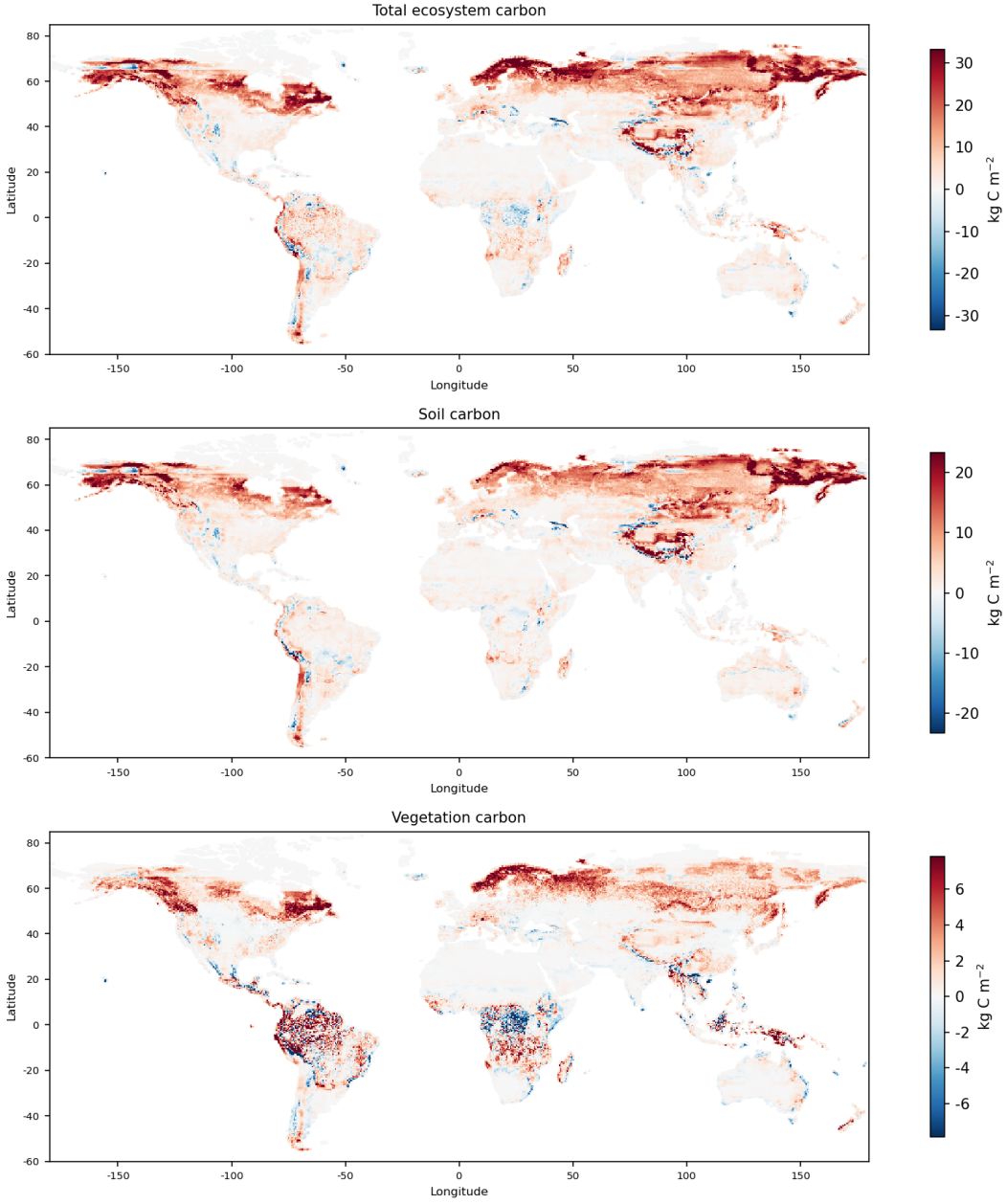


Figure S30. Global-land mean surface downwelling shortwave radiation (1900-2100), ISIMIP-3b MRI-ESM2-0 (solid) versus IMOGEN-coupled (dashed); the projection period is coloured by scenario and the shared historical period (to 2015) is shown in black.

S10 Absolute ecosystem-state difference maps (including the baseline-climatology offset)

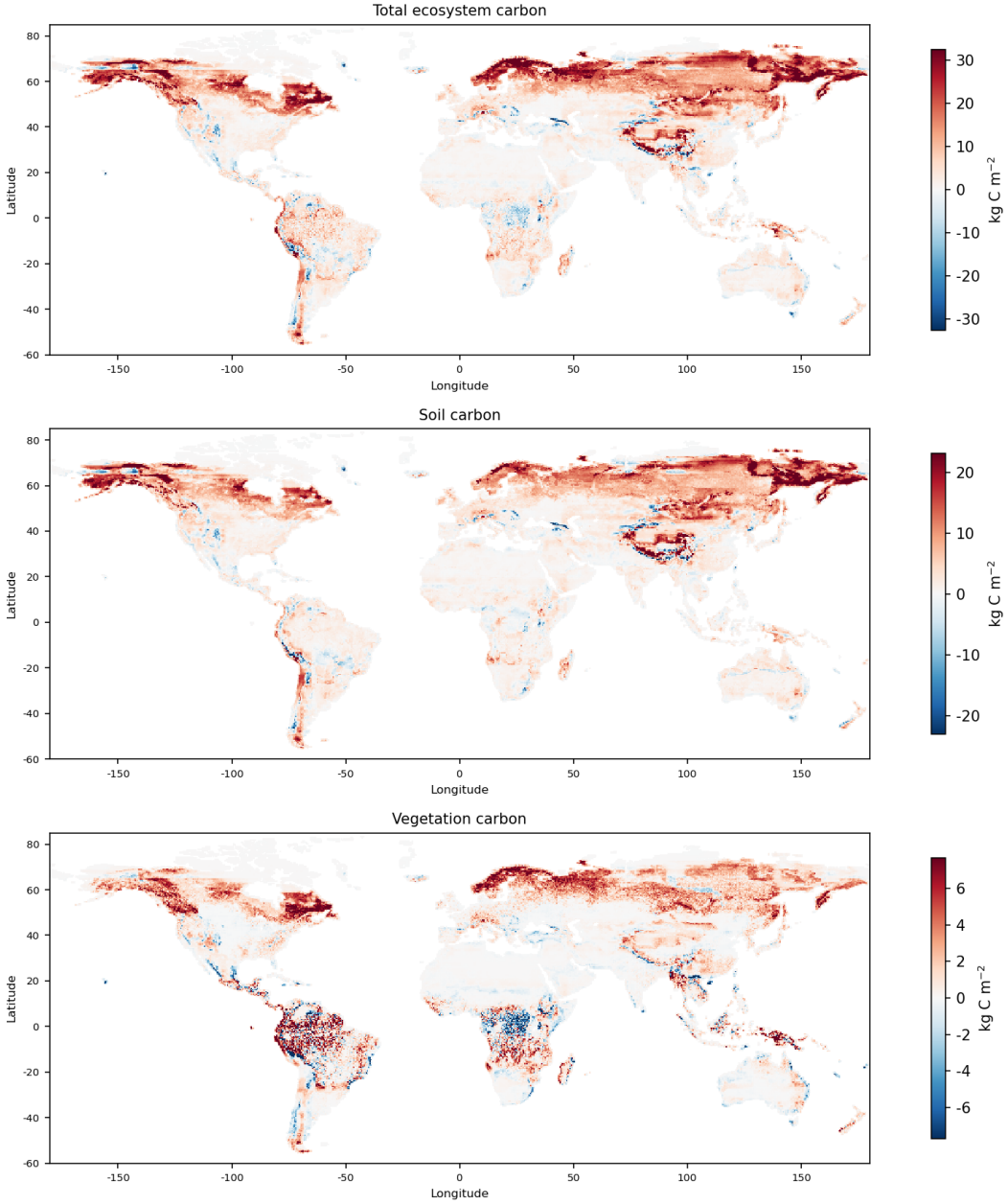
For completeness, this section provides the *absolute* end-of-century (2080-2100) difference maps (IMOGEN-coupled minus ISIMIP-3b prescribed) for ecosystem carbon and crop yield, for all five SSP-RCP scenarios. Unlike the change-based maps of the main text (Figs. 7, 8) and Supplement (Figs. S6, S7) – which difference the present-day-to-end-of-century change between the two configurations and thereby remove the time-invariant baseline-climatology mean-state offset (Sect. 3.4.1) – these maps retain that offset. The large, spatially coherent carbon surplus of the coupled configuration across the boreal and cool-temperate zones seen here is the persistent baseline-climatology offset itself; the change-based maps remove it to isolate the differential response.

end-of-century difference (IMOGEN-coupled - ISIMIP-3b) in ecosystem carbon, SSP1-2.6 (low forcing) (2080-2100); retains the baseline-climatol

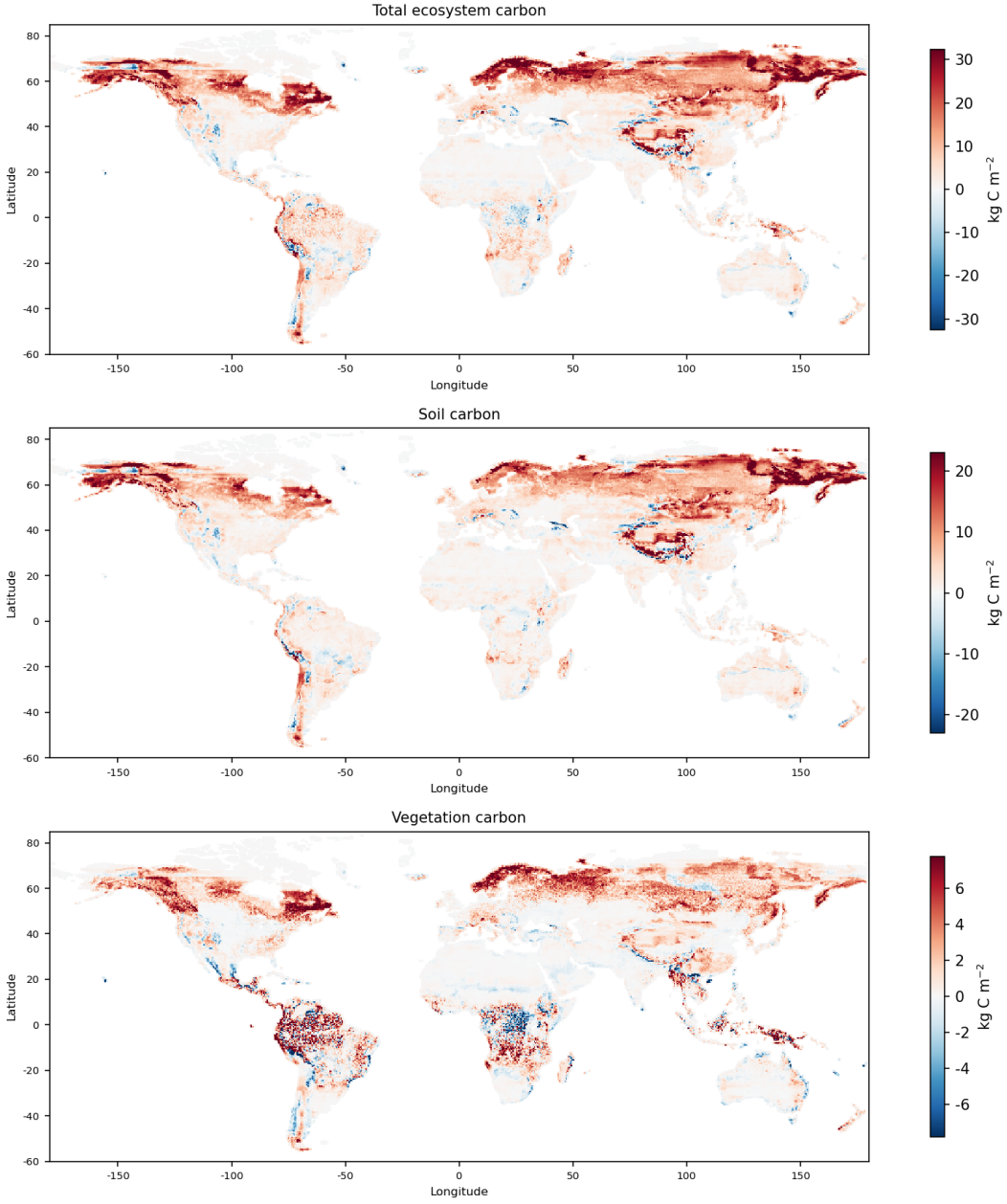


320

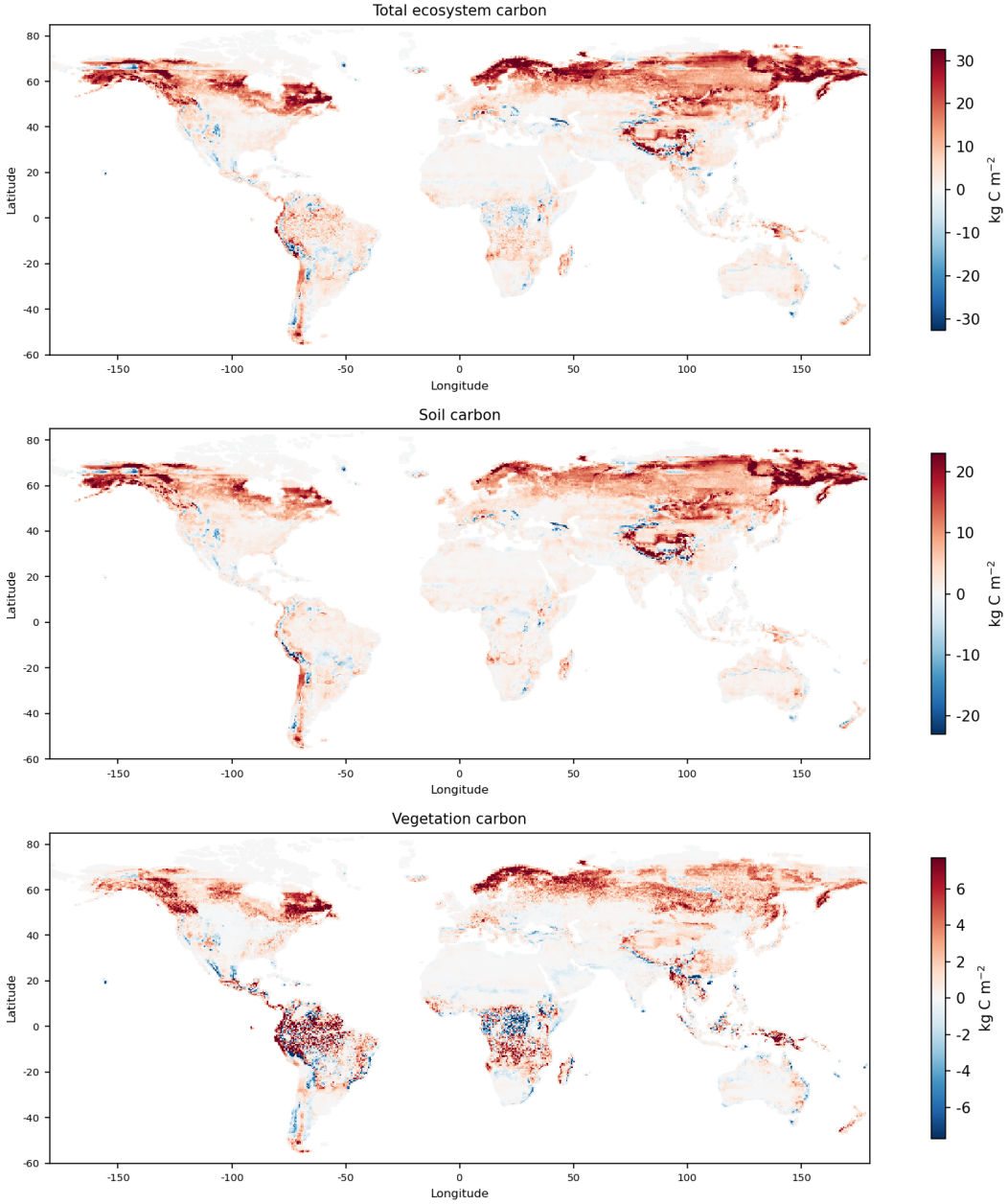
solute end-of-century difference (IMOGEN-coupled - ISIMIP-3b) in ecosystem carbon, SSP2-4.5 (2080-2100); retains the baseline-climatology off



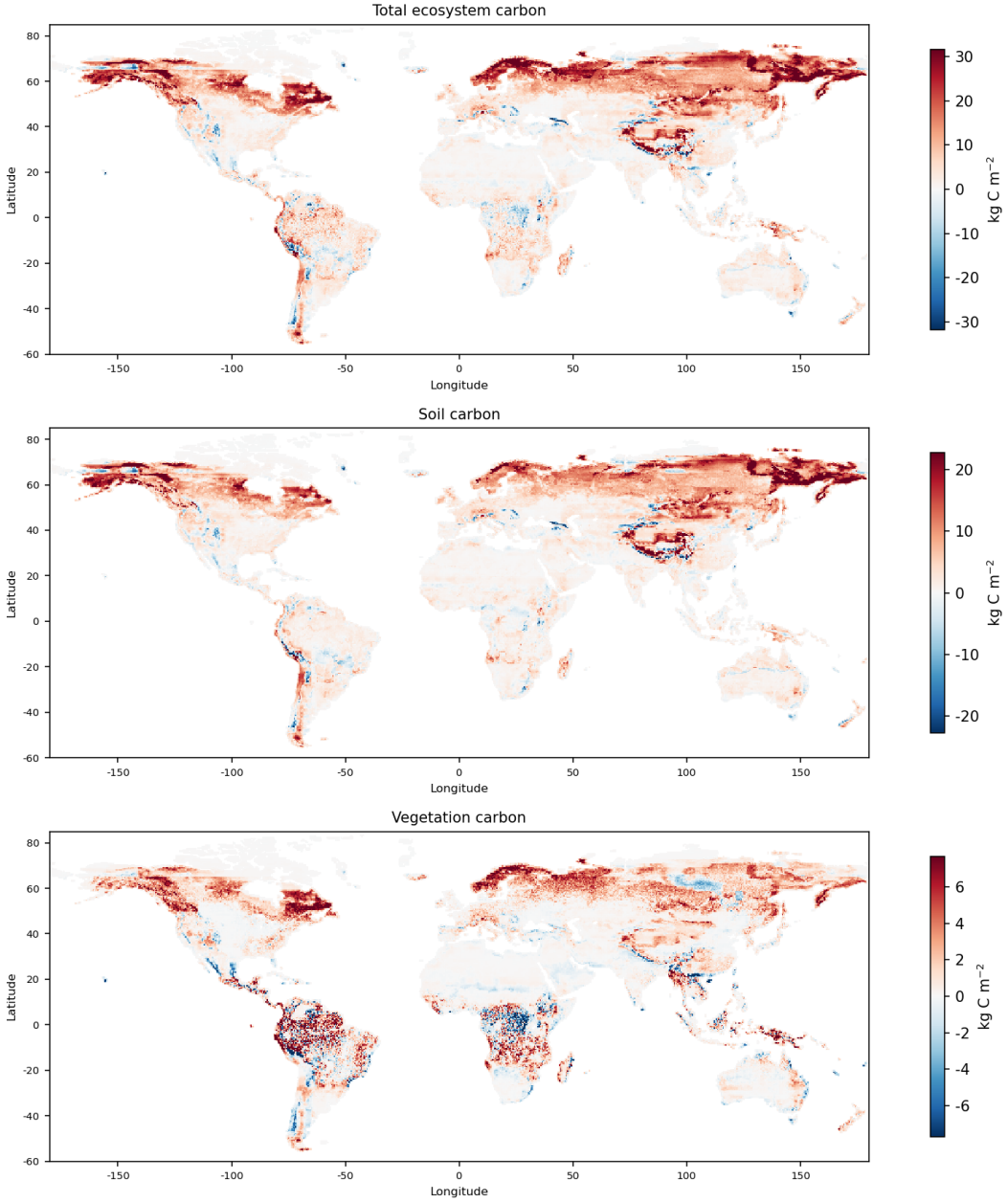
solute end-of-century difference (IMOGEN-coupled - ISIMIP-3b) in ecosystem carbon, SSP3-7.0 (2080-2100); retains the baseline-climatology off



solute end-of-century difference (IMOGEN-coupled - ISIMIP-3b) in ecosystem carbon, SSP4-6.0 (2080-2100); retains the baseline-climatology off

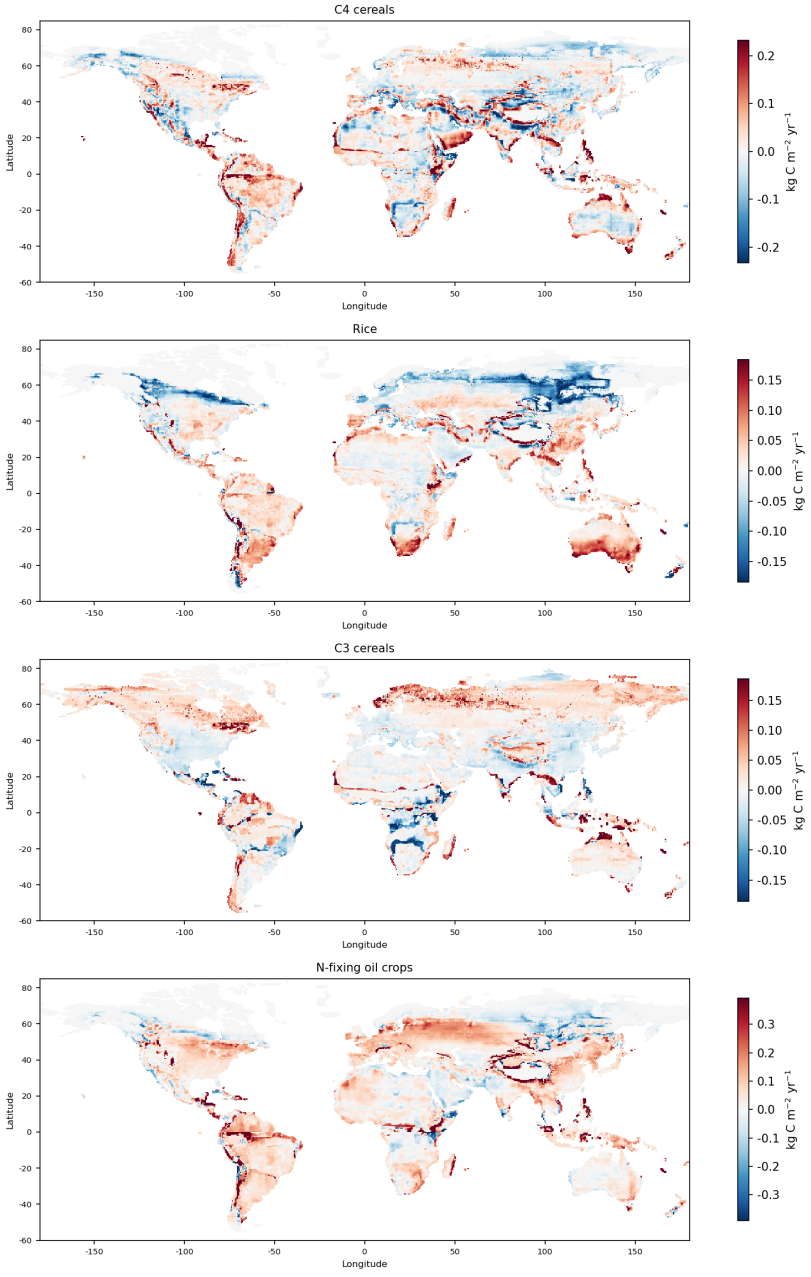


end-of-century difference (IMOGEN-coupled - ISIMIP-3b) in ecosystem carbon, SSP5-8.5 (high forcing) (2080-2100); retains the baseline-climatol



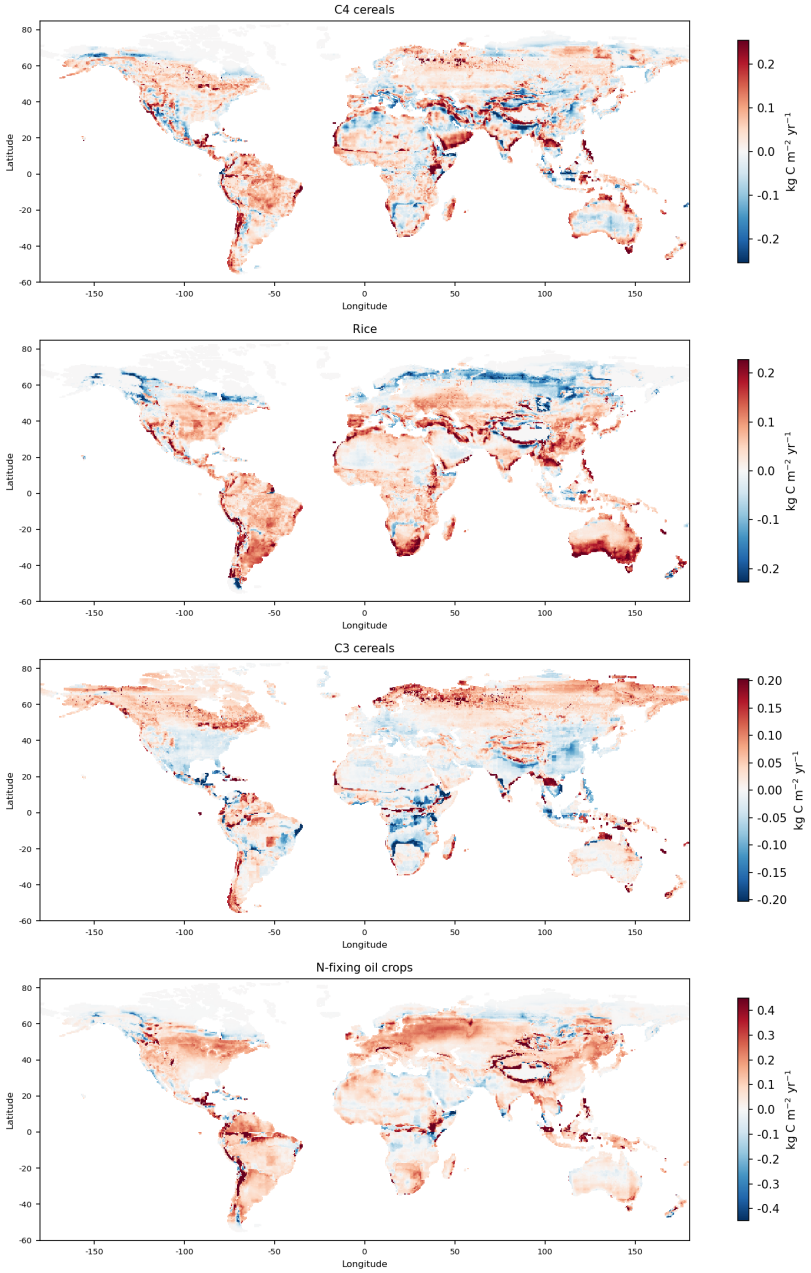
325 **Figure S31.** Absolute end-of-century (2080-2100) spatial difference (IMOGEN-coupled minus ISIMIP-3b prescribed) in ecosystem carbon (total ecosystem carbon, soil carbon, vegetation carbon), for all five SSP-RCP scenarios: (from top) SSP1-2.6, SSP2-4.5, SSP3-7.0, SSP4-6.0, and SSP5-8.5. These maps retain the persistent baseline-climatology mean-state offset (Sect. 3.4.1); the offset-removed, change-based counterparts are Fig. 7 (bracketing scenarios) and Fig. S6 (intermediate scenarios).

ute end-of-century difference (IMOGEN-coupled - ISIMIP-3b) in crop yield, SSP1-2.6 (low forcing) (2080-2100); retains the baseline-climatology

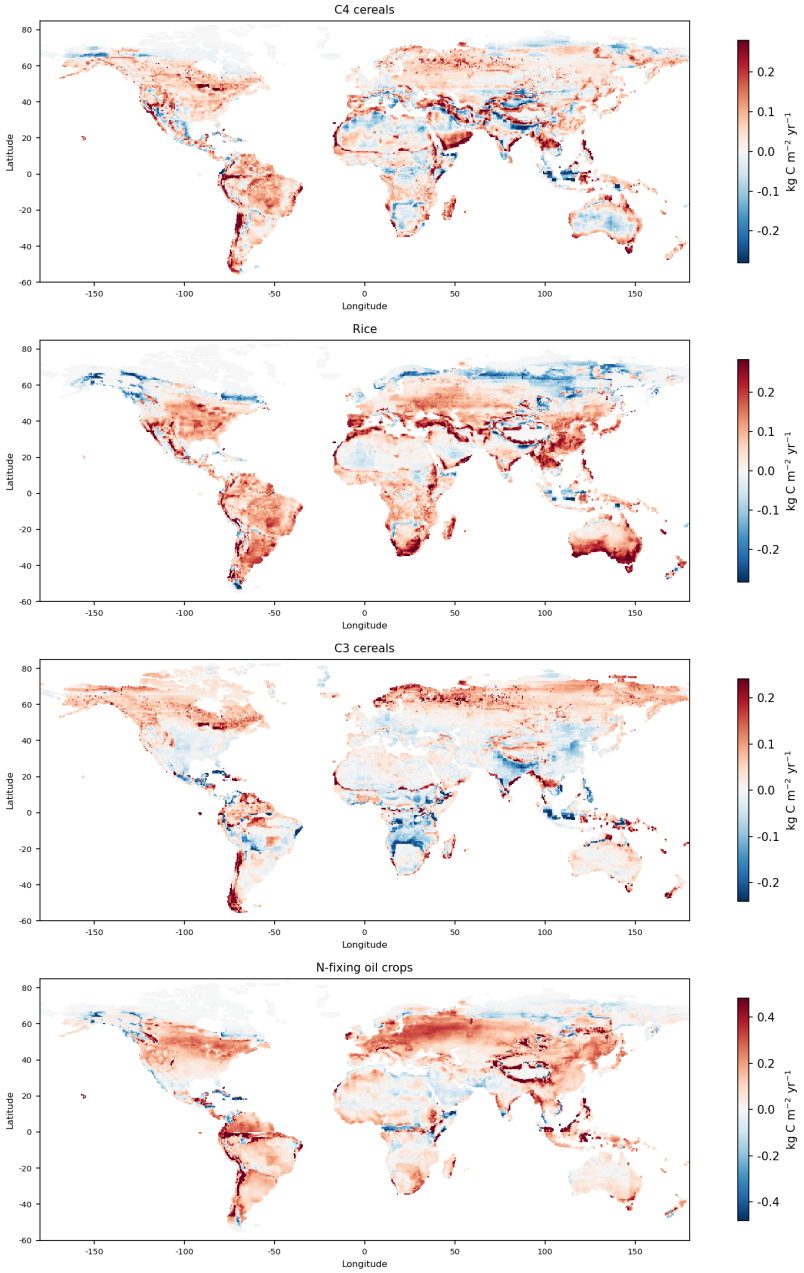


330

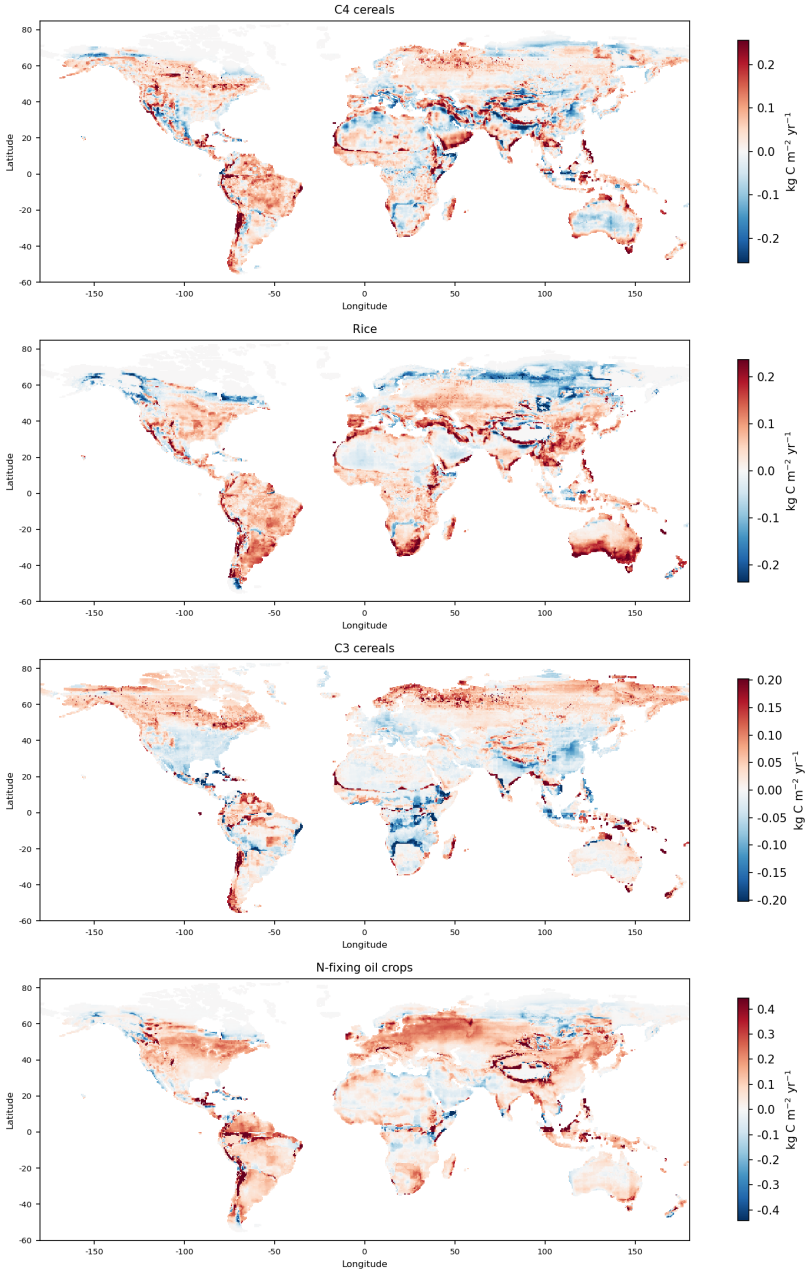
Absolute end-of-century difference (IMOGEN-coupled - ISIMIP-3b) in crop yield, SSP2-4.5 (2080-2100); retains the baseline-climatology offset



Absolute end-of-century difference (IMOGEN-coupled - ISIMIP-3b) in crop yield, SSP3-7.0 (2080-2100); retains the baseline-climatology offset



Absolute end-of-century difference (IMOGEN-coupled - ISIMIP-3b) in crop yield, SSP4-6.0 (2080-2100); retains the baseline-climatology offset



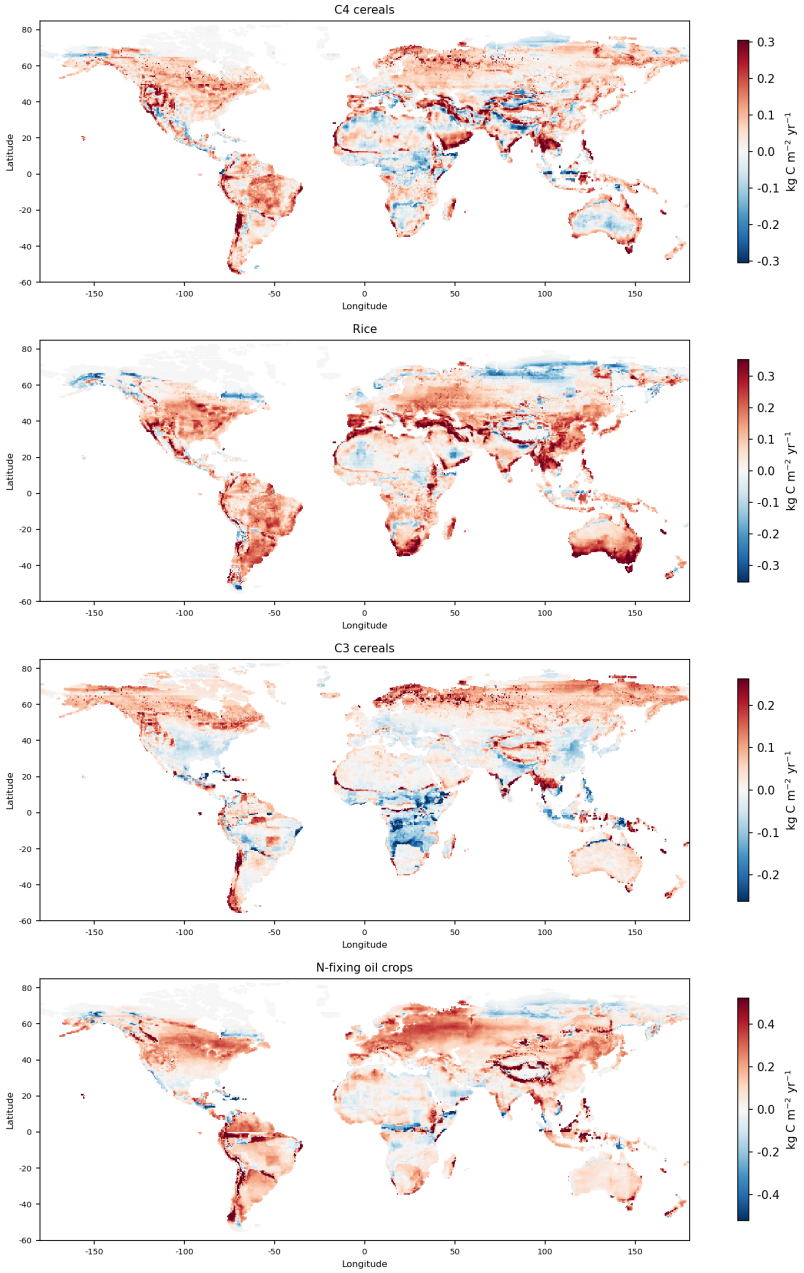


Figure S32. Absolute end-of-century (2080-2100) spatial difference (IMOGEN-coupled minus ISIMIP-3b prescribed) in crop yield (C4 cereals, rice, C3 cereals, N-fixing oil crops), for all five SSP-RCP scenarios: (from top) SSP1-2.6, SSP2-4.5, SSP3-7.0, SSP4-6.0, and SSP5-8.5. The maps show the per-area difference on all grid cells (the aggregate statistics of Table S2 are production-weighted by harvested area); the offset-removed, change-based counterparts are Fig. 8 (bracketing scenarios) and Fig. S7 (intermediate scenarios).

Friedlingstein, P., O'Sullivan, M., Jones, M. W., Andrew, R. M., Hauck, J., Landschützer, P., Le Quéré, C., Li, H., Luijkx, I. T., Olsen, A., Peters, G. P., Peters, W., Pongratz, J., Schwingshackl, C., Sitch, S., Canadell, J. G., Ciais, P., Jackson, R. B.,

and others: Global carbon budget 2024, Earth System Science Data, 17, 965–1039, https://doi.org/10.5194/essd-17-965-2025, 2025.

Saunois, M., Martinez, A., Poulter, B., Zhang, Z., Raymond, P. A., Regnier, P., Canadell, J. G., Jackson, R. B., Patra, P. K., Bousquet, P., Ciais, P., Dlugokencky, E. J., Lan, X., Allen, G. H., Bastviken, D., Beerling, D. J., and others: Global methane budget 2000–2020, Earth System Science Data, 17, 1873–1958, https://doi.org/10.5194/essd-17-1873-2025, 2025.

Tian, H., Pan, N., Thompson, R. L., Canadell, J. G., Suntharalingam, P., Regnier, P., Davidson, E. A., Prather, M., Ciais, P., Muntean, M., Pan, S., Winiwarter, W., Zaehle, S., Zhou, F., Jackson, R. B., and others: Global nitrous oxide budget (1980–2020), Earth System Science Data, 16, 2543–2604, https://doi.org/10.5194/essd-16-2543-2024, 2024.